

QATAR UNIVERSITY

COLLEGE OF ENGINEERING

A HYBRID PIEZOELECTRIC-ELECTROMAGNETIC ENERGY HARVESTING AT

STABILIZATION CYCLES EXCITED BY CONFINED WATER IN PIPELINE

BY

MOHAMED ABDUL AZIZ ARAB

A Thesis Submitted to

the College of Engineering

in Partial Fulfillment of the Requirements for the Degree of

Master of Science in Mechanical Engineering

June 2021

© 2021 Mohamed Arab. All Rights Reserved.

COMMITTEE PAGE

The members of the committee approve the thesis of
Mohamed Abdul Aziz Arab defended on 19/04/2021.

Asan Gani Bin Abdul Muthalif
Thesis Supervisor

Jawaid I. Inayat-Hussain
Committee Member

Jamil Renno
Committee Member

Approved:

Khalid Kamal Naji, Dean, College of Engineering

ABSTRACT

ARAB, MOHAMED, MASTERS: June: 2021 Master of Science in Mechanical Engineering

Title: A Hybrid Piezoelectric-Electromagnetic Energy Harvesting at Stabilization Cycles Excited by Confined Water in Pipeline

Supervisor of Thesis: Asan Gani Bin Abdul Muthalif

Research on green energy has been increasing tremendously in the past few years. Energy harvesting from an industrial pipeline conveying fluid using a hybrid harvester consisting of a piezoelectric beam and electromagnetic mechanism is proposed in this research thesis. Accumulated harvested energy can be stored over time utilizing an external battery to power smart sensing applications in remote locations. Existing harvesters in terms of piezoelectric or electromagnetic parts aim to obtain peak power by tuning techniques in terms of frequency, resistance or by manipulating fluid velocity. To address this nut, a hybrid harvester is proposed to acquire energy at stabilization cycles over unlimited time, providing a steady voltage based on realized 3D simulation in agreement with piezoelectric control algorithm and (EM) governing equation. The study covers water velocities from 0.34 to 1.36 m/sec when lift and transverse fluid forces reveal that water velocity of 1.36 m/sec and new originated velocity of 1.39 m/sec obtained by iteration could have further investigations. For the piezoelectric part, the mean voltages are 37.6 mV and 41.4 mV for water velocity of 1.36 m/sec and 1.39 m/sec, respectively, while mean voltages are 49.7 μ V and 91.8 μ V for water velocity of 1.36 m/sec and 1.39 m/sec respectively from the electromagnetic part.

DEDICATION

I dedicated this thesis to my supervisor and my daughter

ACKNOWLEDGMENTS

I want to express my grateful appreciation to my principal supervisor Dr. Asan for his efforts to guide this thesis on the right lane. The principal committee Dr. Asan has provided endless support over more than a year, especially during the pandemic period, by giving keywords to overcome conventional critical thinking. In fact, without his mentoring, the current thesis would have been unattainable to achieve by its content and timeline.

Additionally, I would like to give my sincere thanks to Dr. Saud Gani for giving his potential time coaching on modern simulation techniques and analysis. Also, Eng Ahmed Osama and Eng. Muhammad Hafizh for their continued assistance on literature review, simulation analysis and interpretation of results.

I thank my study journey partner Eng. Ahmed Jamil, Eng Mohamed Houkan, and Eng. Mohamed Mudather for their technical contribution towards writing this thesis. I take the chance to appreciate the work of the Department of Mechanical and Industrial Engineering at Qatar University, and I am grateful for allowing me to study and graduate under their college.

TABLE OF CONTENTS

DEDICATION	iv
ACKNOWLEDGMENTS	v
LIST OF TABLES	ix
LIST OF FIGURES	xi
Chapter 1: Introduction.....	1
Motivation	2
Aim and Objectives.....	3
Scope of Work.....	4
Organization of Chapters and Flow Chart.....	4
Chapter 2: Literature Review	6
Chapter 3: Methodology	12
Preliminary Study	12
Section1: Basic Setup.....	12
Section 2: The Four Reynolds Number.....	14
Section 3: Piezoelectric Power Formula	15
Section 4: Finding Model Parameters and Variables.....	18
Polypropylene Cylinder	18
Piezoelectric Material	19
Piezoelectric Capacitance.....	21

Cylinder Moment of Inertia.....	22
Cylinder Radius of Gyration	24
Section 5: 2-D CFD Setup of Preliminary Study	25
Section 6: Development of MATLAB Code for Piezoelectric Power.....	33
Section 7: Electromagnetic Induction	34
Governing Equation.....	34
Finding Model Parameters and Variables	37
Development of MATLAB Code for Magnet Velocity.....	39
Finding Electromagnetic Power and Voltage.....	40
3-D Simulation Study.....	42
Section 1: Geometry and Fluid Force Analysis.....	42
Section 2: Piezoelectric Voltage	47
Section 3: Magnet Velocity and Electromagnetic Voltage	49
Chapter 4: Results and discussions.....	51
Preliminary Study	51
Section 1: Fluent Results and Piezoelectric Power.....	51
Section 2: Magnet Velocity, Electromagnetic Voltage and Power	63
3D Simulation Study.....	71
Section 1: ANSYS Fluent Lift and Transverse Forces	71
Section 2: Piezoelectric Voltage.....	73

Section 3: Magnet Velocity and Electromagnetic Voltage	75
Conclusion	79
References	82
Appendix “A”: Sample Matlab code from literature.....	85
Appendix “b”: Piezoelectric matlab codes of preliminary study	86
Appendix “C”: Electromagnetic induction governing equation	91
Appendix “D”: MATLAB Codes for electromagnetic induction	93
Appendix “E”: Non-selected water velocities.....	98

LIST OF TABLES

Table 1. Summary of basic setup measurements.	13
Table 2. Four Reynolds number of the preliminary study	14
Table 3. Model parameters	16
Table 4. Model variables	17
Table 5. PZT versus Polymer PVDF properties [8].	21
Table 6. Summary for fine and mesh simulation setup	32
Table 7. Variables of the electromagnetic induction governing equation	37
Table 8. Parameters of the electromagnetic induction governing equation.....	37
Table 9. Summary of parameters used in MATLAB	39
Table 10. Summary of the control volume mesh	44
Table 11. Summary of the selected option in fluent analysis	45
Table 12. Summary of transient mechanical mesh.....	49
Table 13. Summary of C_L , C_D and Strouhal number for fine mesh	51
Table 14. Summary of C_L , C_D coefficients for medium mesh.....	51
Table 15. Variable and parameters for V_{water} 0.34 m/sec	53
Table 16. mean power for V_{water} of 0.34 m/sec	54
Table 17. Variable and parameters for V_{water} 0.68 m/sec	55
Table 18. Mean power for V_{water} of 0.68 m/sec	56
Table 19. Variable and parameters for V_{water} 1.02 m/sec	58
Table 20. Mean power for V_{water} of 1.02 m/sec	58
Table 21. Variable and parameters for V_{water} 1.36 m/sec	60
Table 22. Mean power for V_{water} of 1.36 m/sec	61
Table 23. Summary of research piezoelectric power	62

Table 24. Summary of MATLAB result for V_{water} (0.34 m/sec).....	63
Table 25. Summary of MATLAB result for V_{water} (0.68 m/sec).....	64
Table 26. Summary of MATLAB Result for V_{water} (1.02 m/sec).....	64
Table 27. Summary of MATLAB Result for V_{water} (1.36 m/sec).....	65
Table 28. Summary of Ansoft Maxwell results for V_{water} (0.34 m/sec).....	66
Table 29. Summary of Ansoft Maxwell result for V_{water} (0.68 m/sec).....	67
Table 30. Summary of Ansoft Maxwell result for V_{water} (1.02 m/sec).....	69
Table 31. Summary of Ansoft Maxwell result for V_{water} (1.36 m/sec).....	70
Table 32. Summary for piezoelectric voltage For V_{water} 1.36 m/sec.....	74
Table 33. Summary for piezoelectric voltage for V_{water} 1.39 m/sec.....	75
Table 34. Summary for electromagnetic voltage for V_{water} 1.36 m/sec.....	78
Table 35. Summary for Electromagnetic Voltage for V_{water} 1.39 m/sec.....	79
Table 36. Summary of piezoelectric parametric (preliminary study).....	80
Table 37. Summary of piezoelectric (3D simulation).....	80
Table 38. Summary of electromagnetic voltage and power (preliminary study).....	81
Table 39. Summary of electromagnetic voltage (3D simulation).....	81

LIST OF FIGURES

Figure 1. Publications and publications including patents from 2005 until 2018 [21].	2
Figure 2. Main flow chart of the research work.....	5
Figure 3. 2D simulation on a cylinder	6
Figure 4. Piezoelectric harvester schematic [23]	7
Figure 5. Schematic of the experimental setup [24].....	8
Figure 6. Schematic of the experimental setup [25].....	9
Figure 7. Electrmagnetic harvester (b) and section view (a) [28].....	10
Figure 8. Piezoelectric beam with cylinder body (Not to scale).....	13
Figure 9. Sketch of the harvester device (not to scale) [5].	17
Figure 10. Electromagnetic mechanism inside the cylinder (not to scale)	18
Figure 11. Direct and Converse Piezoelectric effect [8].....	20
Figure 12. Model: M2814-P1 with capacitance 1.4 nF [9].....	21
Figure 13. CATIA V5 Geometry preparation and applying material	23
Figure 14. CATIA V5 informative properties of the cylinder	24
Figure 15. Schematic of control volume preparation [14].....	26
Figure 16. 2-D control volume setup by ANSYS	27
Figure 17. 2-D Auto-generated global mesh.....	27
Figure 18. Edge size around the cylinder	28
Figure 19. A 30-layer inflation and edge sizing for fine mesh	29
Figure 20. Materials properties of the fluid in the domain	30
Figure 21. Lift and drag monitor specifying axis of interest	30
Figure 22. Lift.out file to estimate Strouhal number	31
Figure 23. Literature MATLAB results for $V_{\text{water}} 0.34 \text{ m/sec}$	33

Figure 24. FBD of electromagnetic induction prototype (not to scale)	36
Figure 25. Sketch of the cylinder components (not to scale).....	38
Figure 26. Overall view of the geometry preparation (Ansoft Maxwell 4.0)	41
Figure 27. Isometric view of the control volume CATIA V5.....	42
Figure 28. Harvester creation on offset plane from pipe inlet	43
Figure 29. Fluent geometry using boolean subtract operation.....	44
Figure 30. Implementation of global and cylinder mesh.....	45
Figure 31. Transverse z-axis forces versus time (V_{water} 0.68 m/sec)	46
Figure 32. Lift y-axis forces versus time (V_{water} 0.68 m/sec).....	47
Figure 33. Isometric view of the harvester	48
Figure 34. Isometric view of the magnet mechanism.....	50
Figure 35. C_L versus time of 15 sec (0.34 m/sec).....	52
Figure 36. C_D versus time of 15 sec (0.34 m/sec)	52
Figure 37. Vortex shedding for (V_{water} 0.34 m/sec).....	53
Figure 38. P_{mean} for V_{water} 0.34 m/sec	54
Figure 39. C_L versus time of 15 sec (0.68 m/sec).....	54
Figure 40. C_D versus time of 15 sec (0.68 m/sec)	55
Figure 41. Vortex shedding for (V_{water} 0.68 m/sec).....	55
Figure 42. P_{mean} for V_{water} (0.68 m/sec).....	56
Figure 43. C_L versus time of 15 sec (1.02 m/sec).....	57
Figure 44. C_D versus time of 15 sec (1.02 m/sec)	57
Figure 45. Vortex shedding for V_{water} (1.02 m/sec).....	57
Figure 46. P_{mean} for V_{water} (1.02 m/sec).....	58
Figure 47. C_L versus time of 15 sec (1.36 m/sec).....	59

Figure 48. C_D versus time of 15 sec (1.36 m/sec)	59
Figure 49. Vortex shedding for V_{water} 1.36 m/sec	60
Figure 50. P_{mean} for V_{water} (1.36 m/sec)	61
Figure 51. Voltage for V_{water} 1.36 m/sec	61
Figure 52. MATLAB results for magnet velocity (V_{water} 0.34 m/sec).....	63
Figure 53. MATLAB results for magnet velocity (V_{water} 0.68 m/sec).....	64
Figure 54. MATLAB results for magnet velocity (V_{water} 1.02 m/sec).....	64
Figure 55. MATLAB results for magnet velocity (V_{water} 1.36 m/sec).....	65
Figure 56. Mean voltage using Ansoft Maxwell for (V_{water} 0.34 m/sec).....	66
Figure 57. Mean power using Ansoft Maxwell for (V_{water} 0.34 m/sec).....	66
Figure 58. Mean voltage using Ansoft Maxwell for (V_{water} 0.68 m/sec)	67
Figure 59. Mean power using Ansoft Maxwell for (V_{water} 0.68 m/sec).....	67
Figure 60. Mean voltage using Ansoft Maxwell for (V_{water} 1.02 m/sec)	68
Figure 61. Mean power using Ansoft Maxwell for (V_{water} 1.02 m/sec).....	68
Figure 62. Mean voltage using Ansoft Maxwell for (V_{water} 1.36 m/sec)	69
Figure 63. Mean power using Ansoft Maxwell for (V_{water} 1.36 m/sec).....	69
Figure 64. Lift and z- force applied on the harvester cylinder (V_{water} 1.36m/sec)	71
Figure 65. Velocity vector over a cylinder for V_{water} 1.36 m/sec	72
Figure 66. Static pressure contour over a cylinder for V_{water} 1.36 m/sec.....	72
Figure 67. Lift and transverse forces applied on the harvester cylinder (V_{water} 1.39m/sec)	73
Figure 68. Mean voltage for piezoelectric (V_{water} 1.36 m/sec).....	74
Figure 69. Mean voltage for piezoelectric (V_{water} 1.39 m/sec).....	75
Figure 70. Mean magnet velocity for (V_{water} 1.36 m/sec)	76

Figure 71. Magnified mean magnet velocity for ($V_{\text{water}} 1.36 \text{ m/sec}$) between 11.7 sec to 18 sec showing steady cycles. 76

Figure 72. Mean magnet velocity for ($V_{\text{water}} 1.39 \text{ m/sec}$) 77

Figure 73. Magnified mean magnet velocity for ($V_{\text{water}} 1.39 \text{ m/sec}$) between 6 sec to 18 sec showing steady cycles..... 77

Figure 74. Electromagnetic voltage ($V_{\text{water}} 1.36 \text{ m/sec}$) 78

Figure 75. Electromagnetic voltage ($V_{\text{water}} 1.39 \text{ m/sec}$) 79

CHAPTER 1: INTRODUCTION

Energy is a hot topic nowadays in the research field; it is the steps to convert one form of energy into another form. Energy can be transformed from a nuclear reactor, windmill, or fossil fuel. Energy generation prior 2000s mainly was fossil fuel energy, where its output contributes to around 87% of world energy (varies every year). Consequently, most CO₂ in metric tons emitted from fossil fuel energy [5].

Nuclear energy contributes about 3%, which is the most expensive in terms of building a reactor and decommissioning its components. Finally, renewable energy contributes about 10% of world energy, and it is known as clean energy as it uses natural power such as wind or solar [27]. The only problem associated with renewable energy generation that it is intermittent, and the overall electricity generation is relatively insufficient.

Vibration-based energy harvesting device can be used to generate electrical power when applying mechanical stress. It is continuing energy, and if utilized optimally by charging a battery, it can widely use in today's industries. The scientific research on piezoelectric harvesting energy has been increasing tremendously since 2005, as shown in Figure 1, and it is continuing [21].

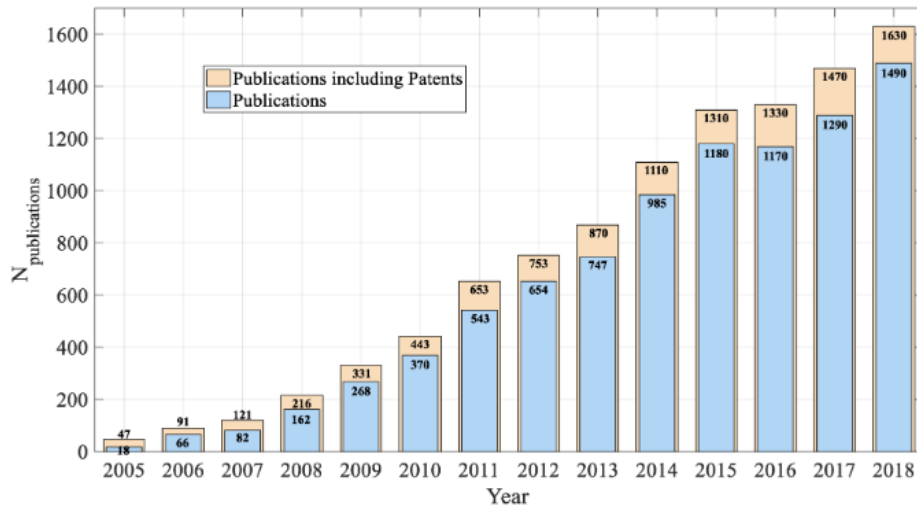


Figure 1. Publications and publications including patents from 2005 until 2018 [21].

The efficiency of the system depends on the materials used in the harvester, having different physical, mechanical, and dielectric constant [22]. Materials such as Lead Magnesium Niobate-Lead Titanate (PMN-PT), Lead Zinc Niobate-Lead Titanate (PZN-PT), Polyvinylidene Difluoride (PVDF), and Lead Zirconate Titanate (PZT).

Electrical current can be also generated by the oscillation motion of a Permanent Magnet (PM) admitted into a coil consisting of a certain number of loops. When a PM moves towards a copper coil, the galvanometer with a sensitive needle will deflect away towards positive Electromotive force (EMF). Consequently, when PM retracts, the needle moves away from zero reading towards negative EMF. There is a zero reading by the galvanometer if the PM is idle. The mechanism described above is discovered by Michael Faraday in the 1830s.

Motivation

Pipes are very important products in all today's industrial sections. Pipes in human

anatomy are blood-vessel carrying blood and nutrition elements to organs. In medical equipment, it is the hoses conveying oxygen for a patient suffering from a disease such as the novel COVID-19 virus pandemic. In electrical engineering, it is the outer duct shell protecting the electrical cables or fibers.

Eventually, in mechanical engineering, pipes are carrying potable water for residential houses or Treated Sewer Effluent (TSE) for processing facilities. A survey made by the researcher exposed a potential gap in the leak-detection in industrial pipelines, especially the laid ones with thousands of meters in the rural areas. Several works were done on energy harvesting devices, and maximum energy was estimated. However, none of them concentrate on energy harvesting from the steady state of the harvester over a time period that ensures a stabilized energy output.

Aim and Objectives

The aim of the current research is to calculate the steady combined output voltage over time from a hybrid mechanism harvester device mounted inside a utility pipe carrying water at 25 °C.

The required objectives to meet the aim are stated as follow:

- i. Perform a parametric study to determine the existing piezoelectric hydro-mechanical model to suit the new prototype dimensions and find its power and voltage.
- ii. Derive a mathematical model for the electromagnetic induction mechanism and estimate the output voltage and power.
- iii. Carryout a 3D simulation analysis to find a suitable water velocities that provide a stable voltage over time by iteration.

- iv. Implement a 3D simulation analysis to find the voltage from piezoelectric and electromagnetic induction based on water velocities selected in objective “iii”.
- v. Compare results from 3D simulation study with the preliminary study “i” and “ii”

Scope of Work

This research work includes the design and dimension of the proposed hybrid harvester under steady water velocity. The design work includes specifying the material properties of each component at a certain environment temperature. The dimensions include the sizing of the main pipe, piezoelectric beam, the electromagnetic components, and positioning inside the pipe. Also, obtaining the steady output voltage versus time from the dual harvester is included.

Hybrid harvester operation on water velocities beyond 3.0 m/sec, storing energy in an external battery, maintenance guides, and energy output from the hybrid harvester from other pipe sizes than specified is not included.

Organization of Chapters and Flow Chart

This research work is organized in a sequenced manner. Chapter 1 provides a brief introduction about electromagnetic and piezoelectric power, also the motivation of the researcher, followed by aim and objectives. Chapter 2 provides a focused literature review and research gap. Chapter 3 gives the details about the preliminary study and the actual 3D simulation study. Similarly, Chapter 4 is organized in the same structure as the methodology, where preliminary study and 3D simulation results were presented

and discussed separately. The conclusion is the final chapter, where a summary is presented along with future recommendations.

The methodology flow chart (Figure 2) starts by specifying the piezoelectric dimensions and materials followed by the performance of the parametric study. Next is to obtain the magnet velocity governing equation and finding the electromagnetic voltage.

So far, piezoelectric voltage and electromagnetic voltage are acquired by preliminary study. The new method to obtain the same voltage is by performing a 3D simulation analysis. Before that, at least one water velocity must be the bridge between preliminary and 3D simulation analysis that is 1.36 m/sec. one more water velocity was obtained and carried on by iteration, which is 1.39 m/sec. Finally, piezoelectric, and electromagnetic voltage were obtained and compared to the preliminary study results.

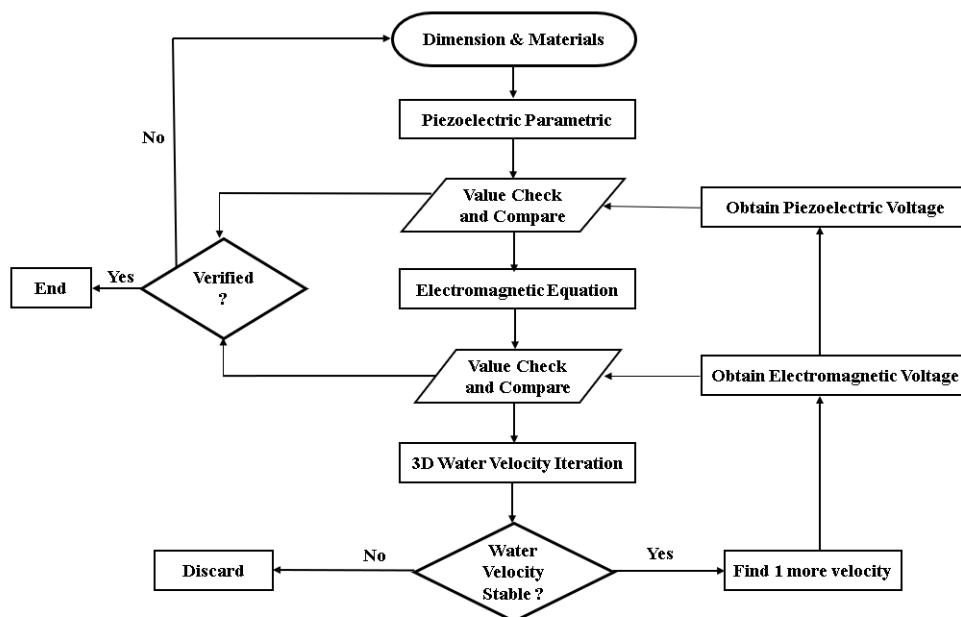


Figure 2. Main flow chart of the research work

CHAPTER 2: LITERATURE REVIEW

The main literature that part of it is used in this research work is piezoelectric harvesting from underwater [5]. The study is to obtain the piezoelectric voltage based on a hydromechanical mathematical model that is originally a patent [4]. Energy harvesting was based on kinetic energy from four water velocities at 22 °C where Reynolds number was obtained for each water velocity based on the cylinder diameter. The harvester is essentially the piezoelectric beam linked to a cylinder submerged in water. The lift coefficient for the four water velocities was a major requirement for the model; a 2D simulation was performed to obtain the maximum lift coefficient without performing a 3D simulation for the same. The difference is that in 2D simulation, the software analyzer engine assumes the cylinder as a beam extended from the pipe wall (see Figure 3) to the bottom of the pipe, where all fluid vectors will spin around the cylinder. In the 3D simulation, the cylinder will be as an actual size suspended in the middle of the flow having the water flow surrounding sides, top, and bottom of the cylinder, which will result in actual cylinder oscillation.

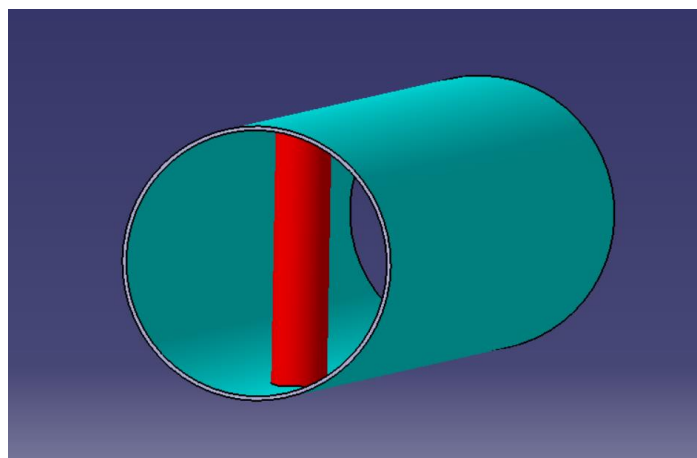


Figure 3. 2D simulation on a cylinder

Using the mathematical model, the mean power for four water velocities was obtained using MATLAB software. For water velocities between 0.34 m/sec to 1.36 m/sec the mean power ranges from 3.95 μ W to 996.25 μ W.

Another study uses a governing equation based on Euler-Bernoulli beam theory and a piezoelectric from Macro Fiber Composite (MFC) where the piezoelectric beam is placed parallel to the water flow downstream of a cylinder. The piezoelectric beam produces voltage by flutter motion from the vortex shedding generated by the cylinder, as shown in Figure 4.

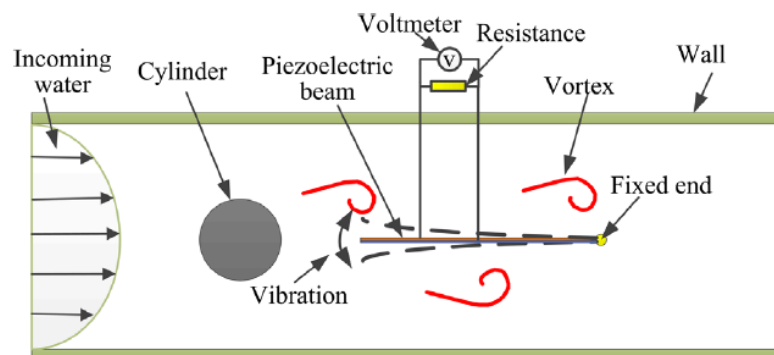


Figure 4. Piezoelectric harvester schematic [23]

The water velocities used is ranging from 0.05 to 0.5 m/sec, and the maximum power generated was at 0.5 m/sec water velocity. The mathematical model results agreed with the experimental laboratory work for all cylinder sizes ranging from 0.03m to 0.05m. Finally, the mathematical model and the experimental work did not present the maximum generated power against time, or the maximum power will remain for how long? Or is it stable?

A recent coupled hybrid model consists of piezoelectric and electromagnetic induction was introduced in 2017. The model converts the kinetic energy of water into electrical energy by experiment. This work aims to prove that a coupled harvester will maximize the output power compared to a single electromagnetic or piezoelectric harvester that is validated throughout the conclusion.

The physical model is basically a PZT (Piezoelectric Transducer) attached to a copper cantilever beam and a cylinder submerged in water. The cylinder is attached to a spring, and a specific type of permanent magnet is hanged in the middle of a coil loop, as shown in Figure 5.

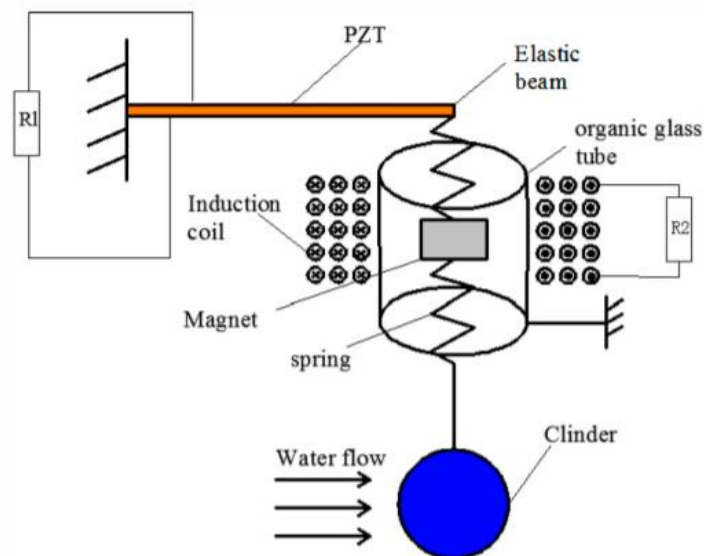


Figure 5. Schematic of the experimental setup [24]

The experiment methodology begins when water is pumped from the water tank into a pipe where the hybrid harvester is fixed. External resistance is connected to the system for adjustment and calibration. With a variety of resistance, the piezoelectric part is plotted, resulting in a maximum power of 1.99 mW, while the same plot is arranged for

the electromagnetic part having a maximum power of 14.56 mW. The total coupled power is 16.55 mW. However, the steady power region is not considered.

Another hybrid harvester model is presented using airfoil energy. The model structure is basically a wound coil, a permanent magnet, and a piezoelectric patch. Airfoil and a cantilever beam are fixed to a frame on the upper cantilever are maintaining the permanent magnet. That PM, by its role, adjusted close to the coil. See Figure 6.

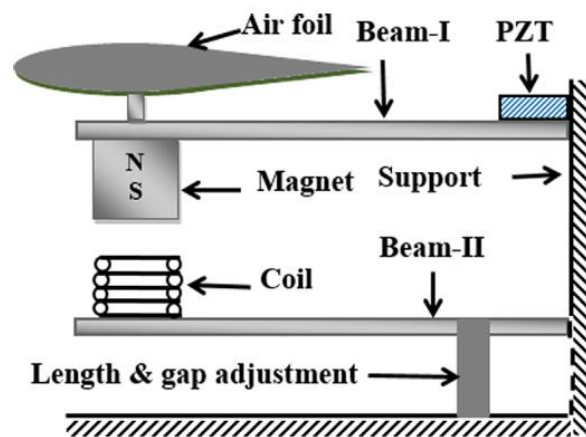


Figure 6. Schematic of the experimental setup [25]

The coupled harvester with air at room temperature, converting wind energy into electrical energy by experiment operating at three different low frequencies. At a certain base excitation, the harvester produces a maximum voltage of 25mV from the electromagnetic part and 114mV from piezoelectric when calibration is adjusted to the optimum conditions. The work uses air as the main fluid, and the hybrid harvester is varying the output voltage by frequency, load resistance, and by varying wind speed. Fixing the airspeed and monitoring the steady output voltage as a function of time is not considered.

In a similar previous work, a design of electromagnetic induction based on Faraday's law is presented. The proposed harvester converts airflow in the pipeline to useful electrical energy. The harvester assembly shown in Figure 7 consists of a stationary magnet and a moving coil that is fixed to a flexible membrane that is vibrating due to the airflow to produce electrical voltage. The maximum power produced is $18600 \mu\text{W}$ at optimum resistance of 4.3 ohm and optimum pressure of 625 pa .

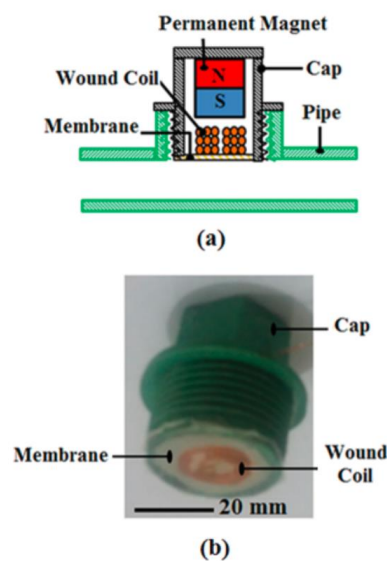


Figure 7. Electrmagnetic harvester (b) and section view (a) [28].

This work aims to obtain the maximum voltage while variating the pressure level of the flow between 0 to 625 Pa with a corresponding flow velocity of 0 to 18 m/sec . The flexible membrane is attached to the pipe wall and vibrating with respect to the fluid (air) pulsating pressure. The pressure is changing by manipulating the motor speed (rotating disc) placed downstream of an air blower. Finally, a comparison table was placed at the end of the research work to compare the maximum voltage produced in this work to other previous works.

The main literature used in this work [5] uses a 2D simulation only. Lift and transverse forces will be identical on the bottom and sides of the cylinder, while the actual harvester size is not simulated against the flow. Additionally, the initial water momentum causing instability motion of the harvester is not presented as the actual 3D simulation is not performed; thus, the steady output power cannot be obtained. The second research work that is based on Euler-Bernoulli beam theory [23] piezoelectric harvester PEH is placed downstream of a cylinder parallel to water flow. By varying water velocity, cylinder diameter, and resistance, the optimum voltage is reached. Here, the aim is to get the maximum voltage. However, the steady output voltage was not obtained based on the water forces. The third research work was a hybrid piezoelectric-electric harvester with a similar design to this research thesis. The aim is to get the maximum voltage by changing resistance. Again, the steady voltage to power any sensor for a long period is not specified.

This thesis will contribute to previous works by filling the unrevealed gap by presenting the actual output voltage as a function of time at a steady region using actual 3D simulation on a hybrid harvester. Initially, water momentum will cause unsteady oscillation motion of the harvester where maximum voltage might be reached instantaneously and drop back eventually. By performing actual 3D simulation on a cylinder and by selecting a steady region, all instantaneous voltage will be very close together, assuring continuous stable energy over time.

CHAPTER 3: METHODOLOGY

Preliminary Study

Section1: Basic Setup

By studying the beginning of the literature, the first step is to calculate the pipe diameter where the harvester will be mounted. The literature [5] does not specify the exact pipe diameter; it only provides a range from 0.0508m to 0.1270m, which is not accurate and did not specify that this is pipe OD or ID. Therefore, a black color UPVC pipe was selected locally in Qatar, manufactured by Hepworth Qatar [1] that is UPVC 250mm class 4 with a thickness of 4.9mm and ID of 240.2mm.

UPVC was selected as it is the only product with minimum wall thickness than HDPE or Ductile Iron which is an advantage for ID size. Below are sample calculations for pipe dimensions given that:

(ID=internal Diameter, OD=Outer Diameter, thk=thickness)

$$OD = 250mm$$

$$ID = 240.2 mm$$

$$ID = OD - (2thk)$$

$$240.2 = 250 - (2(thk))$$

$$thk = \frac{-250 + 240.2}{-2}$$

$$thk = 4.9mm$$

Another measurement to be calculated is the cylinder free space inside the pipe; this can be found by:

$$Movement_H = 0.2402m - 0.04m$$

$$Movement_H = 0.2002m$$

Where $Movement_H$ is horizontal free movement space of the cylinder.

The piezoelectric beam will have a length of 70mm or 0.07m, and the cylinder height is 80mm or 0.08m with 40mm or 0.04m diameter, refer to Figure 8.

Similarly, to find out the vertical Movement_v space is by:

$$\text{Movement}_v = 0.2402m - 0.15m$$

$$\text{Movement}_v = 0.0902m$$

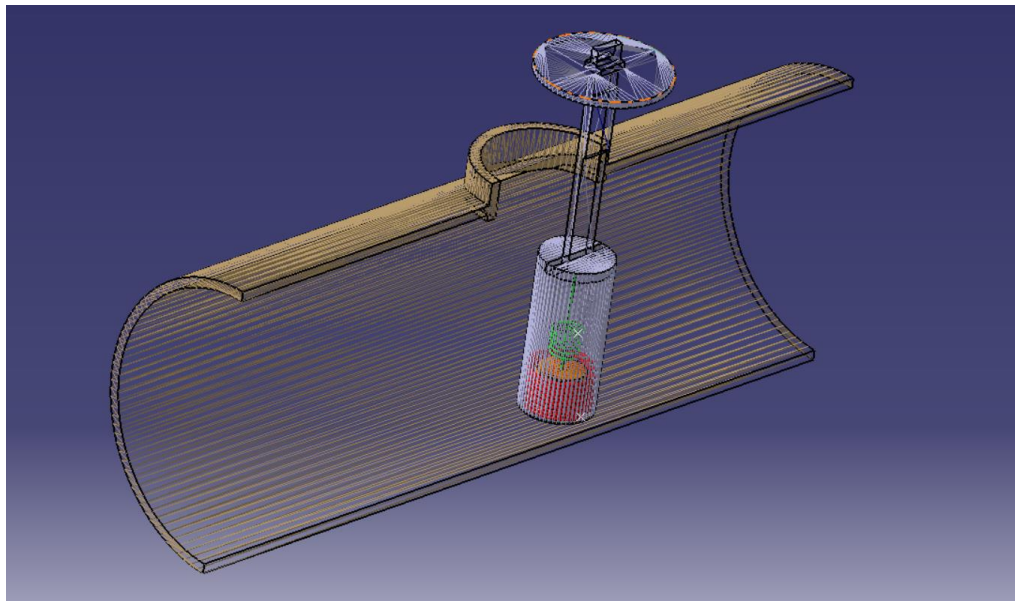


Figure 8. Piezoelectric beam with cylinder body (Not to scale).

As a result, below parameters will be carried out throughout the thesis as per Table 1.

Table 1. Summary of basic setup measurements.

Dimensions	Size/Material	Unit
Pipe materials	UPVC	-
OD	0.250	m
ID	0.2402	m
Thickness	0.0049	m
Piezoelectric beam length	0.07	m
Cylinder height	0.08	m
Cylinder diameter	0.04	m

Section 2: The Four Reynolds Number

Reynolds number is an important value that describes the relationship between fluid velocity and density with the characteristic length of a cylinder. Reynolds number value estimates the behavior of fluid inside a confined space, usually a pipe. The behavior of fluid is either laminar or completely turbulent, based on API 13D guides. When the number is equal to or less than 2100, it means that it is a laminar flow. In contrast, when the number is above 2100, the fluid is completely turbulent [2].

$$Re = \frac{V_{water} D \rho}{\mu} \dots\dots\dots(1)$$

Where V_{water} is the water velocity, D is the diameter of the cylinder, ρ is the density of fluid at a given temperature, and μ is the fluid's dynamic viscosity. Basically, all further calculations will be based on the temperature of 25 °C.

For the preliminary study, four water velocities will be demonstrated in line with the literature [5]. The four velocities along with cylinder characteristic length will result in four Reynolds number as follows:

Table 2. Four Reynolds number of the preliminary study

Water Velocity	Formula	Result	Unit
0.34 m/sec	$Re = \frac{0.34 * 0.04 * 997}{8.91e^{-4}}$	15,000	-
0.68 m/sec	$Re = \frac{0.68 * 0.04 * 997}{8.91e^{-4}}$	30,000	-
1.02 m/sec	$Re = \frac{1.02 * 0.04 * 997}{8.91e^{-4}}$	45,000	-
1.36 m/sec	$Re = \frac{1.36 * 0.04 * 997}{8.91e^{-4}}$	60,000	-

Where water density at 25 °C is 997 kg/m³ and dynamic viscosity of water at the same

temperature is $8.91e^{-4} \frac{NS}{m^2}$ [3].

Section 3: Piezoelectric Power Formula

The piezoelectric harvester model in terms of power output was based on the previous power formula proposed by Francesco Cotton [5]. There are many variables used in the model. However, the water velocity (V_{water}) and lift coefficient CL are the main variables. The beginning of the model is as follows:

$$L_1 \rho_{piezo} A \frac{d^2 r_1}{dt^2} = -ku_1 - \alpha V_1 + F_m \dots\dots\dots(2)$$

Where $L_1 \rho_{piezo} A$ represent the mass of the piezo beam, $-ku_1$ stiffness of the piezo beam, and αV_1 is the oscillation dampening. Hydro-mechanical model and piezoelectric power control model were introduced in the above model, and the derivations continue until finally obtaining the mean power formula:

$$P_{mean} = \left(\frac{\alpha a}{k_{Trans}}\right)^2 \frac{1}{2k_P} \left(\frac{a_1 w_0 C_{Lmax}}{\sqrt{(a_4 - a_2 w_0^2)^2 + (a_3 w_0)^2}}\right)^2 \dots\dots\dots(3)$$

Given:

$$a_1 = \frac{\rho_{water} D V_{water}^2 H_a (2L - H_a)}{4} \dots\dots\dots(4)$$

$$a_2 = (J_{wt} + L_1 \rho_{piezo} A a^2) \dots\dots\dots(5)$$

$$a_3 = \left(f + \frac{\alpha^2 a^2}{K_p K_{trans}} \right) \dots\dots\dots(6)$$

$$a_4 = \left(K_{spring} + \frac{ka^2}{K_{trans}} \right) \dots\dots\dots(7)$$

Model parameters are fixed values to calculate the piezoelectric power varies with water speed; as shown in Table 3, nine parameters were referenced, and six parameters were calculated/investigated.

Table 3. Model parameters

Name	Definition	Value	Unit	Reference	Note
ρ_{water}	Water density	997	kg/m ³	-	-
A	Section of piezoelectric	0.01	m ²	[5]	-
k	Piezoelectric stiffness	123	N/m	[5]	-
K_{trans}	Transduction gain	2	-	[5]	-
f_c	Frictional coefficient	0.01	(N.m.s)/rad	[5]	-
L_l	Length of layer	0.0035	m	[5]	-
a	Force application distance	0.01	m	[5]	-
α	Voltage induced bending factor	100	A.s/m	[5]	-
$\rho_{Cylinder}$	Cylinder density	920	kg/m ³	[5]	Section 4
ρ_{Piezo}	Piezoelectric material density	1780	kg/m ³	-	Section 4
I_z	Cylinder moment of inertia	4.021 e^{-5}	kg*m ²	-	Section 4
C	Piezoelectric capacitance	1.4	nF	-	Section 4
L	Radius of gyration	0.18	m	-	Section 4

Name	Definition	Value	Unit	Reference	Note
H_a	Cylinder height	0.08	m	-	-
w_0	Angular pulsation	5876	rad/sec	-	-
K_{spring}	Spring constant	constant for V_{water}	N/m	[5]	changes for 4 V_{water} only

Similarly, model variables are shown in Table 4. These variables are to be calculated four times at every water speed. For r_1 (piezoelectric beam tip deflection), L (radius of gyration), and (force application distance) refer to Figure 9.

Table 4. Model variables

Name	Definition	Unit	Note
CL_{max}	Maximum lift coefficient	-	To be calculated four times in section 5
t	Time	sec	-
V_{water}	Velocity of water	m/sec	as previously presented (0.34, 0.68, 1.02 and 1.36 m/sec)
K_p	Proportional gain	-	To be calculated four times
r_1	Piezoelectric beam tip deflection	-	Refer to equation 2

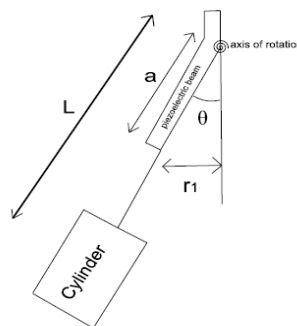


Figure 9. Sketch of the harvester device (not to scale) [5].

Section 4: Finding Model Parameters and Variables

Previously in section 3, the model used to find the piezoelectric power (equation 3) uses specific dimensions and parameters according to the cylinder size and piezoelectric body. However, in this research work, the harvester cylinder size and piezoelectric beam/materials were enlarged as the cylinder interior will host an electromagnetic induction mechanism, as shown in Figure 10. The green spiral body is a spring controlling the radial motion of the magnet, the orange cylinder is the moving magnet, and the red helical body is a copper coil.

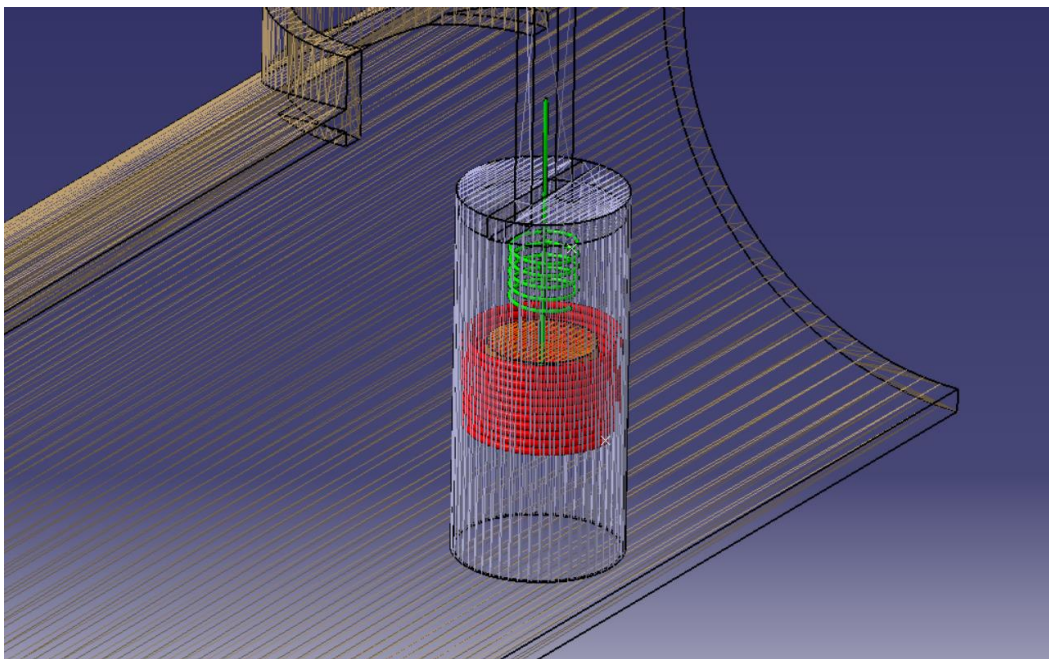


Figure 10. Electromagnetic mechanism inside the cylinder (not to scale)

As the cylinder and the piezoelectric beam dimensions differ, the parameters and variables must be changed accordingly.

Polypropylene Cylinder

The cylinder is submerged in water at all times, so it must be water-resistant; also, it must be made from low-density materials. It was found that plastic materials are most appropriate for the cylinder. Plastic is either thermoplastic or thermoset. Thermosets mainly soft materials when heated, it will harden, and a cross-linking microstructure is maintained. This microstructure prevents chain slipping; additional heat will degrade the material rather than liquefying it, that's why thermoset cannot be recycled [6]. On the other hand, thermoplastics are pellets that continuously soften when exposed to heat and getting harder when cooled. The majority of thermoplastics are soluble using certain solvents and can burn. The molten temperatures differ based on polymer structure. Thermoplastics are sensitive to heat due to the hydrocarbon chains that they are made of; degradation is highly possible when exposed to a source of heat for enough period. Several materials such as polyethylene and polyvinyl chloride are typical examples of them.

Polypropylene was selected as a cylinder material because of its excellent properties of fluid and chemical resistance, beside it is one of the lowest densities (920 kg/m^3). In addition, polypropylene is high-temperature resistance, and it is most favorable for manufacturing injection molded bottles and funnels [7].

Piezoelectric Material

Piezoelectric body is one of the main components in the harvester assembly. It can be made from various smart materials and classified as green energy and future replacement of fossil fuel. Piezoelectric effect can be direct or converse, as shown in Figure 11.

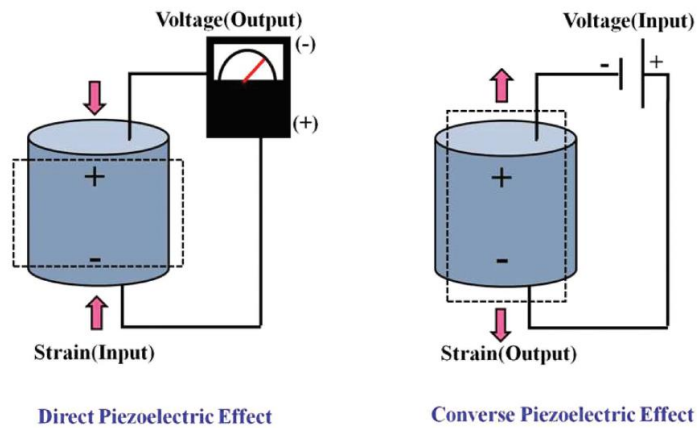


Figure 11. Direct and Converse Piezoelectric effect [8]

The direct effect is applying an external force to the piezoelectric body; this method is used in the proposed harvester model, while the converse effect is associated with actuators. The four main categories of piezoelectric materials are ceramics (i.e Lead-Zirconate-Titanate), polymers (i.e PVDF), single crystals (i.e Lithium Niobate), and polymer composites (Polyamides-PZT) [8].

Lead-Zirconate-Titanate (PZT) is a metallic oxide-based ceramic having greater flexibility than its predecessor i.e, Barium Titanate [9]. PZT can withstand high applied pressure comparing to polymer type, but the latter is lighter and better behaviors in mechanical flexibility. See Table 5.

Table 5. PZT versus Polymer PVDF properties [8].

Properties/parameters	Piezo-ceramics (PZT)	Piezo-polymers (PVDF)
Piezoelectricity	High	Low
Acoustic impedance ($10^6 \text{ kg m}^{-2} \text{ s}^{-1}$) ^{a)}	High (30) ^[34]	Low (2.7) ^[34]
Density (10^3 kg m^{-3})	7.5 ^[34]	1.78 ^[34]
Relative permittivity (ϵ/ϵ_0)	1200 ^[34]	12 ^[34]
Piezo-strain constant ($10^{-12} \text{ C N}^{-1}$)	$d_{31} = 110$, ^[34] $d_{33} = 225\text{--}590$ ^[35]	$d_{31} = 23$, ^[34] $d_{33} = -33$ ^[34]
Piezo-stress constant ($10^{-3} \text{ V m N}^{-1}$) ^{a)}	$g_{31} = 10$, ^[34] $g_{33} = 26$ ^[36]	$g_{31} = 216$, ^[34] $g_{33} = -330$ ^[34]
Electromechanical coupling factor (% at 1 KHz)	$k_{31} = 30$ ^[34]	$k_{31} = 12$ ^[34]
Dielectric constant	1180 ^[37]	10–15 ^[37]
Mechanical flexibility ^{a)}	Poor	Outstanding
Curie temperature ($^{\circ}\text{C}$)	386 ^[37]	80 ^[37]

Due to the above-mentioned properties (mainly PZT density 7500 kg/m^3) and because water forces are low due to the water velocity selected, polymer PVDF (density 1780 kg/m^3 type was chosen).

Piezoelectric Capacitance

In focus on piezoelectric PVDF polymer type, a specific commercial product was found by the researcher that is piezo d_{33} Model: M2814-P1 (elongator type) having a capacitance value of 1.4 nF at room temperature [9]. See Figure 12.

Model	active length in mm	active width in mm	overall length in mm	overall width in mm	Capacitance in nF $\pm 20\%$	free strain in ppm $\pm 10\%$	blocking force in N $\pm 10\%$
M2503-P1	25	3	46	10	0.34	788	21
M2807-P1	28	7	38	13	0.93	1035	62
M2814-P1	28	14	38	20	1.40	1160	146

Figure 12. Model: M2814-P1 with capacitance 1.4 nF [9]

Cylinder Moment of Inertia

The cylinder of the harvester is made from polypropylene with a density of 920 kg/m³. The cylinder moment of inertia value is essential for power formula equation (2). As per this research design, the cylinder height is 0.08 m, and the cylinder diameter is 0.04m. Thus, it must be calculated. The moment of inertia in angular motion is analogous to mass in translational motion. Specifically, when the cylinder in angular motion, its concentrated mass is away from the center of rotation. Moreover, the moment of inertia relay on the location of the center of rotation [11].

The required moment of inertia here is about the z-axis with respect to 3D drawing in CATIA V5. The main formula derived from integral calculus is equation 8.

$$I_z = 0.5 MR^2 \dots\dots\dots(8)$$

Where M is the mass of the cylinder and R is the radius of the cylinder. The specific mass of the cylinder body is 0.101 kg, so CATIA v5 was used to find the value of I_z . Firstly, the geometry was prepared by the researcher as per Figure 13.

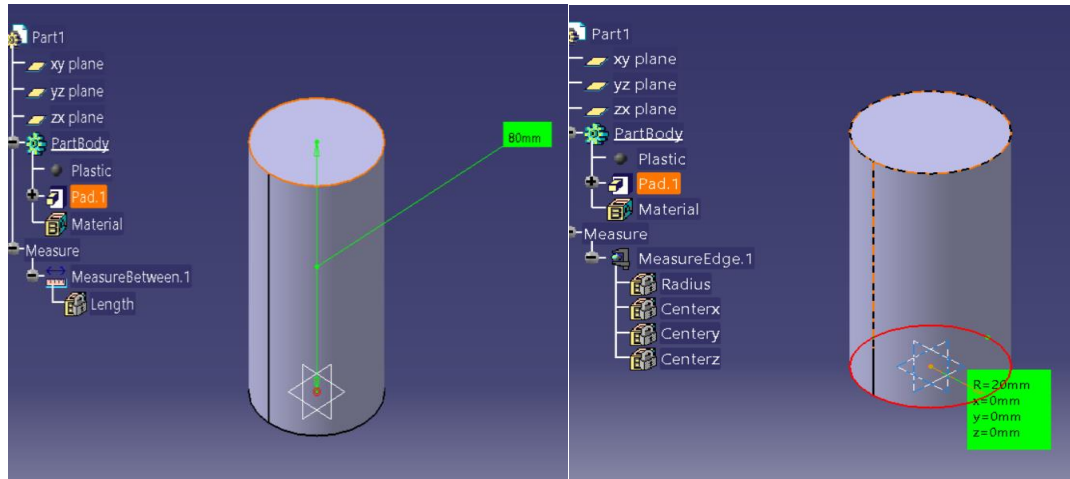


Figure 13. CATIA V5 Geometry preparation and applying material

The material applied is polypropylene. CATIA V5 has its own database; as soon as the material is applied, the density, color, and other physical and mechanical properties will be applied.

The simulation software will calculate the body's mass based on the given geometry and the material assigned.

Next, by highlighting the cylinder body and by choosing the properties option, an informative window will display. The moment of inertia about three axes were given, while the axis of interest is the z-axis, as shown in Figure 14.

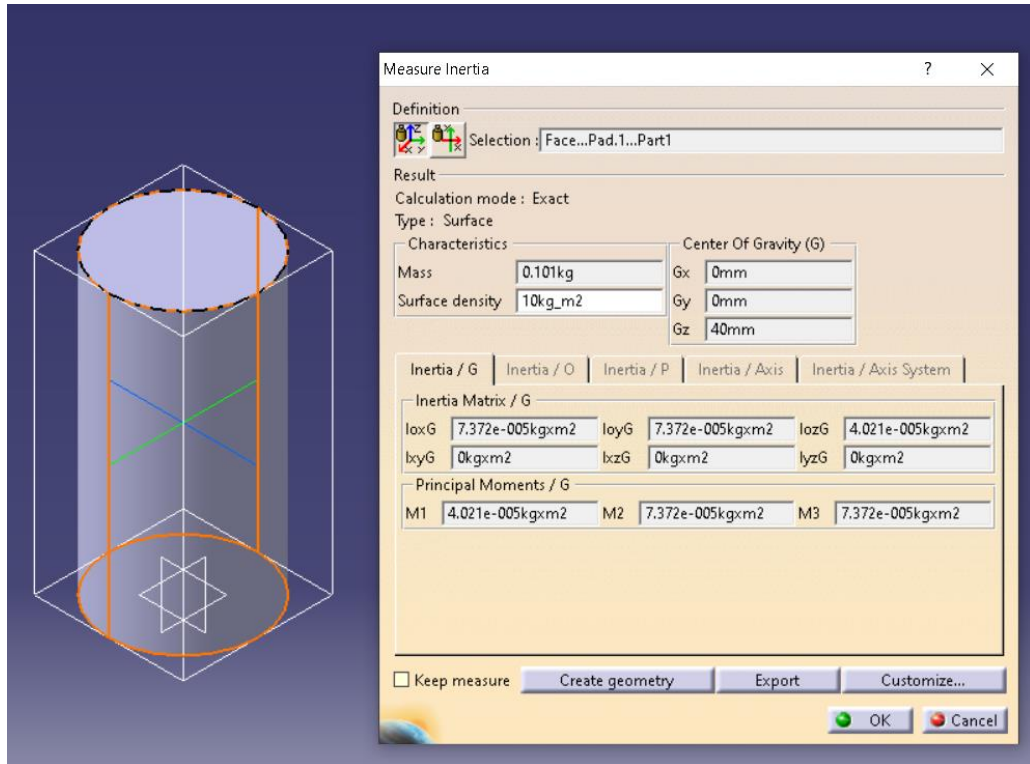


Figure 14. CATIA V5 informative properties of the cylinder

Finally, the moment of inertia about the z-axis is $iozG$ is $4.02e^{-5} \text{ kg.m}^2$.

Cylinder Radius of Gyration

As a definition, the radius of gyration of a cylindrical body is an invisible distance from the body centroid at which the area of cross-section is imagined to be focused on a point in order to obtain the same moment of inertia; it is denoted by L [12]. Finding radius of gyration is simply using equation (9)

$$L = \sqrt{\frac{I_z}{m}} \dots\dots\dots(9)$$

Where I_z is the moment of inertia about the axis of interest, m is the mass cylindrical body. Plugging in the values and evaluating the formula will result in $L=0.020$ m.

Section 5: 2-D CFD Setup of Preliminary Study

The aim of this section is to find the maximum lift coefficient of the cylinder body in the UPVC pipe. Lift coefficient C_L depends on the water velocity V_{water} , lift force F_L which is the perpendicular force to the input stream, cylinder diameter D , ρ density of water at a given temperature, and (U_∞) freestream velocity [5].

$$C_L = \frac{F_L}{0.5\rho_{water}U_\infty^2 D} \dots\dots\dots(10)$$

The lift coefficient is calculated against flow time in fluid transient motion assuming steady flow. C_L is unitless, and it expresses the ratio between the perpendicular force and the pipe contents. Basically, C_L value is gradually increasing over time until stabilizing, indicating the maximum lift coefficient. The turbulent model used in this research work $K\omega-SST$ which is validated by Mentor [13]. Similarly, drag coefficient is another aerodynamic factor that can be calculated along with the CFD analysis.

$$C_D = \frac{F_D}{0.5\rho_{water}U_\infty^2 D} \dots\dots\dots(11)$$

Where F_D is the dragging force in parallel with the stream, cylinder diameter D , ρ density of water at a given temperature, and (U_∞) freestream velocity [5].

Finally, the Strouhal number is a commonly presented value to describe the oscillation flow in aerodynamic.

$$St = \frac{f_s \cdot D}{U_\infty} \dots\dots\dots(12)$$

Where f_s is basically the frequency of the vortex shedding behind the cylinder, D is the

diameter of the targeted cylinder, U_∞ is the free water stream velocity [5].

The final value of C_L , C_D , and ST using Computational Fluid Dynamic absolutely depends on the 2-D control volume setup, pressure or density-based Navier-Stoke equation, and the mesh size with its number of elements. The control volume was prepared and validated by the researcher as per MD Rahman [14].

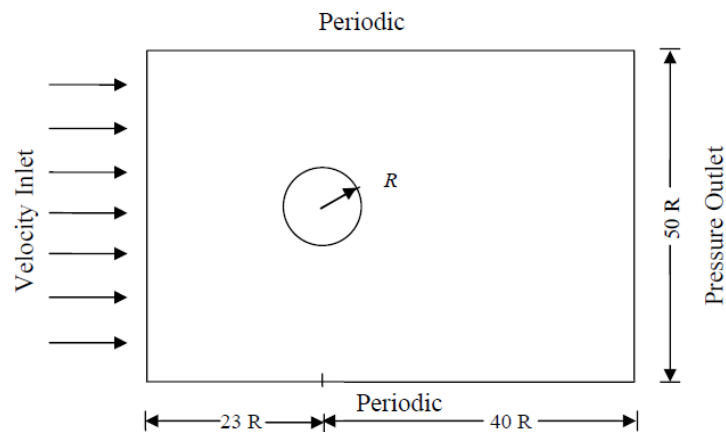


Figure 15. Schematic of control volume preparation [14].

The researcher maintained the control volume preparation in Figure 15. However, the internal diameter of the pipe was kept to 240.2mm as actual pipe diameter and not $50R$, as changing the internal diameter of the actual UPVC pipe will critically change the accuracy of the results for every corresponding water velocity 0.34 m/sec, 0.68 m/sec, 1.02 m/sec, and 1.36 m/sec. On the other hand, other parameters such as $23R$ upstream of the cylinder and $40R$ downstream the cylinder were used refer to Figure 16. The UPVC internal pipe wall was selected as a free slip condition wall as it was validated, where the slip wall allows the solver to compute the water velocity vector parallel to the wall [15].

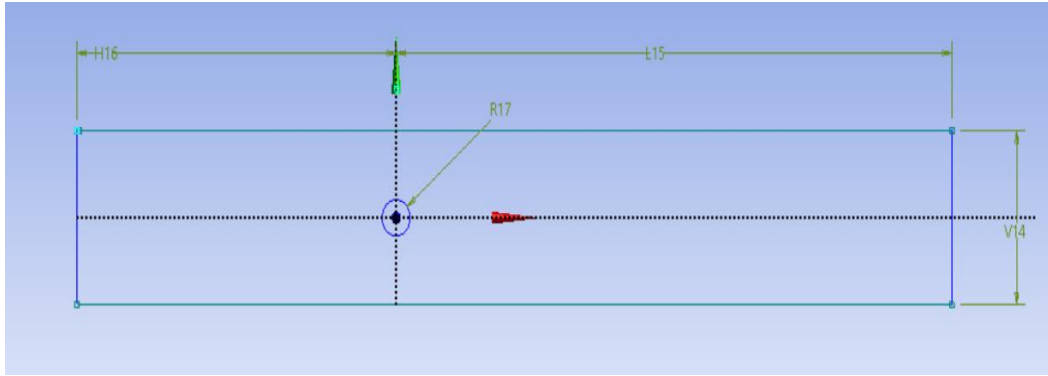


Figure 16. 2-D control volume setup by ANSYS

The left boundary is the water inlet, the opposing boundary is the pressure outlet set to zero. Body thickness is 0m, H16 is 0.46m, L15 is 0.8mm, V14 is 0.2402 m, and R17 is the cylinder radius of 0.02m.

Meshing is an essential factor for accurate solver results in ANSYS fluent. After control volume establishment and boundary condition preparations, ANSYS will generate a basic mesh that is editable. At least two methods of mesh sizing must be specified and compared.

As a result, fine and medium mesh were conducted and compared after enhancing the current auto-generated mesh as per Figure 17.

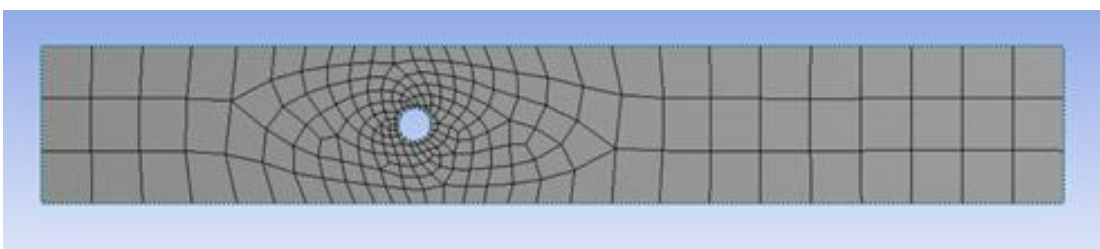


Figure 17. 2-D Auto-generated global mesh

Fluent is applying global meshing in order to discretize the domain and analyze it numerically by an implicit first or second-order method. Next, the global mesh was

changed to a triangular method rather than rectangular. Critical analysis will be concentrated around the cylinder where the un-meshed hole is located, the solver will assume the unmeshed area as a solid wall, and all the water velocity will flow around it. As this is a 2D control volume, the solver will assume that this is an infinite cylinder column extended from the pipe ceiling to the bottom of the pipe.

The global mesh size is 4mm for fine mesh and 6mm for medium mesh. The mesh here was enhanced. However, the mesh around the cylinder must be further reduced by edge sizing, where the selected edge is the cylinder boundaries. For fine mesh, the edge size is 0.75mm and for medium mesh is 1.25mm.

After implementing the edge sizing of the cylinder, one final step must be applied that is inflation. Inflation is the re-organization of the mesh nodes by layers for enhanced solver results as the solver is calculating results from neighboring nodes to the next. See Figure 18 for mesh before the inflation implementation.

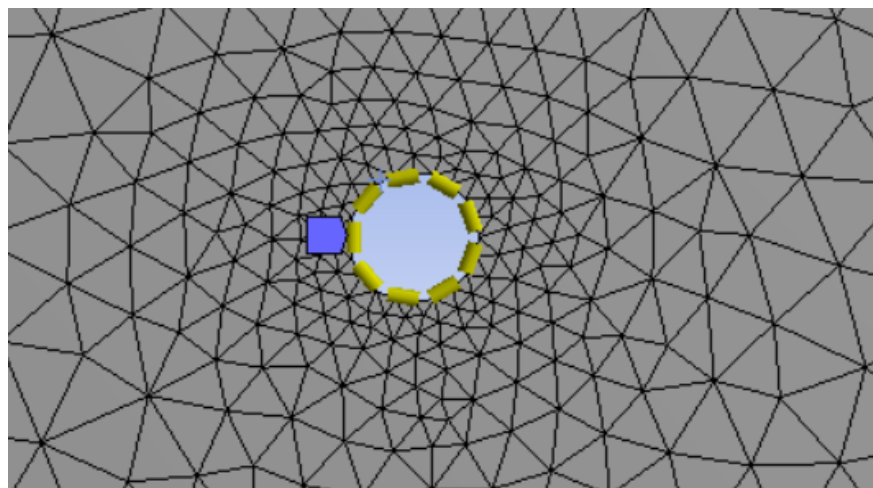


Figure 18. Edge size around the cylinder

Inflation by first layer thickness was applied to the cylinder edge with 1mm layer

thickness for fine and 1.5mm layer for medium mesh. Moreover, maximum layers of 30 and 20 were applied to the fine and medium mesh, respectively. The inflation option was validated with Stringer [15], where the result is shown in Figure 19.

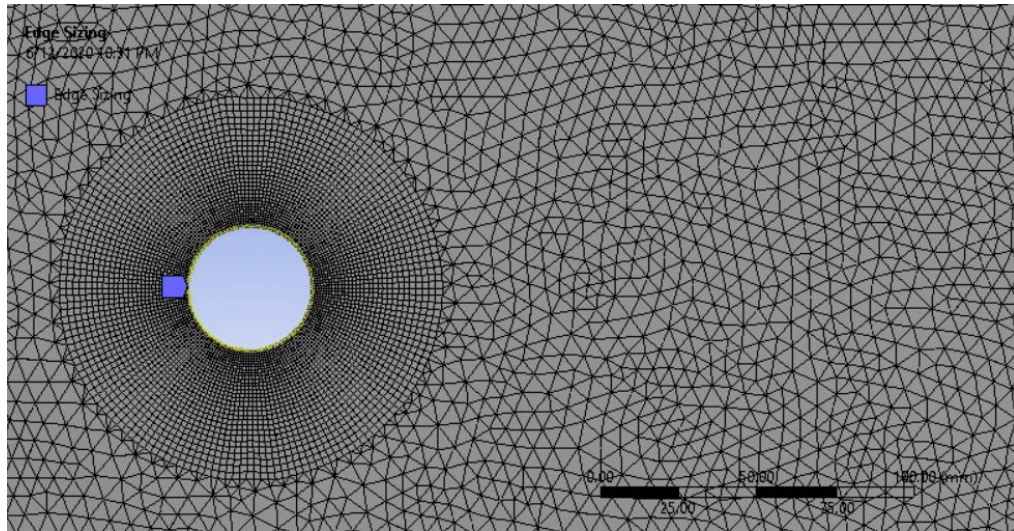


Figure 19. A 30-layer inflation and edge sizing for fine mesh

The relevance center is medium, and smoothing is medium for the medium prototype, while the fine option was selected for the fine mesh.

For the solver, the viscous model $K\omega-SST$ two-equation was selected along with the transient model so the solver can calculate the lift and drag coefficient against time. For the fluid type inside the boundary condition, by default, it is room temperature of air.

This option must be changed as per Figure 20 to water liquid with a density of 997 kg/m^3 at 25°C and a dynamic viscosity of $8.91e^{-4} \frac{\text{NS}}{\text{m}^2}$ as previously estimated in section 2.

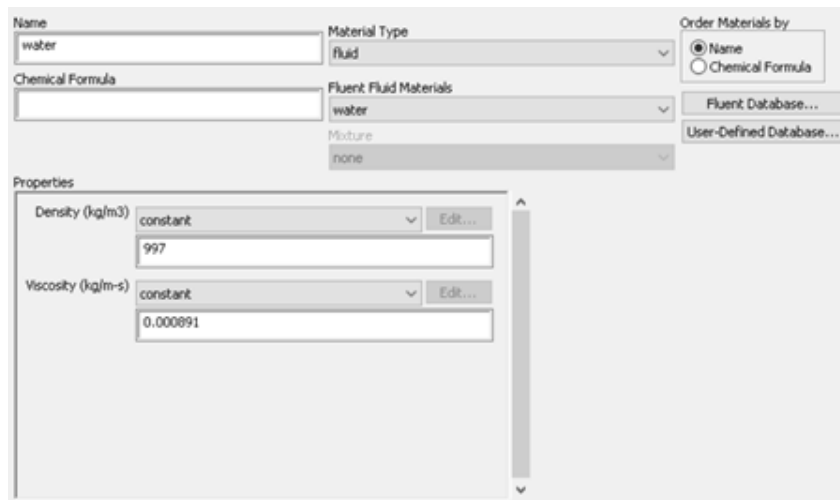


Figure 20. Materials properties of the fluid in the domain

The Initialization method used is realized along with second order implicit numerical solving method. Furthermore, the solution initialization is hybrid. Before running the simulation, a lift and drag monitor must be created, where the lift coefficient axis monitor is y-axis (normal to stream) and drag coefficient in the z-axis (parallel to stream). See Figure 21.

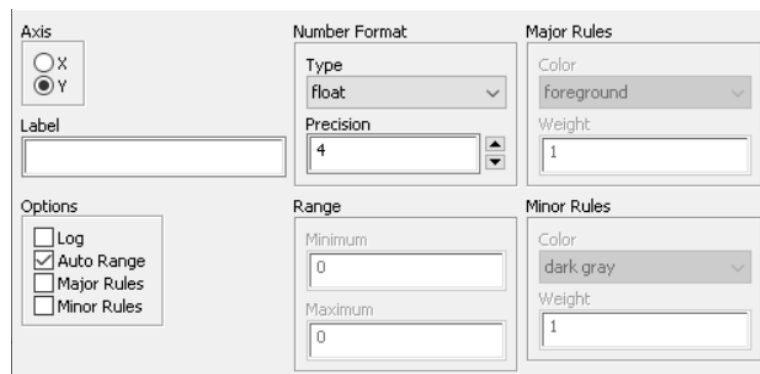


Figure 21. Lift and drag monitor specifying axis of interest

As a final step Strouhal number is calculated using a different method for fine mesh only; just after running the simulation for lift and drag monitors, the following steps were used.

The report file must be saved to the local drive for each velocity of water V_{water} .

- i. Once the calculation is done for C_L , go to Plots, then FFT
- ii. Select Y-Axis Function to the magnitude
- iii. Select X-axis function to Strouhal Number
- iv. Click load input file
- v. Select the saved file which is lift Strouhal number i.e 123.out (See Figure 22)

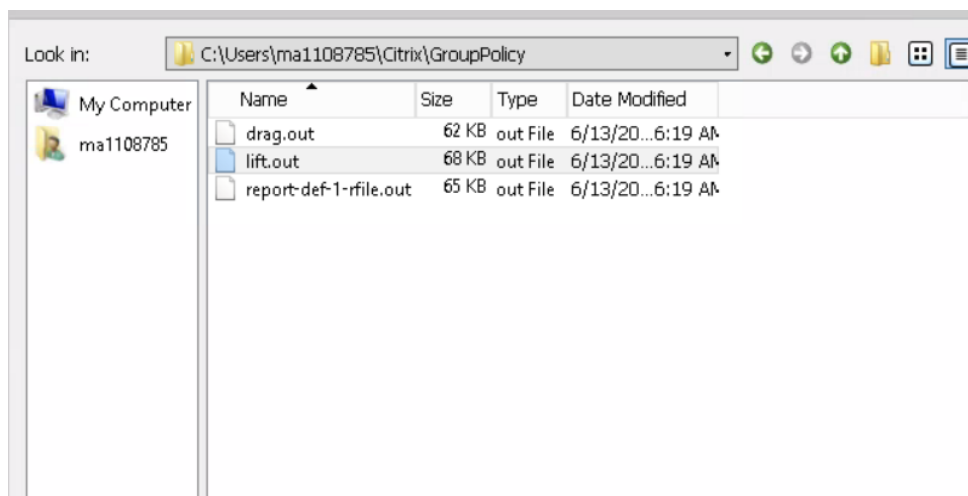


Figure 22. Lift.out file to estimate Strouhal number

- vi. Click Plot FFT
- vii. Click write FFT and save it in local C:\\
- viii. Open MS excel sheet
- ix. Import the saved file above in Excel, and two-column data will show
- x. Use the command Max and select the first column data
- xi. The Strouhal number maximum number will show; repeat this step for every V_{water} .

Strouhal number value was not used in physical calculations; it is obtained for comparison with previous published work as shown in Results and Discussions. Table 6. demonstrates the summary of the options used for fine and medium mesh.

Table 6. Summary for fine and mesh simulation setup

Definition	Fine Mesh	Medium Mesh	Unit
Calculations step time	0.003	0.003	Sec
Total time	15	15	Sec
Preview			-
Number of elements	19,000	9,377	Nodes
Inflation	Yes Layer: 30 First layer: 1mm Growth Rate: 2.5	Yes Layer: 20 First Layer: 2mm Growth Rate: 2.0	-
Edge sizing	Yes Size: 0.75mm	Yes Size: 1.25mm	-
Global sizing	Min:4mm Max: 6mm Smoothing: High Relevance center: Fine, Growth Rate: 2.5	Min:5 Max: 8mm Smoothing: Medium Relevance center: Medium, Growth Rate: 2.0	-
Triangle method	Yes	Yes	-
Numerical method	Second-order implicit	Second-order implicit	-
Initialization	Hybrid	Hybrid	-

The solution for C_L , C_D , and Strouhal number were completed; please refer to Chapter 4 (Results and Discussions).

Section 6: Development of MATLAB Code for Piezoelectric Power

After obtaining the variables and parameters from sections 4 and 5, MATLAB code must be developed to obtain the piezoelectric power. It is expected that the piezoelectric power will change due to the variations of cylinder diameter, height, piezoelectric density, and capacitance. The literature is using a cylinder with 0.01 m, while the current research is using 0.04m. According to the power formula by Francesco Cotton [5], the power is plotted against K_p (proportional gain) ranging from 0 to 10 A/V.

After analyzing, the literature MATLAB code, See Figure 23 also refer to Appendix “A” literature sample MATLAB code. The variables and parameters were changed accordingly to new values found in sections 4 and 5.

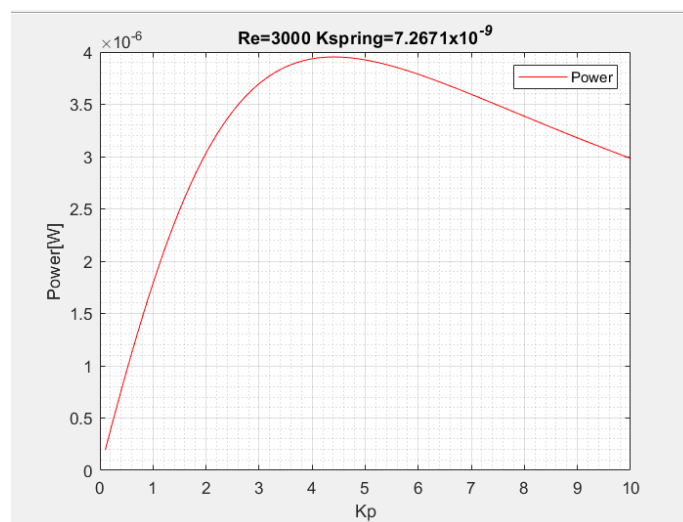


Figure 23. Literature MATLAB results for $V_{\text{water}} 0.34 \text{ m/sec}$

Refer to results and discussions for the new power values in the current research. Also,

refer to appendix ‘B’ for the new MATLAB Codes. Finally, For the same speed of V_{water} 1.36 m/sec and by re-arranging equation 3 given that:

$$P_{mean} = \left(\frac{\alpha a}{k_{Trans}}\right)^2 \frac{1}{2k_p} \left(\frac{a_1 w_0 C_{Lmax}}{\sqrt{(a_4 - a_2 w_0^2)^2 + (a_3 w_0)^2}}\right)^2 \dots\dots\dots(3)$$

Given that,

$$P = V_1 i = K_p V_1^2 \dots\dots\dots(13).[5]$$

Where V_1 is piezoelectric voltage, and i is piezoelectric current

$$V_{mean} = \sqrt{\left(\frac{\alpha a}{k_{trans}}\right)^2 \left(\frac{1}{2k_p^2}\right) \left(\frac{a_1 w_0 C_{Lmax}}{\sqrt{((a_4 - a_2 w_0^2)^2 + (a_3 w_0)^2)}\right)^2} \dots(14)$$

Section 7: Electromagnetic Induction

The piezoelectric calculations were completed as a preliminary study. Another component will be added to the harvester model, which is magnetic induction. The magnet will be placed inside the cylinder body and move in radial motion inside the cylinder. Basically, the cylinder diameter and height were increased to host the new mechanism of electromagnetic induction.

Governing Equation

Faraday’s law is the original law that governs electromagnetic induction through a circular loop (coil). Referring to equation (15), the electromagnetic force in volts, N is the number of loops of the coil, $d\Theta$ is the area of the coil multiplied by magnetic flux

(m²*Tesla), which is Weber. dt is change in time of the magnet

$$V_{emf} = -N \frac{d\Theta}{dt} \dots\dots\dots(15)$$

As the preliminary study continues and the power of piezoelectric was identified for four water velocities, it is necessary to obtain the electromagnetic induction in terms of power as well. To do so, a governing equation must be developed to figure out the magnet velocity first. A free-body diagram shown in Figure 24 illustrates the initial and final position of the cylinder hosting electromagnetic induction mechanism where the magnet is moving only in radial motion. The root equation is newton's second law, but firstly engineering dynamic rotational acceleration equation is presented.

$$a_r = (\ddot{r} - r\dot{\theta}^2)_{e_r} + \cancel{(r\ddot{\theta} + 2\dot{r}\dot{\theta})}_{e_\theta} \dots\dots\dots(16)$$

Where e_r represent the radial acceleration of the magnet and e_θ is the angular acceleration component set to zero as the magnet is moving in radial motion only.

Where r is the total length of the piezoelectric beam and magnet.

$$r = l + x$$

r must be constant distance. However, x is variable as the magnet is moving radially.

so:

$$\frac{dr}{dt} = \frac{d(\cancel{l} + x)}{dt} \longrightarrow \frac{dr}{dt} = \frac{dx}{dt} \longrightarrow \text{so} \quad \ddot{r} = \ddot{x} \text{ and } \dot{r} = \dot{x}$$

$$\sum \vec{F} = ma \dots\dots\dots(17)$$

The main equation that governs the magnet velocity is equation (18).

$$mg \cos \theta - kx = m(\ddot{r} - r\dot{\theta}^2)$$

$$mg \cos \theta - kx = m(\ddot{x} - (l + x)\dot{\theta}^2)$$

Re-arranging

$$m\ddot{x} + x(k + m\dot{\theta}^2) = mg \cos \theta + ml\dot{\theta}^2 \dots\dots\dots(18)$$

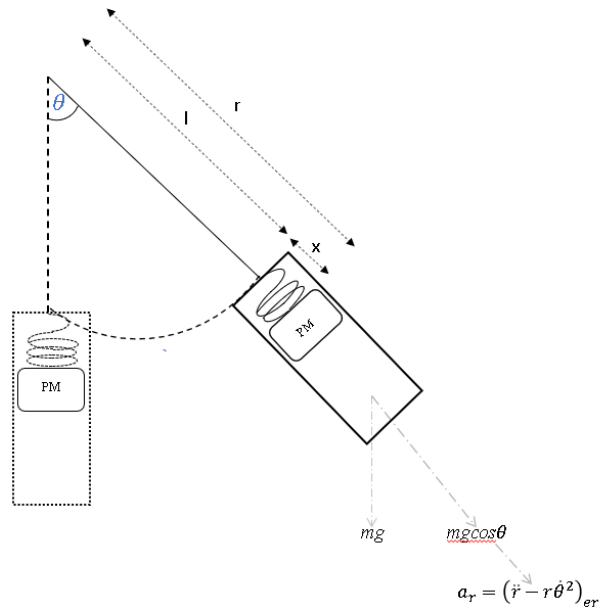


Figure 24. FBD of electromagnetic induction prototype (not to scale)

The second-order differential equation (18) was solved to find the magnet displacement $x(t)$ as a function of time. Additionally, $x(t)$ was derived to obtain the magnet velocity $x(t)'$ as a function of time. For details, please refer to Appendix C. The model variables are presented in Table 7, where the link between the water velocity variables and electromagnetic induction variables is $\dot{\theta}$ (rotational speed) from hydro-mechanical model equation 19 $w(t)$ [5], where $\sin(w_0 t)$ assumed minimum for simplification.

$$w(t) = \frac{a_1 w_0 C L_{\max}}{\sqrt{(a_4 - a_2 w_0^2)^2 + (a_3 w_0)^2}} \sin(w_0 t) \dots\dots\dots(19) [5]$$

Table 7. Variables of the electromagnetic induction governing equation

Name	Definition	Unit	Note
x	Magnet displacement	m	-
t	MATLAB simulation time	sec	5 seconds
\ddot{x}	Magnet acceleration	m/sec ²	To be calculated four times using MATLAB
$\dot{\theta}$	Rotational speed of cylinder [5]	Rad/sec	To be calculated four times using MATLAB

Similarly, the parameters of governing equation are shown in Table 8

Table 8. Parameters of the electromagnetic induction governing equation

Name	Definition	Value	Unit	Note
m	Magnet mass	0.178	Kg	Refer to next module
k	Spring constant	35.71	N/m	Refer to next module
l	Piezoelectric beam length	0.07	m	-

Finding Model Parameters and Variables

According to equation 18, some parameters must be fixed while the variables will be calculated using MATLAB. Both variables and parameters will contribute to finding the electromagnetic induction velocity as a function of time.

Figure 25. illustrate the essential components inside the cylinder. The copper coil consists of 33 loop $N=33$, made from copper coil with a diameter of 0.0015m or $d_{wire} =$

0.0015 m. The length of the coil is $L_{wire}=4.14$ m, the copper resistivity $\rho_{copper}=1.68e^{-8}$ ohm-meter [16], and the coil height is $Coil_{height}=0.0495$ m that can be estimated by the product of d_{wire} , N the number of loops and the loop pitch, which is having a value of 1.

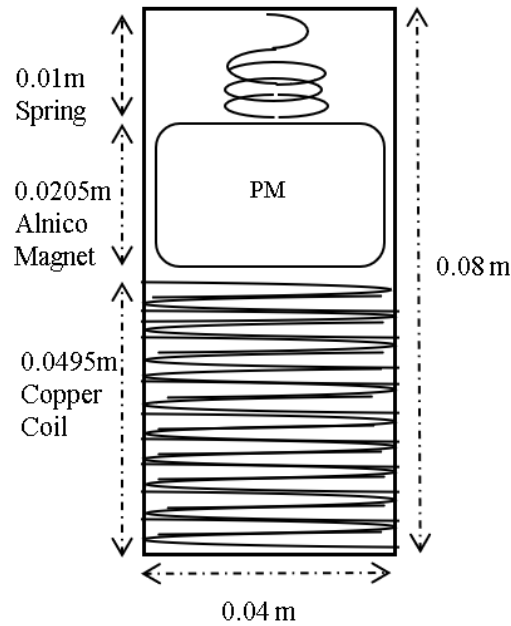


Figure 25. Sketch of the cylinder components (not to scale)

The permanent magnet (PM) is made from a ferrite or ceramic magnet called Alnico magnet, one of the most powerful magnets found in nature, having a magnetic flux between 0.5 to 1.0 Tesla $T=0.5$ Tesla, where the minimum value of 0.5 is considered [17]. Alnico Permanent magnet is classified into many grades depending on purity and composition, wherein the current research Alnico grade 5 is used, which is most popular. (Alnico 5) having a density of $\rho_{pm}=6,900$ kg/m³ [18]. As a comparison, a commercial fridge magnet is about 0.001 tesla.

Alnico 5 is having a height of $mag_{height}=0.0205$ m and a diameter equal to cylinder diameter of 0.04m. As a result, the mass of the permanent magnet is 0.178 kg.

Hook's law equation (20) is used to determine the spring constant where the gravitational acceleration is 9.81 m/sec^2 and the mass of the magnet is 0.178 kg . The spring constant k maximum value is $k=35.71$, whereas maximum elongation of the magnet is used. The variable Δx is the difference between the initial and the final position of the magnet.

$$k = \frac{m_{pm}g}{\Delta x} \dots\dots\dots(20)$$

Development of MATLAB Code for Magnet Velocity

After identifying the electromagnetic induction parameters and calculating variables, also by equations (18) and (19), MATLAB code can be composed to estimate the magnet velocity. Equation (19) the rotational speed is the link between the water characteristics and the magnetic induction, where the lift coefficient CL_{max} , water velocity V_{water} , K_p (Proportional gain from the piezoelectric model), and K_{spring} (from piezoelectric model) were changed accordingly for every corresponding V_{water} of 0.34 m/sec , 0.68 m/sec , 1.02 m/sec , and 1.36 m/sec . Refer to Table 9 for a summary of the parameters used. Additionally, refer to Appendix "D" for MATLAB codes.

Table 9. Summary of parameters used in MATLAB

Name	Definition	Value	Unit
m	Magnet mass	0.178	Kg
k	Spring constant	35.71	N/m
l	Piezoelectric beam length	0.07	m
N	Number of coil loops	33	-
d_{wire}	Wire diameter	0.0015	m
$Coil_{Height}$	Cooper coil height	0.0495	m
mag_{height}	Magnet height	0.0205	m
B	Magnetic flux	0.5	Tesla
L_{wire}	Length of coil wire	4.14	m

Name	Definition	Value	Unit
ρ_{copper}	Copper wire resistivity	$1.68e^{-8}$	Ohm-meter
A_{coil}	Internal area of coil loop	0.0010	m^2
ρ_{alnico5}	Alnico 5 density	6,900	Kg/m^3

Finding Electromagnetic Power and Voltage

As the magnet velocities were found using MATLAB codes and the results were presented in the Results and Discussion section, finding the electromagnetic voltage and power is essential to achieve this task. Ansoft Maxwell 4.0 was the simulation software that aid in finding the voltage and power given the mean velocity of the magnet. The first step is to prepare the geometry, where the coil having a thickness of equal to $d_{\text{wire}}= 0.0015m$ was constructed with a height of 0.0495m and specified material as copper. The second constructed item is the (blue band); it is a virtual space of vacuum required by the simulation software, whereas magnet can move in the band domain only, and it must be at least double the size of the coil height. The third constructed object is the permanent red magnet having a diameter of 0.04m and a height of 0.0205m. Refer to Figure 26 for illustrations.

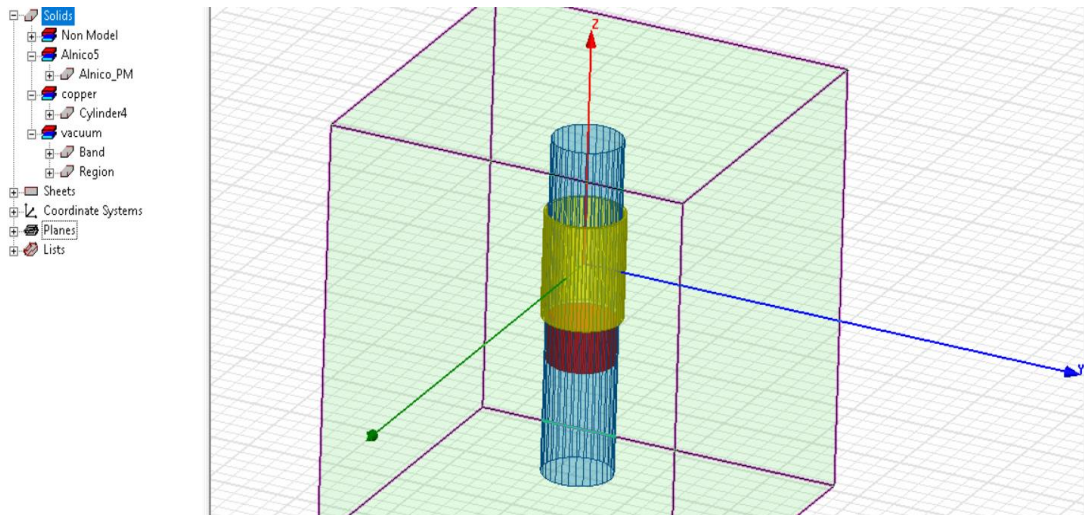


Figure 26. Overall view of the geometry preparation (Ansoft Maxwell 4.0)

Ansoft Maxwell is having a predefined repository of materials and their properties. Alnico Grade 5,9 and 10 can be used as well, whereas Alnico 5 was selected. Before initializing the simulation, the design setup must be specified, such as the magnet velocity, the coil's resistance, and the mesh. The magnet velocity can be specified under motion setup in the model preparation, where the input velocity is constant along the simulation period. Here the specified velocities for four simulations were the mean velocity of the maximum sin wave obtained in MATLAB; Refer to Results and Discussions. The excitation setup in Ansoft Maxwell represents the coil resistance where stranded type along with 33 conductors were specified. The formula $R_c =$

$$\frac{\rho_{wire} L_{wire}}{\frac{\pi d_{wire}^2}{4}}$$

is used to determine the total resistance of the copper wire having a length of 4.14m, the resistivity of $1.68e^{-8}$ ohm-meter, and d_{wire} of 0.0015m which evaluate to 0.0394 ohms. Finally, the mesh operation was split into two regions. The first region is the vacuum blue band (the exterior mesh), and the second one is the coil (the interior); both meshes were set a length-based mesh with mesh elements of 1000 nodes for both bodies. The simulation started. Please refer to the Results and Discussions.

3-D Simulation Study

Section 1: Geometry and Fluid Force Analysis

In this section, a 3D realistic simulation will be completed using ANSYS Fluent and ANSYS transient to determine the piezoelectric voltage and the electromagnetic voltage on steady oscillation motion of the cylinder versus time. The first step is to construct the pipe, the cylinder and position it exactly as in 2D in the preliminary study using CATIA V5. Refer to Figure 27.

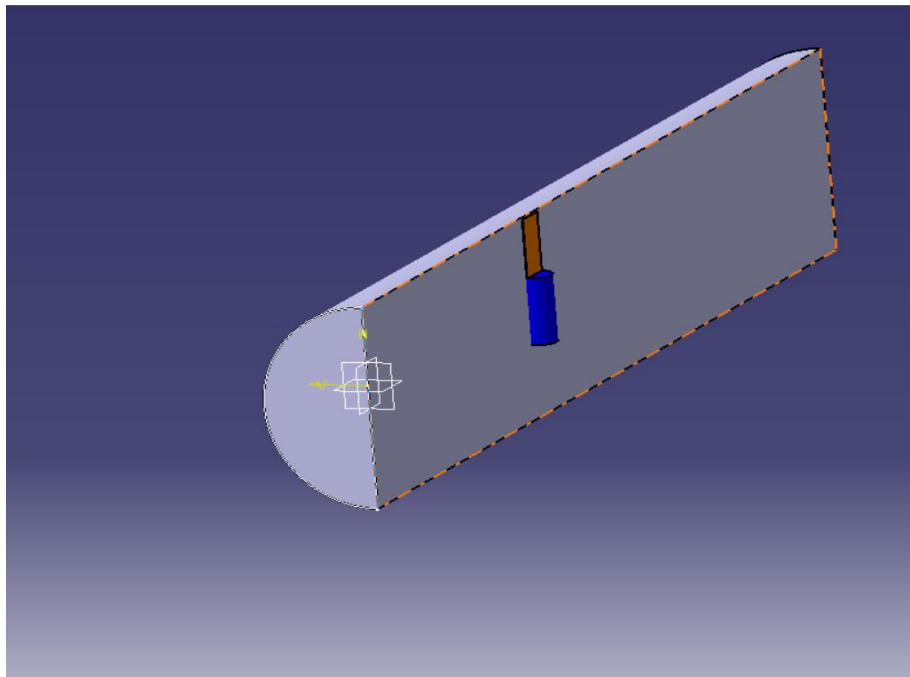


Figure 27. Isometric view of the control volume CATIA V5

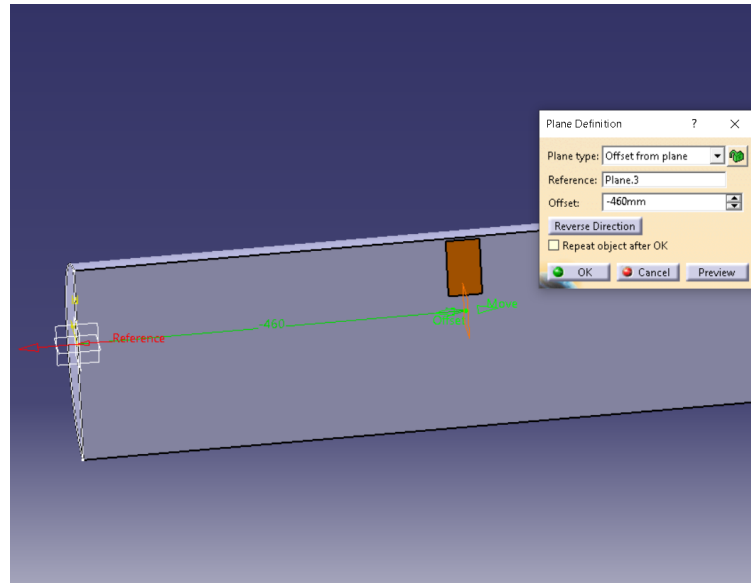


Figure 28. Harvester creation on offset plane from pipe inlet

The pipe body is specified as ID 0.2402m (here, the OD of the pipe is not used as the ID is the meshing domain). The length of the pipe is 1.260m, and the harvester is placed 0.460m from the pipe inlet, as shown in Figure 28. In addition, the cylinder diameter is 0.04m having a height of 0.08. On the other hand, the piezoelectric beam is 0.07m and 0.0015m in height and thickness, respectively. Next, CATIA V5 geometry was linked to ANSYS Fluent geometry for pre-analysis setup.

Boolean subtract operation Figure 29 was performed on the harvester body to remove material. This step is essential; otherwise, the software engine will generate a mesh inside the cylinder and assume no cylinder walls or barriers.

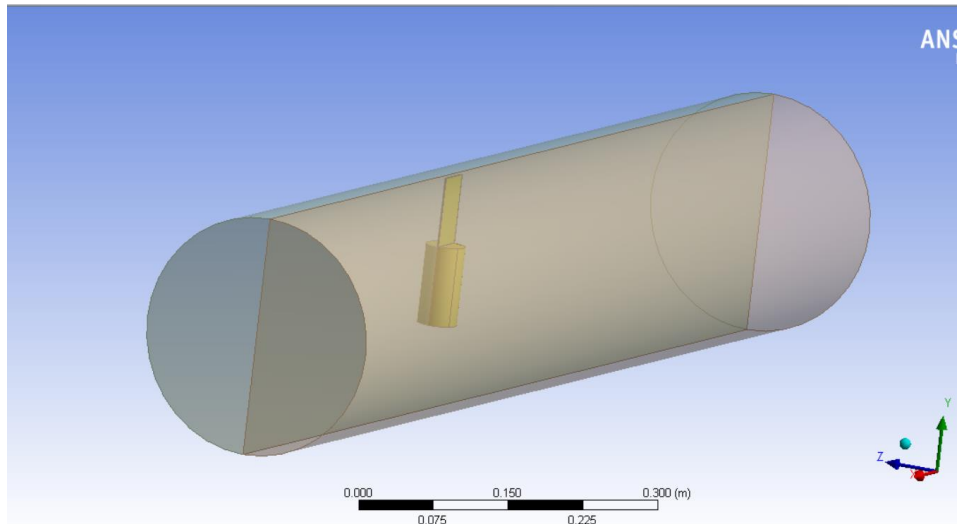


Figure 29. Fluent geometry using boolean subtract operation

The next step is to generate a global and cylinder mesh. As the forces of the z-axis (transverse force) and y-axis (lift force) will be monitored, it is crucial to apply a finer mesh on the cylinder exterior. A summary of global and cylinder mesh is shown in Table 10.

Table 10. Summary of the control volume mesh

Option	Global mesh	Cylinder mesh
Method	Tetrahedrons	Tetrahedrons
Element size	0.005 m	0.0015m
Solver type	Fluent	Fluent
Growth Rate	1.2	1.2
Smoothing	Medium	Medium
Inflation	No	No

In Figure 30, the mesh implementation was completed prior to fluent analysis for the lift and transverse force. The high dense cavity is the cylinder walls; the mesh is applied on the cylinder exterior only.

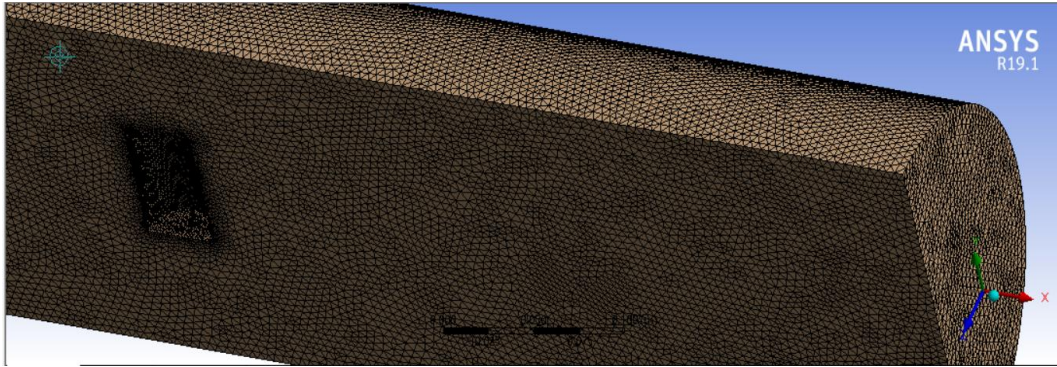


Figure 30. Implementation of global and cylinder mesh

In fluent analysis setting, it is essential to use the correct option as used in 2D analysis setting. However, the availability of options is slightly different from 2D to 3D model. The inlet water velocity will be iterated to cover a wide range of low water velocity V_{water} whereas the selected V_{water} must show a steady lift and transverse force that will oscillate the cylinder in a steady motion over time. A summary of used options is demonstrated in Table 11.

Table 11. Summary of the selected option in fluent analysis

Option	Selection
Solver type	Pressure based
Time	Transient (solver analyze against time)
Viscous model	SST 2 equation
Materials	Water liquid at 25°C (density=997 kg/m ³)
Viscosity	0.000891 kg/m*sec
Water velocity	Iteration for (0.68,1.29,1.36,1.39,1.8 ,2.72) m/sec
Transient formulation	Second order implicit
Report Files: lift force	y-direction vertical
Report Files: z-force	z-direction- sides of cylinder
Residuals	1e-6
convergence condition	Default
Initialization	Hybrid
Time-step	0.1 sec
Number of steps	180
Total time	0.1*180= 18 seconds
Iteration per time step	20

The first simulation for V_{water} of 0.68 m/sec was completed. This water speed was not selected for further processing as lift force, and transverse force are not overlap. Thus, the cylinder will oscillate in one direction only (left side), where this motion will affect the bending of the piezoelectric beam and the radial motion of the magnet (see Figure 31 and 32). Furthermore, V_{water} of 1.29 m/sec, V_{water} 1.80 m/sec, and V_{water} 2.72 m/sec were not selected for the same reason. Refer to Appendix “E” for their forces results.

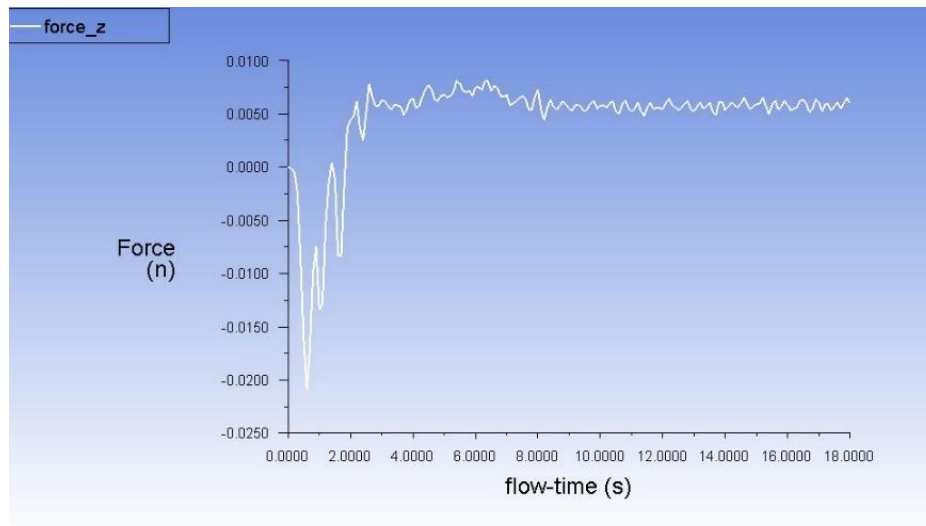


Figure 31. Transverse z-axis forces versus time (V_{water} 0.68 m/sec)

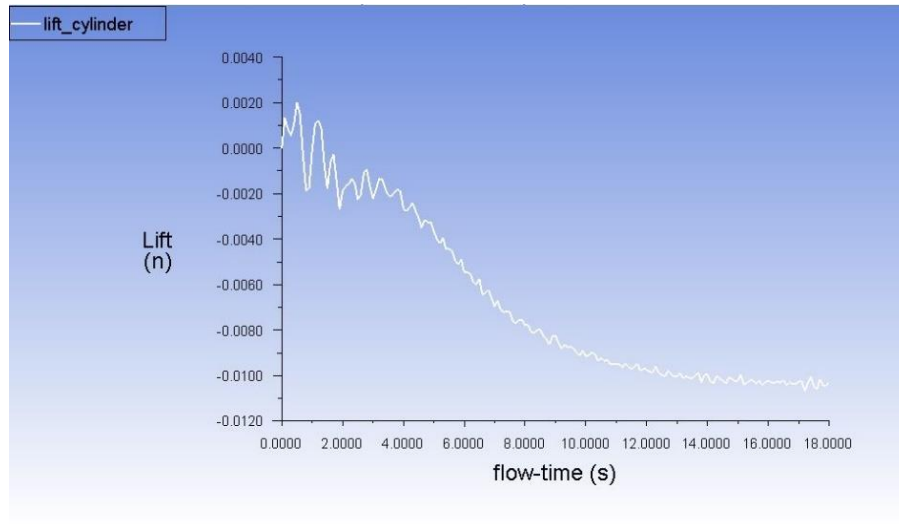


Figure 32. Lift y-axis forces versus time (V_{water} 0.68 m/sec)

Only two water velocities will be selected based on the results forces, which are V_{water} 1.36 m/sec and V_{water} 1.39 m/sec. See the Results and Discussion section for more details.

Section 2: Piezoelectric Voltage

After the completion of ANSYS fluent analysis for transverse and lift forces on V_{water} 1.36 m/sec and V_{water} 1.39 m/sec, these forces will be applied to the cylinder body for further processing. ANSYS transient mechanical v19.1 was the software package used where all 180 data points representing 18 seconds of total simulation time were stored.

The harvester body was prepared as presented in Figure 33. Here the cylinder diameter is 0.04m and a height of 0.08m; on the other hand, the piezoelectric beam is 0.07m in height and thickness of 0.0015m.

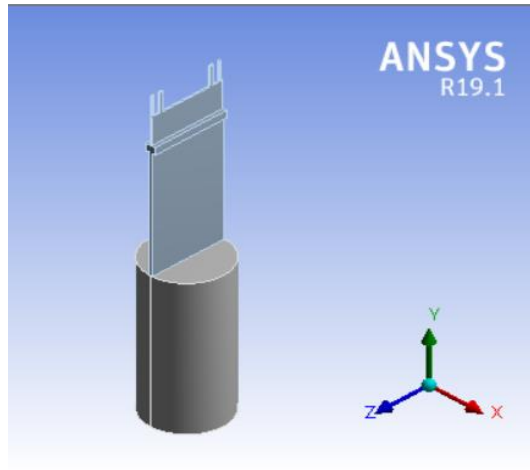


Figure 33. Isometric view of the harvester

Materials assignment is an important step to obtain accurate results; this can be configured in ANSYS engineering data management. For the cylinder, the specified material is polypropylene with a density of 920 kg/m^3 , Young's modulus of 1325 Mpa , shear modulus of 509 Mpa , and tensile yield strength of 34 Mpa [19]. Likewise, the material properties for the piezoelectric beam is PVDF having a density of 1780 kg/m^3 , young's modulus of 2450 Mpa , and tensile strength 53.5 Mpa [20].

The environment temperature was set to 25°C for all the simulation progress. For the specific requirements of the simulation, the top horn of the piezoelectric beam was fixed to restrict the motion in the dragging axis. An extension package was installed on ANSYS 19.1 (Piezo and Mems) for piezoelectric voltage analysis. The next step before running the analysis is to prepare the mesh. Refer to Table 12 for a summary of applied mesh on the piezoelectric beam and cylinder.

Table 12. Summary of transient mechanical mesh

Option	Selection	Applied on
Method	Tetrahedrons	Cylinder and piezoelectric
Solver	Mechanical APDL	Cylinder and piezoelectric
Element Size	0.002 m	Cylinder and piezoelectric
Transition	Fast	Cylinder and piezoelectric
Smoothing	High	Cylinder and piezoelectric

The analysis was completed for 18 seconds on both water velocities of 1.36 m/sec and 1.39 m/sec. Refer to Results and Discussion sections.

Section 3: Magnet Velocity and Electromagnetic Voltage

A critical analysis will be completed in this section; the magnet velocity and electromagnetic voltage for corresponding water velocity of 1.36 m/sec and 1.39 m/sec using ANSYS Transient Mechanical *v19.1*. The same transverse and lift forces will be applied on a cylinder wall, hosting the magnet mechanism that is hanged by a spring, as shown in Figure 34. The exact materials were applied to the piezoelectric beam and the cylinder. Moreover, new material was introduced into the system that is Alnico 5 (the magnet), having a density of 6,900 kg/m³. Alnico 5 material property was adjusted manually in ANSYS engineering data management.

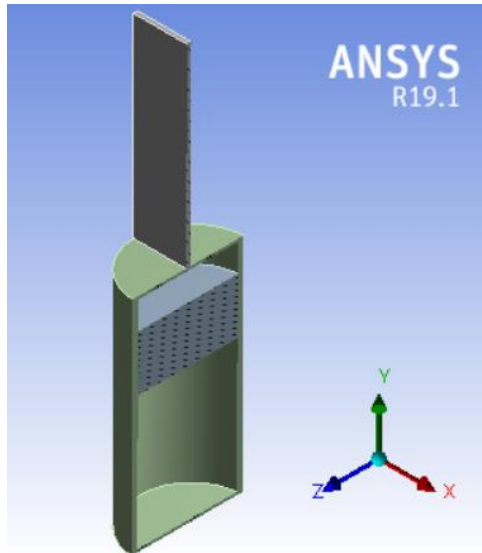


Figure 34. Isometric view of the magnet mechanism

The top surface of the magnet is connected to the ceiling of the cylinder via a spring with no separation option having a spring constant of 20 N/m (this value was the maximum acceptable value by ANSYS). Similar to piezoelectric simulation, the mesh element size is 0.002m, fast transition, medium span angle, and high smoothing. Refer to Results and discussions for details of the outcome.

For the electromagnetic voltage, another analysis was added based on the magnet velocity, which is the magnet displacement. With mean magnet velocity and mean displacement, the initial and final time can be calculated for each time step between 10 to 18 sec for water velocity of 1.36 m/sec and between 4 to 18 sec for water velocity of 1.39 m/sec. Using a data processing sheet and Faraday's law equation (15), the electromagnetic voltage is estimated. The average displacement of the magnet inside the coil is 0.027m, and the coil original designed height is 0.0495m. Thus, the magnet will cut the flux of 17 coil loops only. See Results and Discussions

CHAPTER 4: RESULTS AND DISCUSSIONS

Preliminary Study

Section 1: Fluent Results and Piezoelectric Power

ANSYS fluent has completed solving for C_L , C_D , and Strouhal number using 0.003 as step size and a total time of 15 sec. Fluent is calculating the required coefficients every 0.003 sec from a total time of 15 sec, which makes a total number of steps to be 5000 iterations. Table 13 summarize the results for fine mesh.

Table 13. Summary of C_L , C_D and Strouhal number for fine mesh

Water velocity	0.34 m/sec	0.68 m/sec	1.2 m/sec	1.36 m/sec
Reynolds number	15,000	30,000	45,000	60,000
Maximum lift coefficient C_L	0.85	0.375	0.2625	0.22
Maximum drag Coefficient C_D	0.79	0.650	0.625	0.558
Strouhal number	0.219	0.197	0.186	0.181

Consequently, Table 14 summarizes the results for medium mesh excluding Strouhal number.

Table 14. Summary of C_L , C_D coefficients for medium mesh

Water velocity	0.34 m/sec	0.68 m/sec	1.2 m/sec	1.36 m/sec
Reynolds number	15,000	30,000	45,000	60,000
Maximum lift coefficient C_L	0.31	0.225	0.2	0.155
Maximum drag coefficient C_D	0.68	0.625	0.6	0.558
Strouhal number	-	-	-	-

Fine mesh results values generally higher than medium-mesh results. Selections of values to be used in MATLAB code and generating the power were taken from fine mesh results that agreed with Norberg [26] in terms of ST and C_L . While agrees with Stringer in C_D [15]

For the V_{water} of 0.34 m/sec C_L C_D versus time is shown along with a summary of variables and parameters.

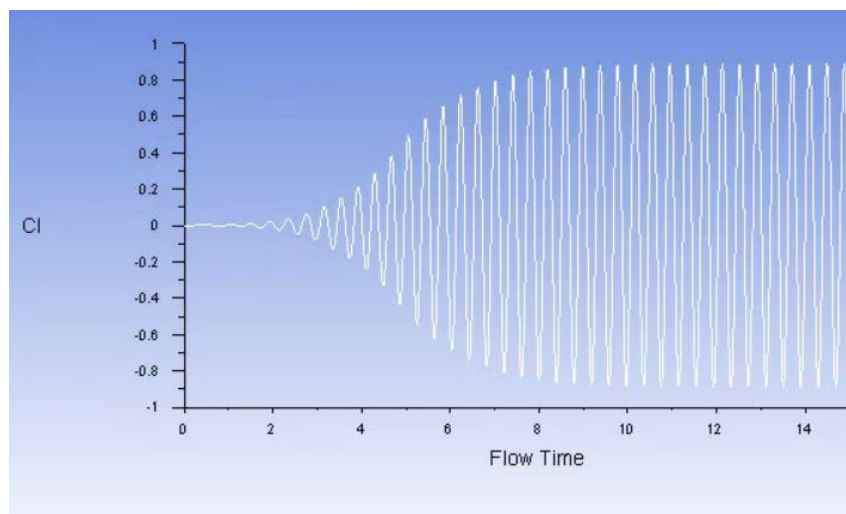


Figure 35. C_L versus time of 15 sec (0.34 m/sec)

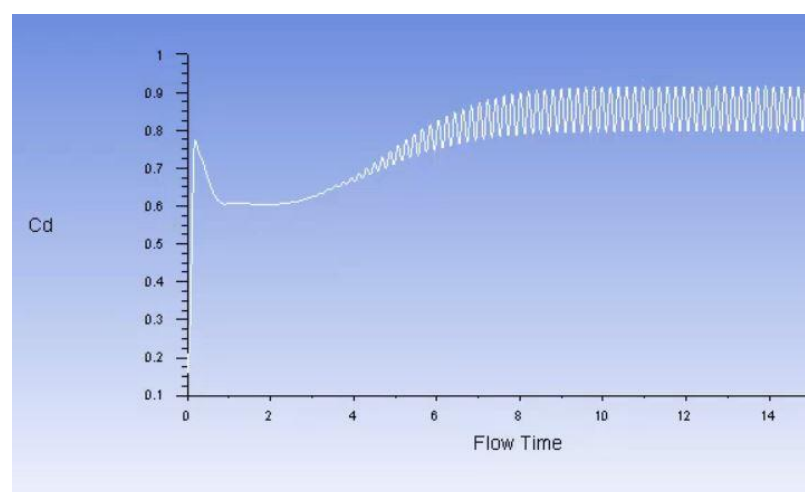


Figure 36. C_D versus time of 15 sec (0.34 m/sec)

Moreover, the vortex shedding behind the cylinder is shown in Figure 37.

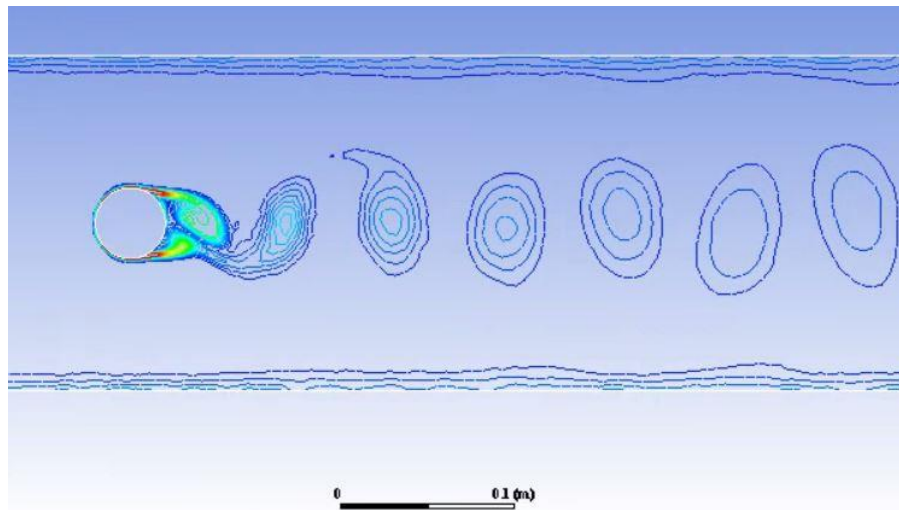


Figure 37. Vortex shedding for ($V_{\text{water}} 0.34 \text{ m/sec}$)

Table 15. Demonstrate the summary of $V_{\text{water}} 0.34 \text{ m/sec}$ variables and parameters that are considered in MATLAB for piezoelectric power

Table 15. Variable and parameters for $V_{\text{water}} 0.34 \text{ m/sec}$

Description	Value	Unit
Reynolds number	15,000	-
Velocity	0.34	m/s
CL_{max}	0.85	-
ρ_{pizo} (density of piezoelectric)	1780	Kg/m^3
$\rho_{\text{water at } 25^\circ\text{C}}$	997	Kg/m^3
C_{d33} (piezoelectric capacitance)	1.4	nF
L (Radius of gyration)	0.020	m
J_{wt} Moment of inertia about z-axis	4.021×10^{-5}	kg.m^2
H_a cylinder height	0.08	m
D_{cylinder}	0.04	m

The mean power for $V_{\text{water}} 0.34/\text{sec}$ as a result of MATLAB code is shown in Figure 38.

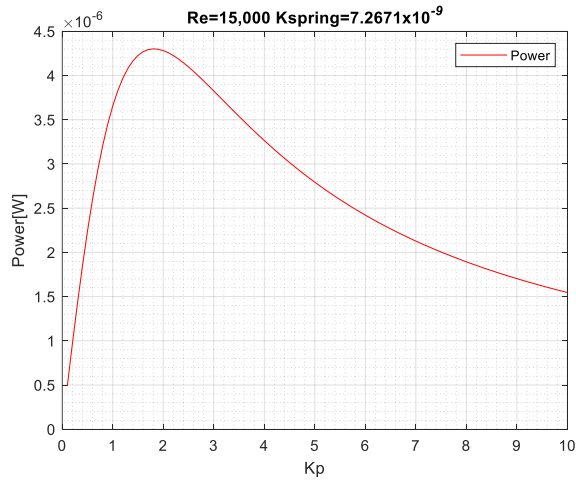


Figure 38. P_{mean} for V_{water} 0.34 m/sec

Table 16. mean power for V_{water} of 0.34 m/sec

Re	V_{water}	Power μW	$K_p(\text{optimal})$ A/V	K_{spring} optimal N/m [5]
15,000	0.34 m/sec	4.3	1.814	7.2671×10^{-9}

For the V_{water} of 0.68 m/sec the $C_L C_D$ versus time is shown along with a summary of variables and parameters.

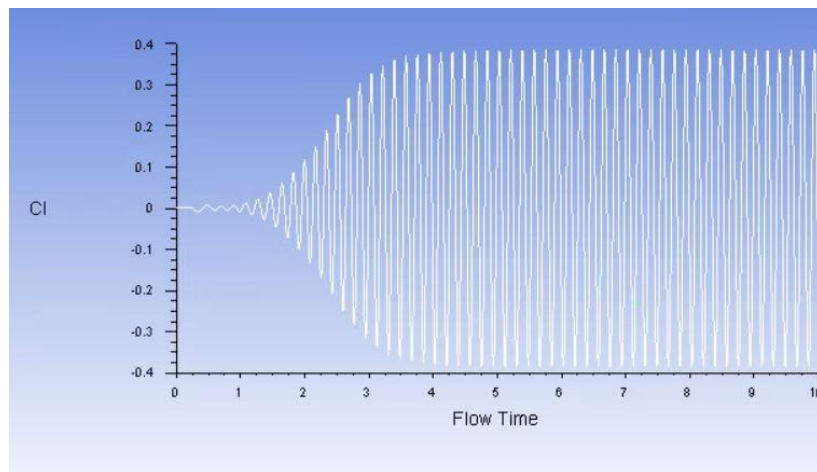


Figure 39. C_L versus time of 15 sec (0.68 m/sec)

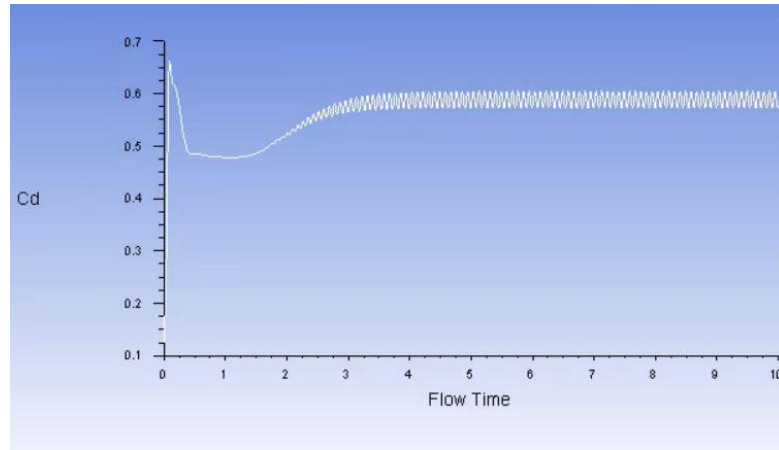


Figure 40. C_D versus time of 15 sec (0.68 m/sec)

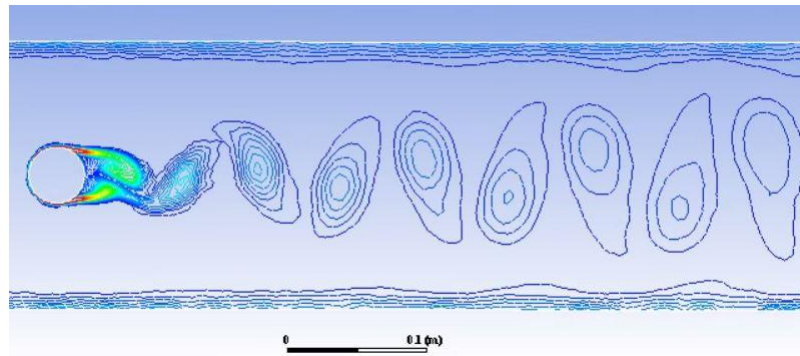


Figure 41. Vortex shedding for (V_{water} 0.68 m/sec)

Table 17. Demonstrate the summary of V_{water} 0.68 m/sec variables and parameters that are considered in MATLAB for piezoelectric power.

Table 17. Variable and parameters for V_{water} 0.68 m/sec

Description	Value	Unit
Reynolds number	30,000	-
Velocity	0.68	m/s
CL_{max}	0.375	-
ρ_{pizo} (density of piezoelectric)	1780	Kg/m^3
ρ_{water} at 25°C	997	Kg/m^3
C_{d33} (piezoelectric capacitance)	1.4	nF
L (Radius of gyration)	0.020	m
J_{wt} Moment of inertia about z-axis	4.021×10^{-5}	kg.m^2
H_a cylinder height	0.08	m
D_{cylinder}	0.04	m

Mean power for $V_{\text{water}} 0.68/\text{sec}$ as a result of MATLAB code is shown in Figure 42.

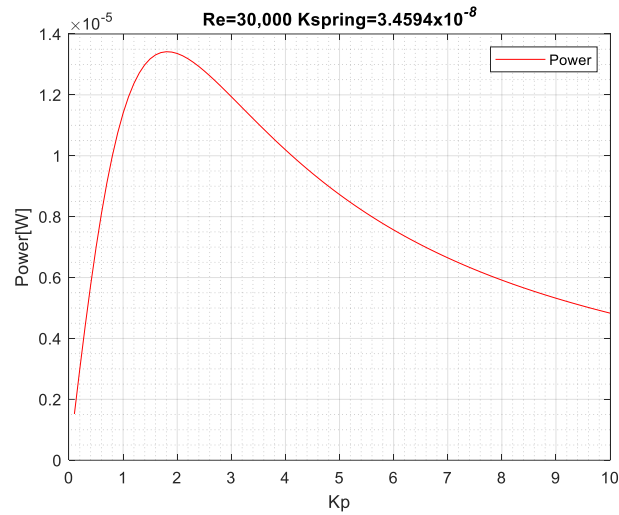


Figure 42. P_{mean} for V_{water} (0.68 m/sec)

Table 18. Mean power for V_{water} of 0.68 m/sec

Re	V_{water}	Power μW	$K_p(\text{optimal})$ A/V	$K_{\text{spring}}(\text{optimal})$ N/m [5]
30,000	0.68 m/sec	13.4	1.8175	3.4594×10^{-8}

For the V_{water} of 1.02 m/sec the $C_L C_D$ versus time is shown along with a summary of variables and parameters.

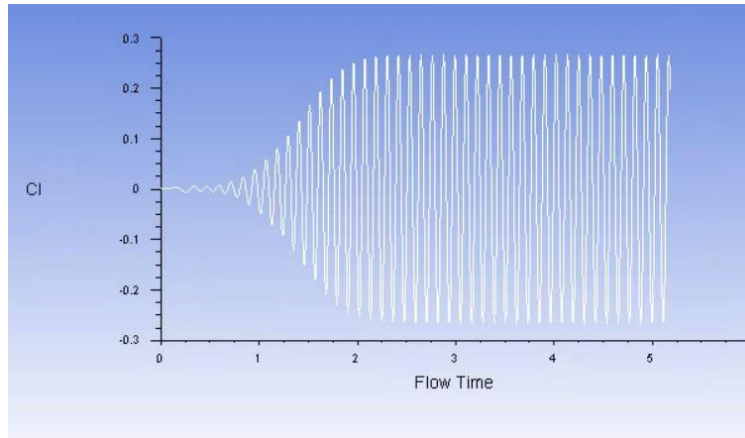


Figure 43. C_L versus time of 15 sec (1.02 m/sec)

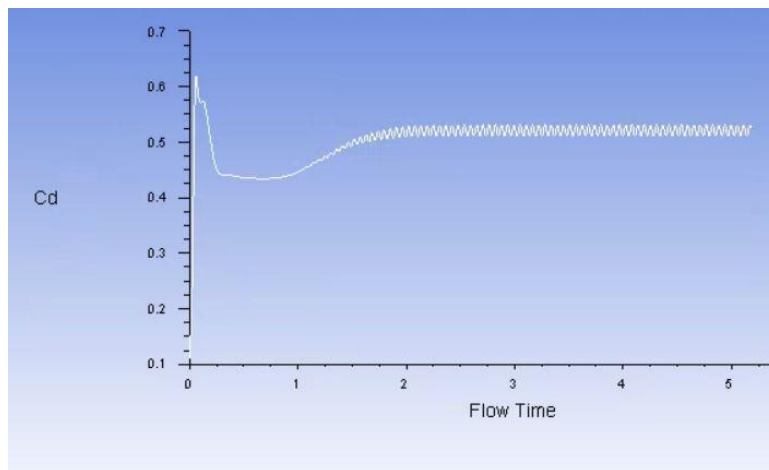


Figure 44. C_D versus time of 15 sec (1.02 m/sec)

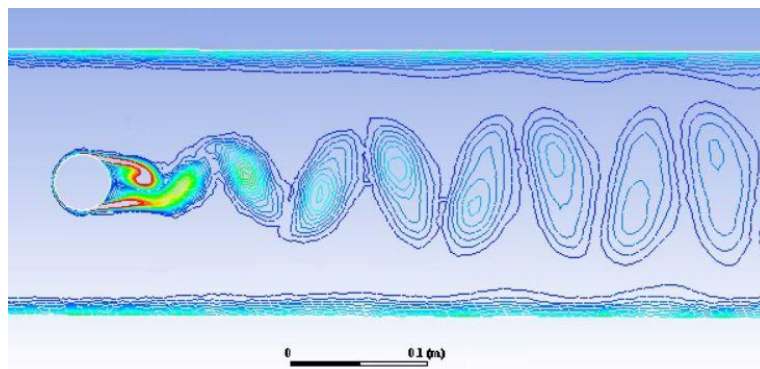


Figure 45. Vortex shedding for V_{water} (1.02 m/sec)

Table 19. Demonstrate the summary of V_{water} 1.02 m/sec variables and parameters that

are considered in MATLAB for piezoelectric power

Table 19. Variable and parameters for $V_{\text{water}} 1.02 \text{ m/sec}$

Description	Value	Unit
Reynolds number	45,000	-
Velocity	1.02	m/s
CL_{max}	0.2625	-
ρ_{pizo} (density of piezoelectric)	1780	Kg/m^3
$\rho_{\text{water at } 25^\circ\text{C}}$	997	Kg/m^3
C_{d33} (piezoelectric capacitance)	1.4	nF
L (radius of gyration)	0.020	m
J_{wt} moment of inertia about z-axis	4.021×10^{-5}	kg.m^2
H_{a} cylinder height	0.08	m
D_{cylinder}	0.04	m

Mean power for $V_{\text{water}} 1.02 \text{ m/sec}$ as a result of MATLAB code is shown in Figure 46.

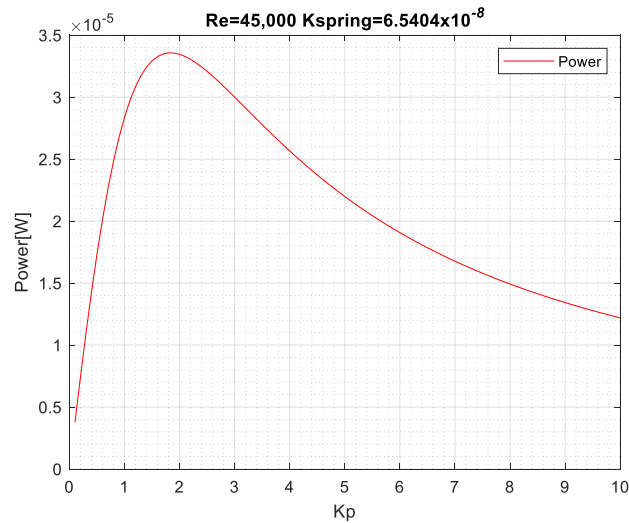


Figure 46. P_{mean} for $V_{\text{water}} (1.02 \text{ m/sec})$

Table 20. Mean power for V_{water} of 1.02 m/sec

Re	V_{water}	Power μW	K_{p} (optimal) A/V	K_{spring} (optimal) N/m [5]
45,000	1.02 m/sec	33.6	1.8339	6.5404×10^{-8}

For the V_{water} of 1.36 m/sec the $C_L C_D$ versus time is shown along with a summary of variables and parameters.

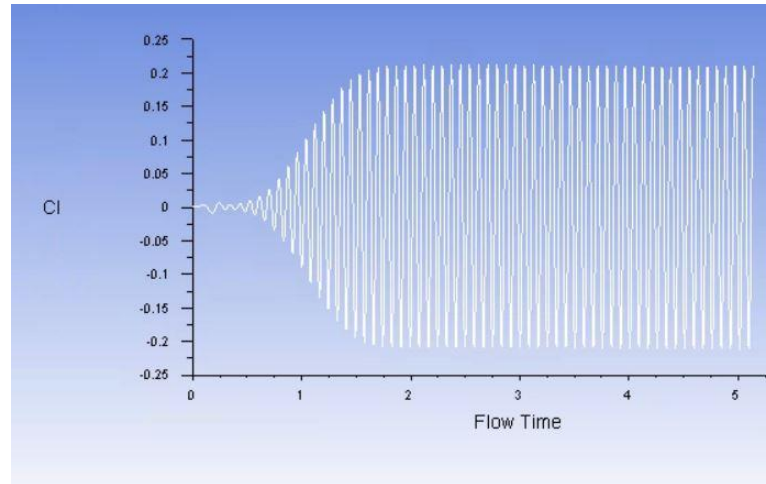


Figure 47. C_L versus time of 15 sec (1.36 m/sec)

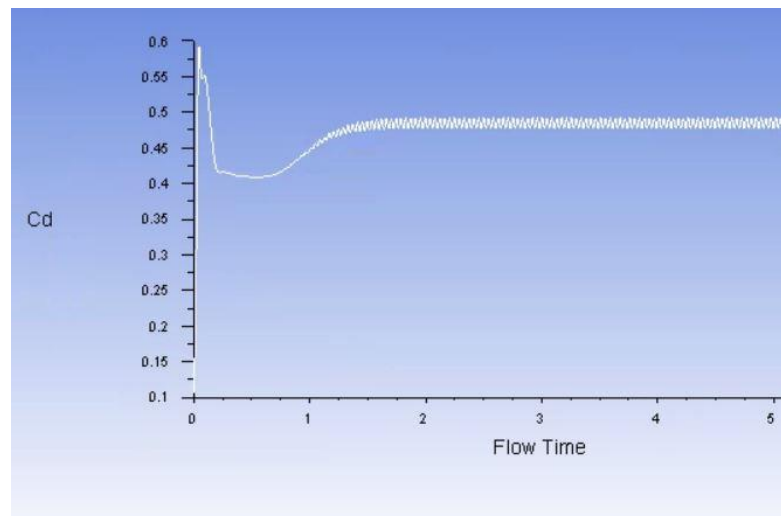


Figure 48. C_D versus time of 15 sec (1.36 m/sec)

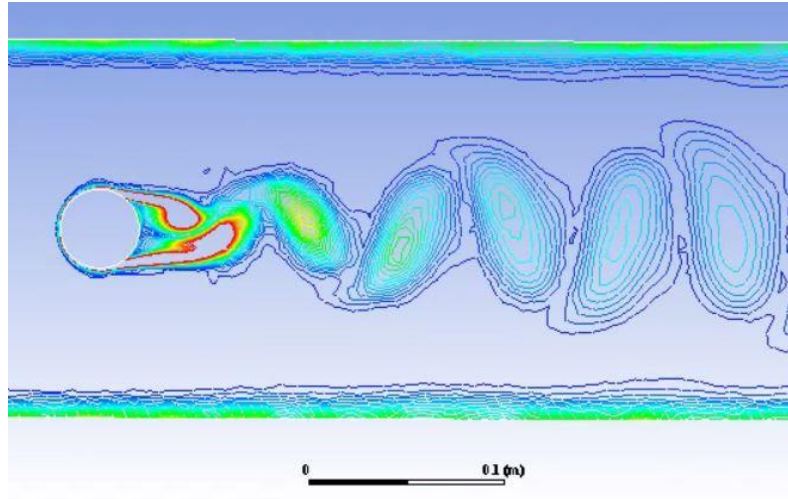


Figure 49. Vortex shedding for $V_{\text{water}} 1.36 \text{ m/sec}$

Table 21. Demonstrate the summary of $V_{\text{water}} 1.36 \text{ m/sec}$ variables and parameters that are considered in MATLAB for piezoelectric power

Table 21. Variable and parameters for $V_{\text{water}} 1.36 \text{ m/sec}$

Description	Value	Unit
Reynolds number	60,000	-
Velocity	1.36	m/s
CL_{max}	0.22	-
ρ_{pizo} (density of piezoelectric)	1780	Kg/m^3
ρ_{water} at 25°C	997	Kg/m^3
C_{d33} (piezoelectric capacitance)	1.4	nF
L (radius of gyration)	0.020	m
J_{wt} moment of inertia about z-axis	4.021×10^{-5}	kg.m^2
H_a cylinder height	0.08	m
D_{cylinder}	0.04	m

Mean power for $V_{\text{water}} 1.36 \text{ m/sec}$ as a result of MATLAB code is shown in Figure 50.

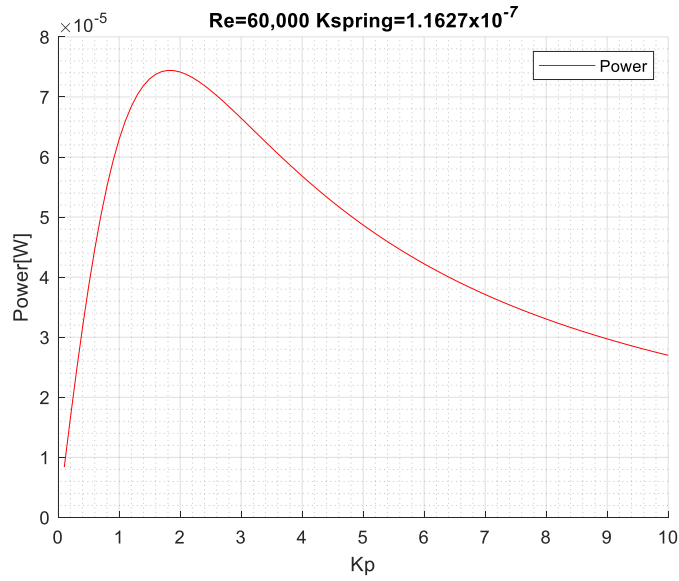


Figure 50. P_{mean} for V_{water} (1.36 m/sec)

Figure 51 present the MATLAB results for maximum voltage for V_{water} 1.36 m/sec

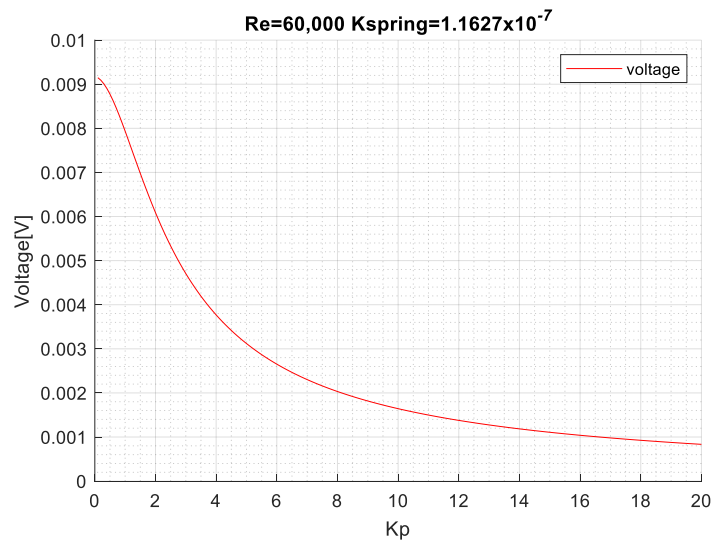


Figure 51. Voltage for V_{water} 1.36 m/sec

Table 22. Mean power for V_{water} of 1.36 m/sec

Re	V_{water} m/sec	Power μW	K_p A/V	K_{spring} optimal N/m [5]	V_{mean} (mVolt)
60,000	1.36	74.4	1.8311	1.1627×10^{-7}	9.1

Calculations have been completed and determined using the new variables and parameters. Both new and the literature power output is in microwatt while literature power is higher than the newly calculated power and voltage. This is due to many values used in MATLAB, such as the radius of gyration (that has a potential impact on the final value). The value changed from 0.08 m to 0.020 m. Moreover, changing the value of piezoelectric capacitance from 1.0 to 1.4 nF has a minor impact. Also, the piezoelectric stiffness new value for PVDF could not be estimated, so it was kept to 123 N/m as per the literature, although this value has minor effect on the final result.

The density of piezoelectric materials changed from 5319 kg/m³ to 1780 kg/m³, which was a minor reduction factor in MATLAB. Finally, K_{spring} (spring constant of piezoelectric material) was a constant value for the four water velocities; this value must be estimated as the piezoelectric material changed from ceramic to polymer type. However, K_{spring} has a medium impact on results, but it's recommended to be obtained.

Table 23. Summary of research piezoelectric power

V_{water} m/sec	Current P_{mean} μ W	Literature [5] P_{mean} μ W	Current V_{mean} mVolt	Current K_p A/V	Literature [5] K_p A/V
0.34	4.3	3.95	N/A	1.814	4.412
0.68	13.4	108.15	N/A	1.8175	4.419
1.02	33.6	395.12	N/A	1.8339	4.459
1.36	74.4	996.25	9.1	1.8311	4.452

Section 2: Magnet Velocity, Electromagnetic Voltage and Power

The simulations using MATLAB were completed for four water velocities using equations (18) and (19) where CL_{max} , V_{water} , Kp (Proportional Gain), and K_{spring} were changed according to each corresponding V_{water} .

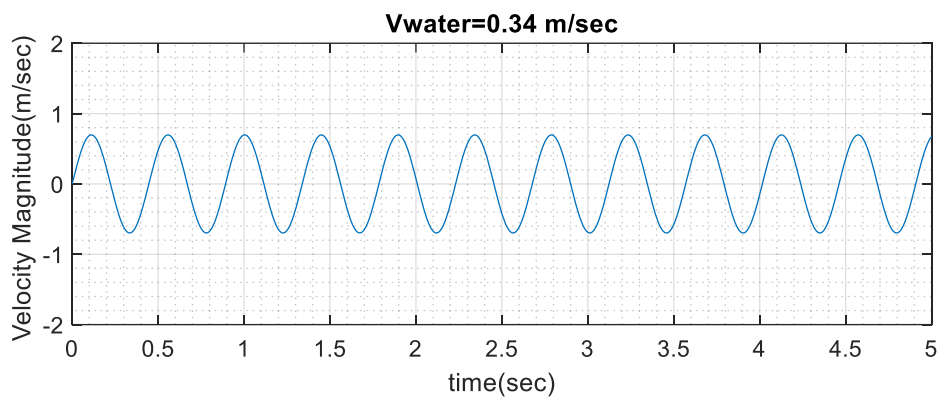


Figure 52. MATLAB results for magnet velocity (V_{water} 0.34 m/sec)

Table 24. Summary of MATLAB result for V_{water} (0.34 m/sec)

Re	V_{water} m/sec	Magnet velocity Vel_{max} m/sec	Magnet velocity Vel_{mean} m/sec
15,000	0.34	0.696613	0.443742

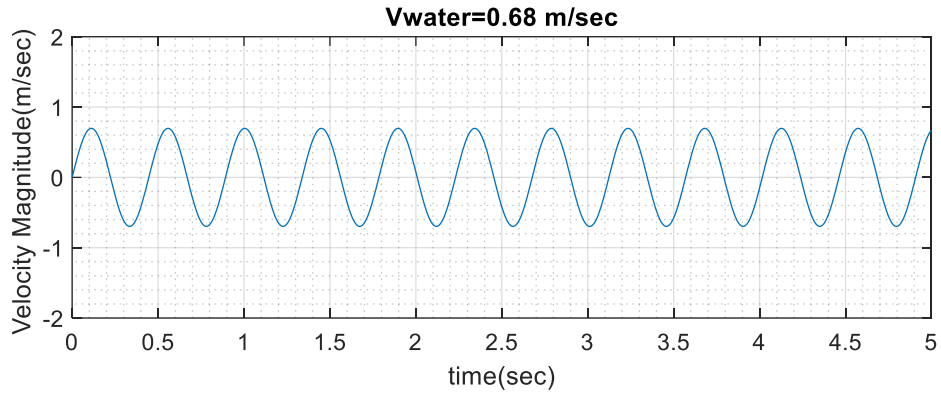


Figure 53. MATLAB results for magnet velocity ($V_{\text{water}} 0.68 \text{ m/sec}$)

Table 25. Summary of MATLAB result for $V_{\text{water}} (0.68 \text{ m/sec})$

Re	$V_{\text{water}} \text{ m/sec}$	Magnet Velocity $Vel_{\text{max}} \text{ m/sec}$	Magnet Velocity $Vel_{\text{mean}} \text{ m/sec}$
30,000	0.68	0.696614	0.443743

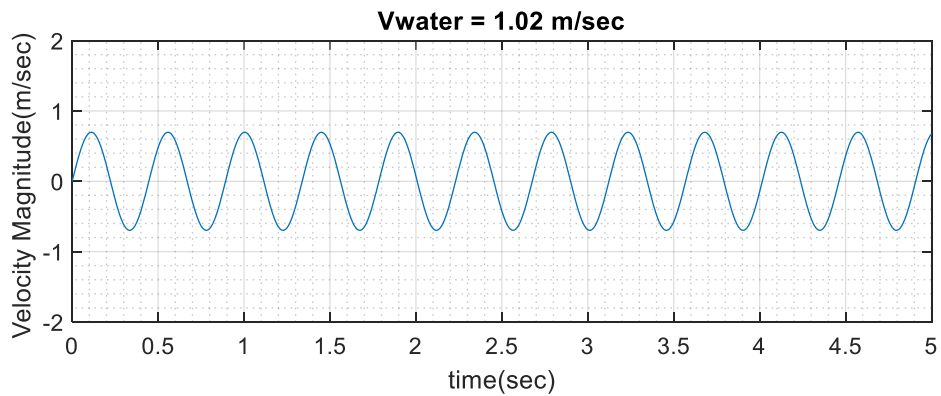


Figure 54. MATLAB results for magnet velocity ($V_{\text{water}} 1.02 \text{ m/sec}$)

Table 26. Summary of MATLAB Result for $V_{\text{water}} (1.02 \text{ m/sec})$

Re	$V_{\text{water}} \text{ m/sec}$	Magnet Velocity $Vel_{\text{max}} \text{ m/sec}$	Magnet Velocity $Vel_{\text{mean}} \text{ m/sec}$
45,000	1.02	0.696615	0.443744

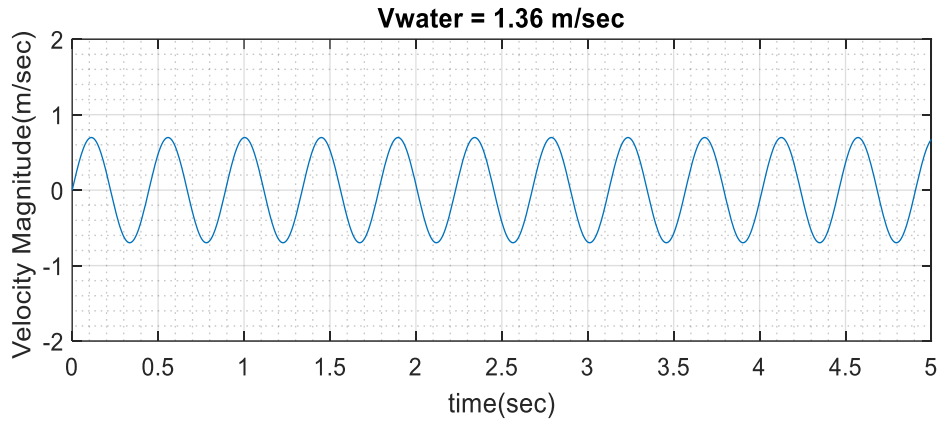


Figure 55. MATLAB results for magnet velocity ($V_{\text{water}} 1.36 \text{ m/sec}$)

Table 27. Summary of MATLAB Result for $V_{\text{water}} (1.36 \text{ m/sec})$

Re	$V_{\text{water}} \text{ m/sec}$	Magnet Velocity $Vel_{\text{max}} \text{ m/sec}$	Magnet Velocity $Vel_{\text{mean}} \text{ m/sec}$
60,000	1.36	0.696617	0.443745

The mean velocities were used to determine the electromagnetic voltage and power using Ansoft Maxwell.

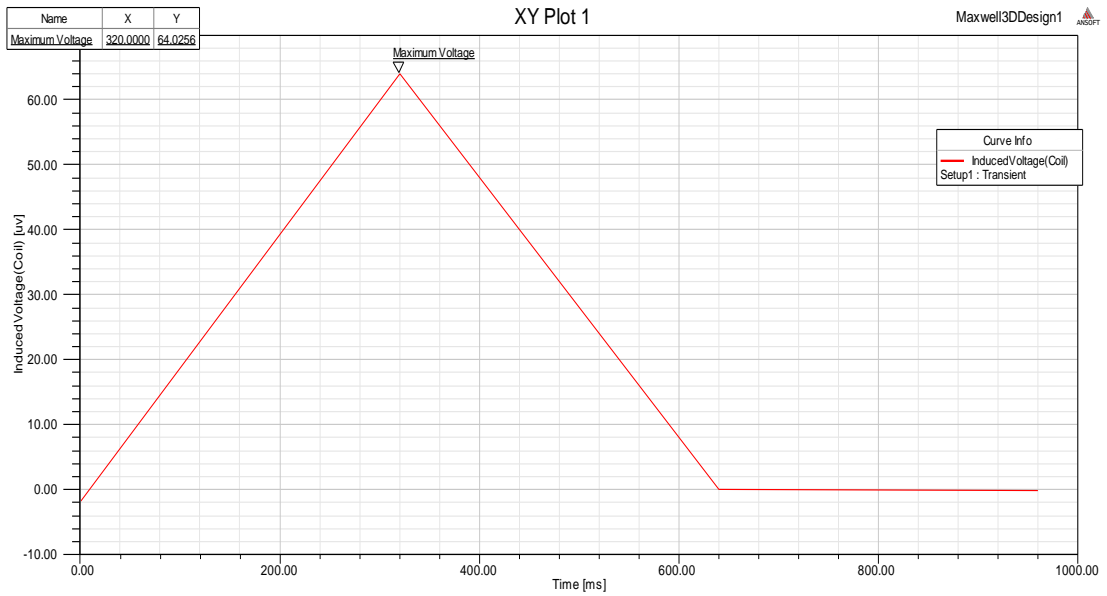


Figure 56. Mean voltage using Ansoft Maxwell for ($V_{\text{water}} 0.34 \text{ m/sec}$)

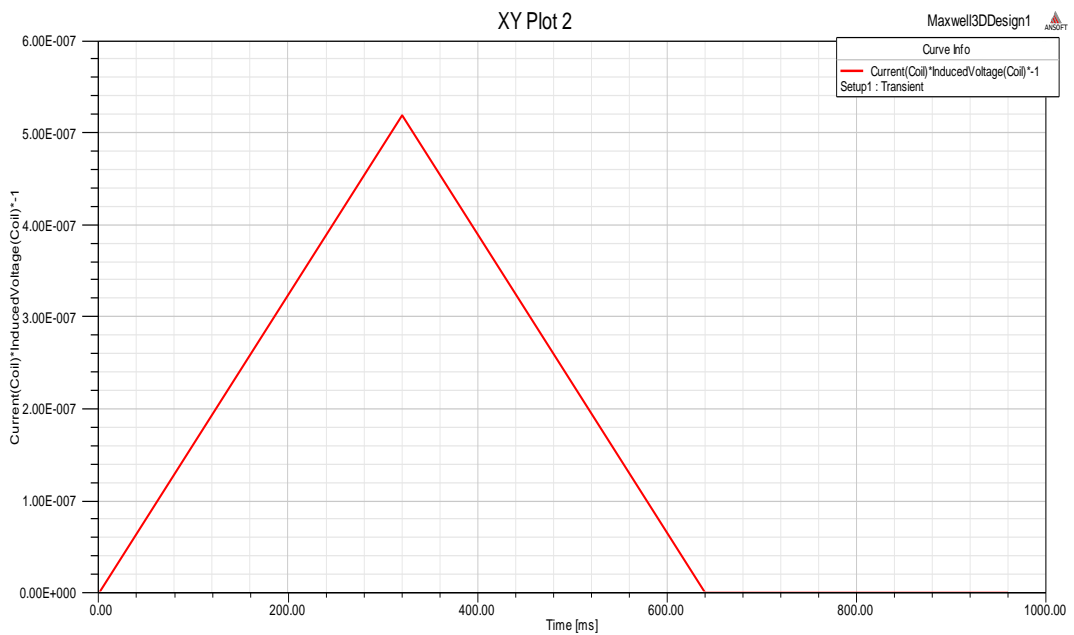


Figure 57. Mean power using Ansoft Maxwell for ($V_{\text{water}} 0.34 \text{ m/sec}$)

Table 28. Summary of Ansoft Maxwell results for $V_{\text{water}} (0.34 \text{ m/sec})$

Re	V_{water} m/sec	Magnet velocity Vel_{mean} m/sec	V_{mean} (volts) μV	P_{mean} (Watt)
15,000	0.34	0.443742	64.31	$5.21e^{-7}$

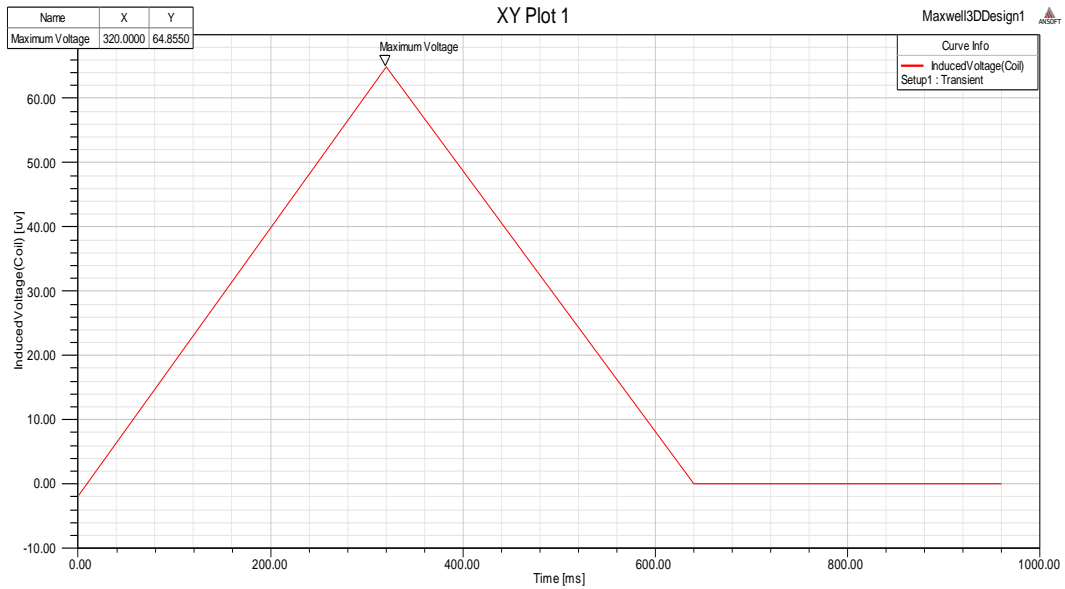


Figure 58. Mean voltage using Ansoft Maxwell for (V_{water} 0.68 m/sec)

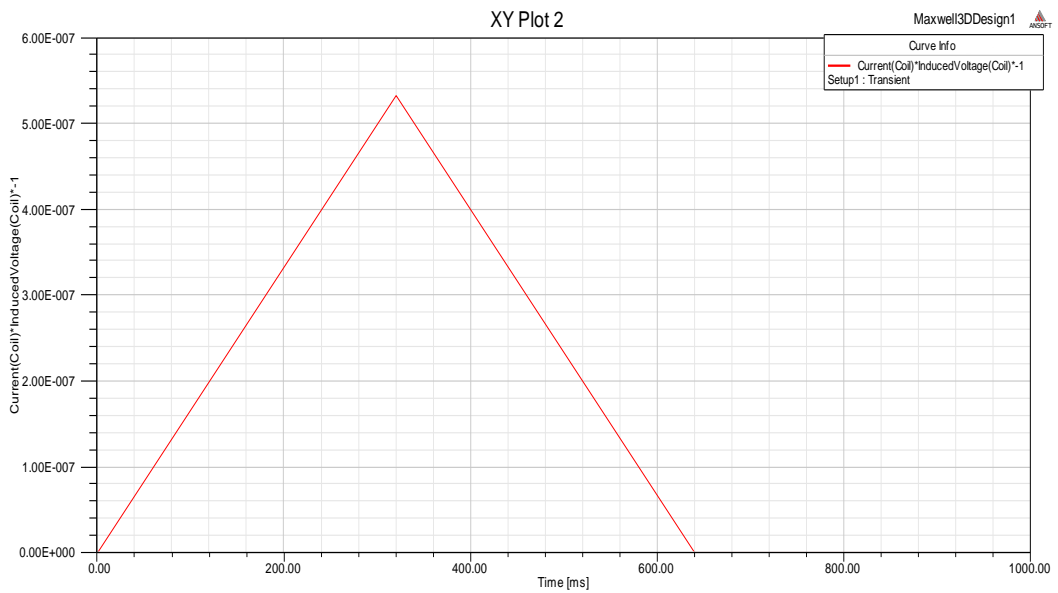


Figure 59. Mean power using Ansoft Maxwell for (V_{water} 0.68 m/sec)

Table 29. Summary of Ansoft Maxwell result for V_{water} (0.68 m/sec)

Re	V_{water} m/sec	Magnet velocity V_{elmean} m/sec	V_{mean} (volts) μV	P_{mean} (Watt)
30,000	0.68	0.443743	64.65	$5.25e^{-7}$

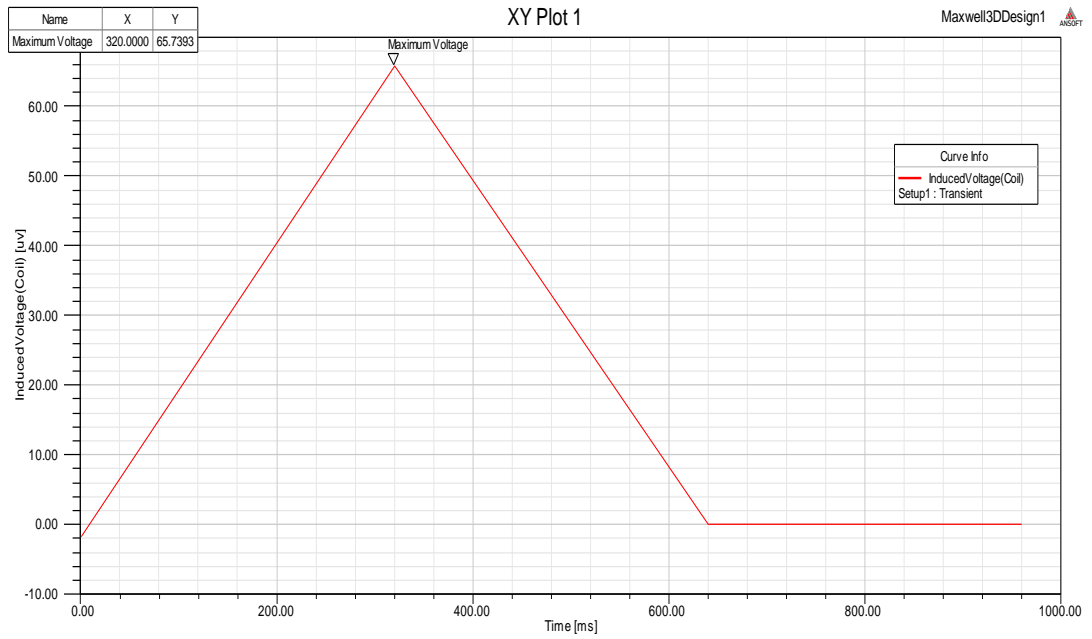


Figure 60. Mean voltage using Ansoft Maxwell for ($V_{\text{water}} 1.02 \text{ m/sec}$)

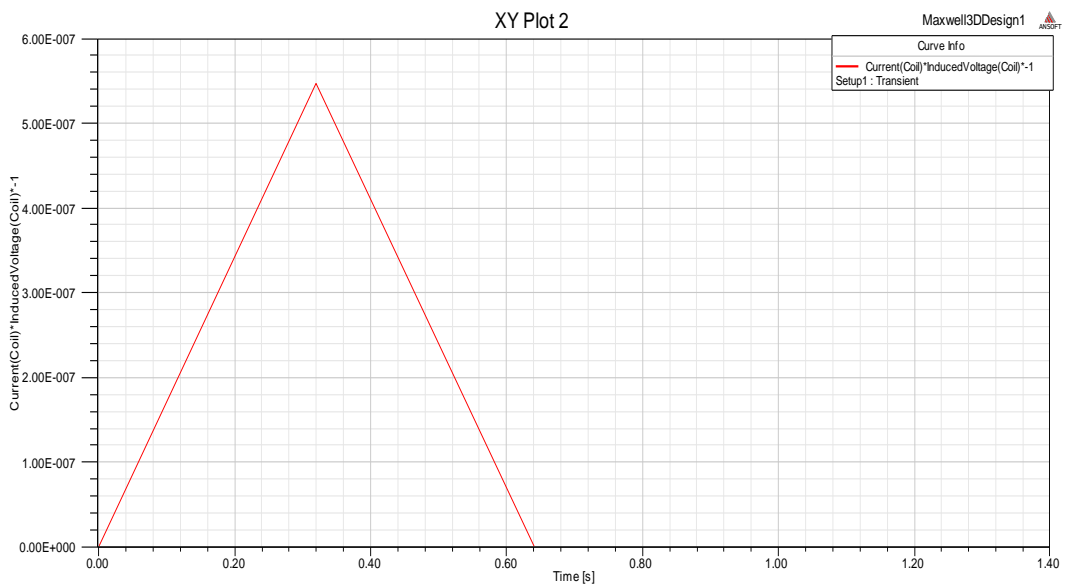


Figure 61. Mean power using Ansoft Maxwell for ($V_{\text{water}} 1.02 \text{ m/sec}$)

Table 30. Summary of Ansoft Maxwell result for V_{water} (1.02 m/sec)

Re	V_{water} m/sec	Magnet velocity V_{elmean} m/sec	V_{mean} (volts) μV	P_{mean} (Watt)
45,000	1.02	0.443744	65.73	$5.39e^{-7}$

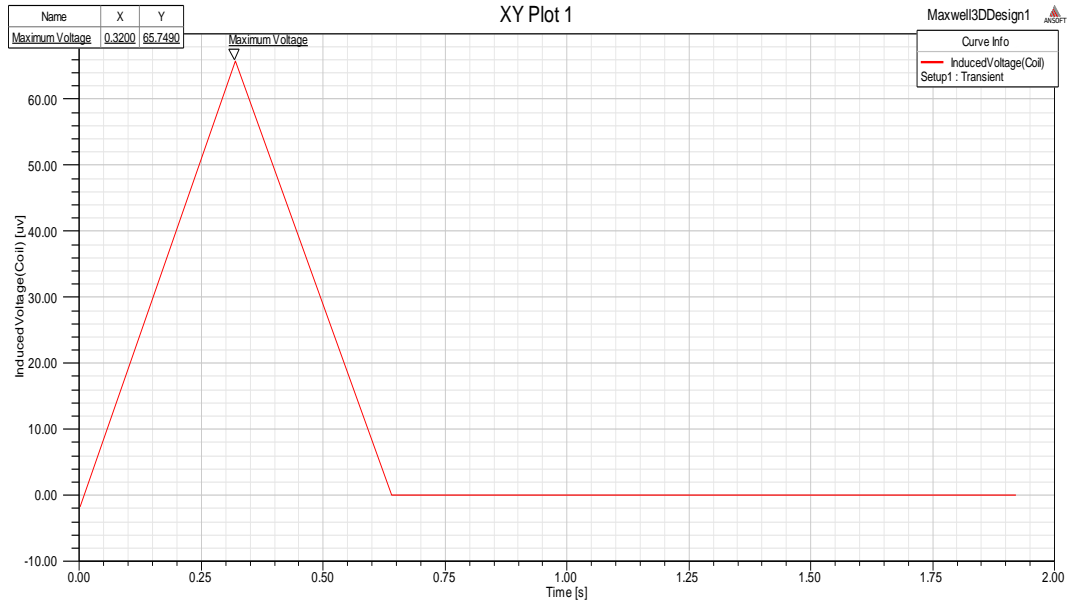


Figure 62. Mean voltage using Ansoft Maxwell for (V_{water} 1.36 m/sec)

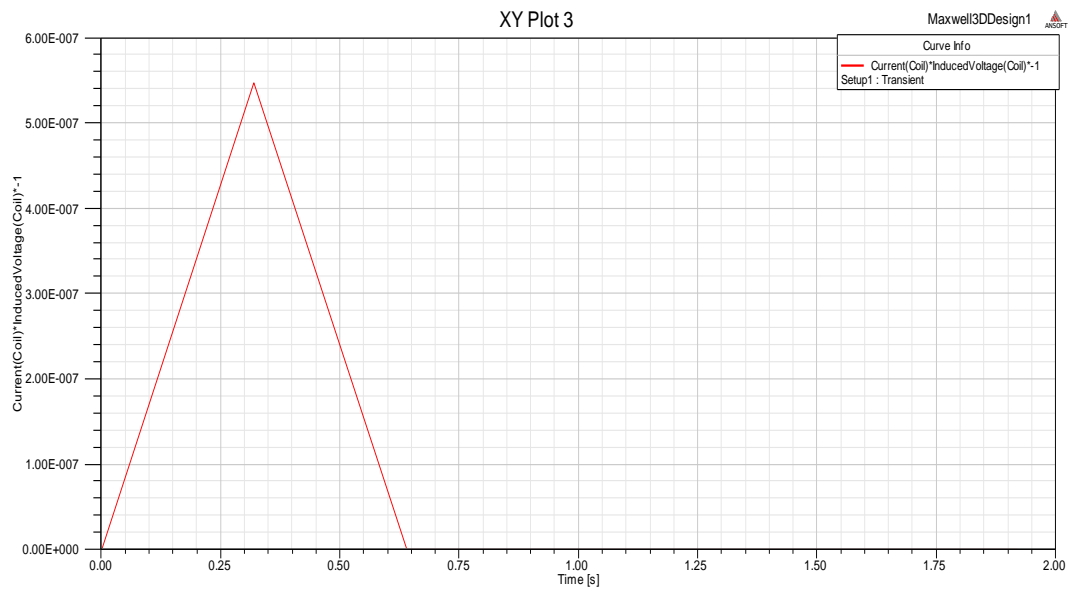


Figure 63. Mean power using Ansoft Maxwell for (V_{water} 1.36 m/sec)

Table 31. Summary of Ansoft Maxwell result for V_{water} (1.36 m/sec)

Re	V_{water} m/sec	Magnet velocity Vel_{mean} m/sec	V_{mean} (volts) μV	P_{mean} (Watt)
60,000	1.36	0.443745	65.89	$5.43e^{-7}$

MATLAB code for magnet velocity was found to be Vel_{max} 0.696613 m/sec as a maximum value with a mean velocity of Vel_{mean} of 0.443742 m/sec for corresponding V_{water} of 0.34 m/sec. Both types of velocities were gradually increased as V_{water} increases. For example, V_{water} of 0.68 m/sec the found maximum velocity Vel_{max} is 0.696614 m/sec with Vel_{mean} of 0.443743 m/sec with a difference with respect to V_{water} 0.34 of $1e^{-6}$ m/sec only. This is due to many variables involving in finding the magnet velocities; performing a change of CL_{max} , V_{water} , K_p , and K_{spring} will contribute minor change in equation (18).

In Ansoft Maxwell, four mean velocities were used to find the mean voltage and power. Therefore, the mean power and voltage results were based on the input mean velocities of the magnet. Four main drawbacks of Ansoft Maxwell. Firstly, the input magnet velocity will remain constant along the simulation period. As a result, the software will generate and repeat the same mean power and voltage for whatever simulation time. Secondly, the moving magnet must reach the end of the coil for getting power and voltage results. For instance, the magnet cannot stop in the middle of the coil and retract. Thirdly, the magnet moves in one direction (forward only) and cannot reverse to generate negative voltage, where this issue is clearly shown in all figures presented above. Finally, the mesh control options are very limited, unlike in ANSYS.

3D Simulation Study

Section 1: ANSYS Fluent Lift and Transverse Forces

In this results section, water velocities will be selected based on ANSYS Fluent analysis results. The first selected water velocity is 1.36 m/sec because transverse forces and lift forces overlap each other, especially between 10 to 18 seconds. As a result, when applying these forces (see Figure 64) on a harvester cylinder, the last will oscillate in a steady motion that will provide a steady piezoelectric and electromagnetic power and voltage over time.

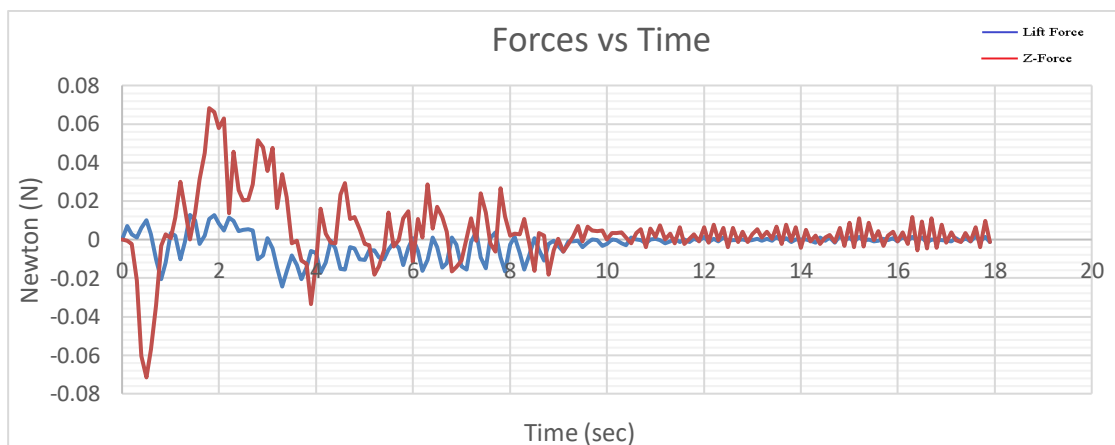


Figure 64. Lift and z- force applied on the harvester cylinder (V_{water} 1.36m/sec)

Velocity vector results were presented to visualize how the water surrounds the cylinder for V_{water} 1.36 m/sec shown in Figure 65. Velocity vectors are spinning around, on top and bottom of the cylinder walls.

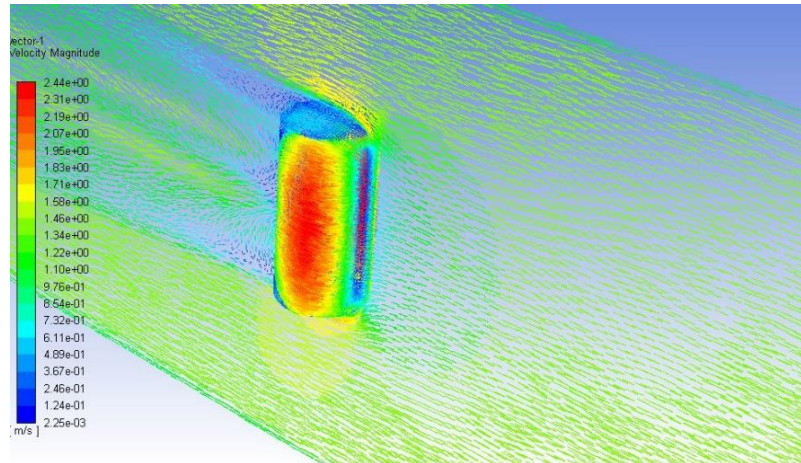


Figure 65. Velocity vector over a cylinder for $V_{\text{water}} 1.36 \text{ m/sec}$

Another illustration is presented from fluent result file, which is pressure contour over the cylinder as shown in Figure 66. The red contour represents the highest pressure due to the water impact, unlike on the sides of the cylinder, where the pressure is lowest due to the high-water velocity on that spot.

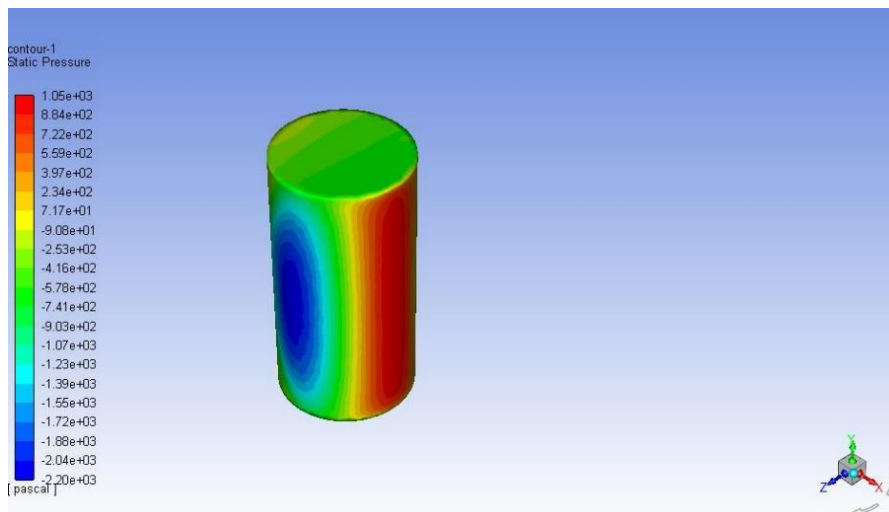


Figure 66. Static pressure contour over a cylinder for $V_{\text{water}} 1.36 \text{ m/sec}$

The second selected water velocity is 1.39 m/sec as its showing even enhanced overlapping transverse and lift forces, especially between 4 to 18 seconds, as shown in Figure 67.

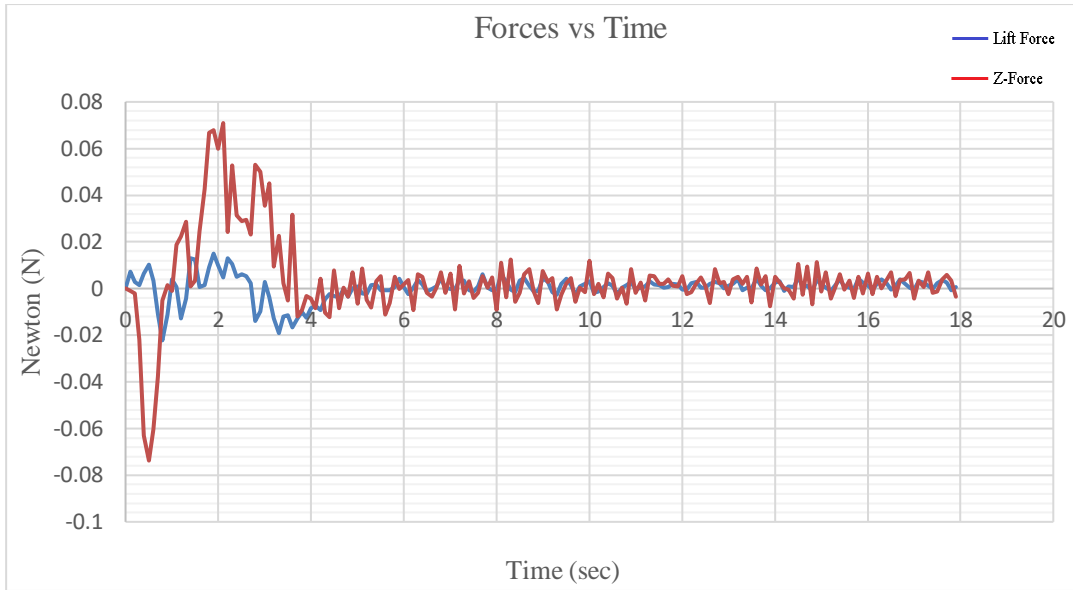


Figure 67. Lift and transverse forces applied on the harvester cylinder (V_{water} 1.39m/sec)

Section 2: Piezoelectric Voltage

Transient analysis was completed for water velocity of 1.36 m/sec and 1.39 m/sec. For the water velocity 1.36 m/sec, the focused region is between 10 to 18 seconds because this region is the most comfortable region where the cylinder will oscillate in steady cycles. Unlike the first region 0 to 10 seconds, wherein this region, the transverse and lift forces will initially cause an unusual impact on the cylinder, causing unsteady motion. Refer to Figure 68 for illustration.

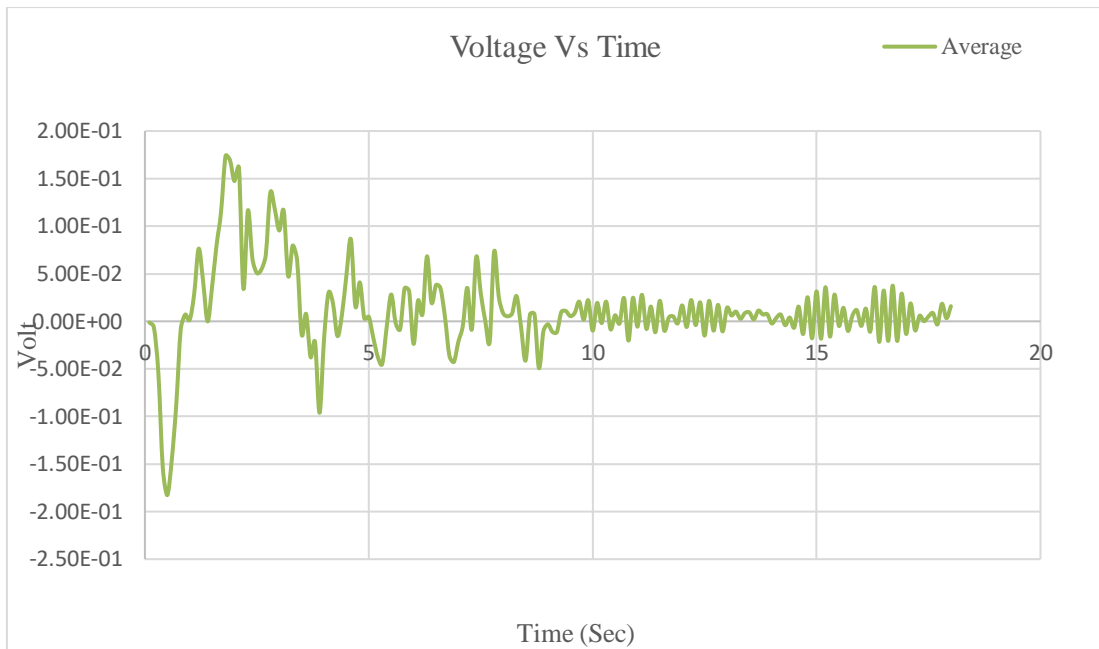


Figure 68. Mean voltage for piezoelectric (V_{water} 1.36 m/sec)

Table 32. Summary for piezoelectric voltage For V_{water} 1.36 m/sec

Re	V_{water} (m/sec)	Mean Voltage V_{mean} (mV)	Instantaneous Time (sec)
60,000	1.36	37.6	16.7

For water velocity of 1.39 m/sec, the considered region is between 4 to 18 seconds, as shown in Figure 69. Also, It is clearly visible that piezoelectric voltage versus time in Figure 69 is inherited from the water combined forces presented in Figure 67.

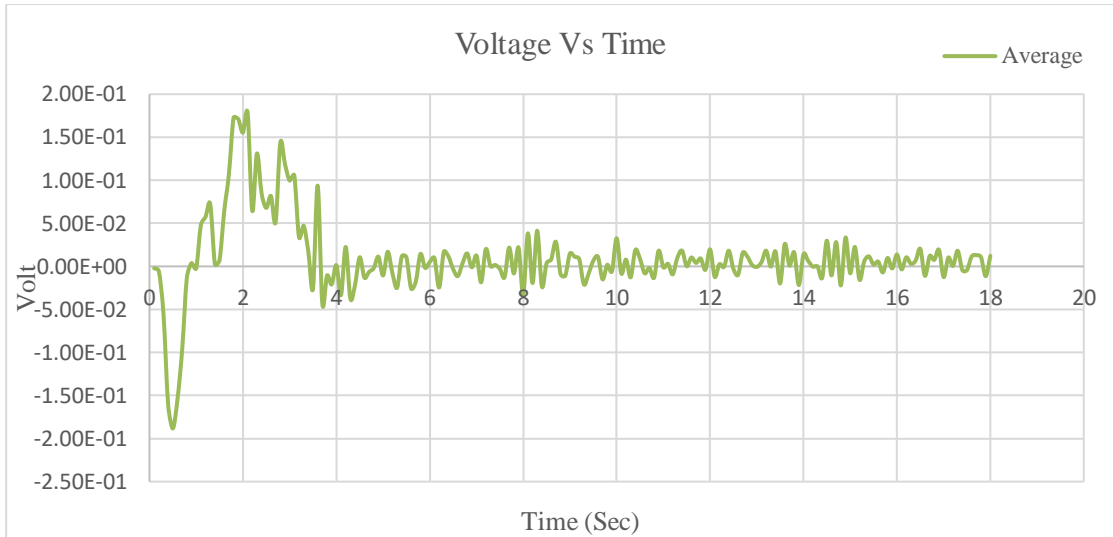


Figure 69. Mean voltage for piezoelectric ($V_{\text{water}} 1.39 \text{ m/sec}$)

Table 33. Summary for piezoelectric voltage for $V_{\text{water}} 1.39 \text{ m/sec}$

Re	$V_{\text{water}}(\text{m/sec})$	Mean Voltage V_{mean} (mV)	Instantaneous Time (sec)
62,000	1.39	41.4	8.3

Section 3: Magnet Velocity and Electromagnetic Voltage

Analysis was completed for magnet velocity for corresponding water velocity of 1.36 m/sec and 1.39 m/sec. The region of interest for the $V_{\text{water}} 1.36 \text{ m/sec}$ is between 10 to 18 seconds as the same transverse and lift forces were applied on the magnet. Even though the analysis for magnet velocity started at 10 seconds, the first 2 seconds from 10 to 12 sec will be subjected to unsteady spikes due to the combined forces as initial momentum is applied on the magnet housing. See Figure 70 for details. The steady region after 11.7 sec is visually close to zero. However, it is not, but in fact, this is the steady cycles. Refer to Figure 71 for $V_{\text{water}} 1.36 \text{ m/sec}$ and Figure 73 for $V_{\text{water}} 1.39 \text{ m/sec}$.

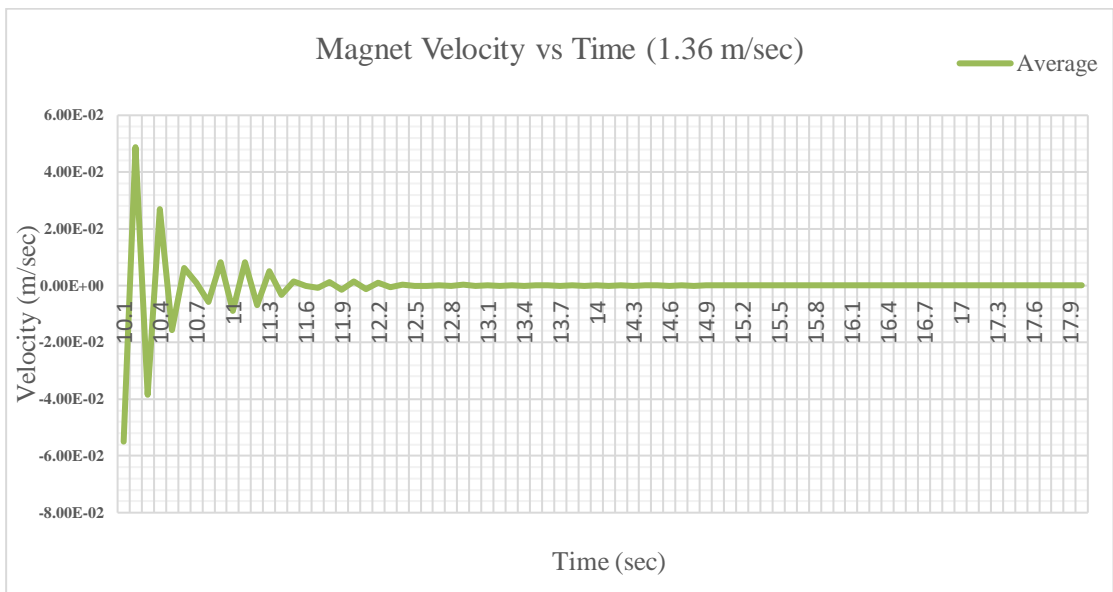


Figure 70. Mean magnet velocity for (V_{water} 1.36 m/sec)

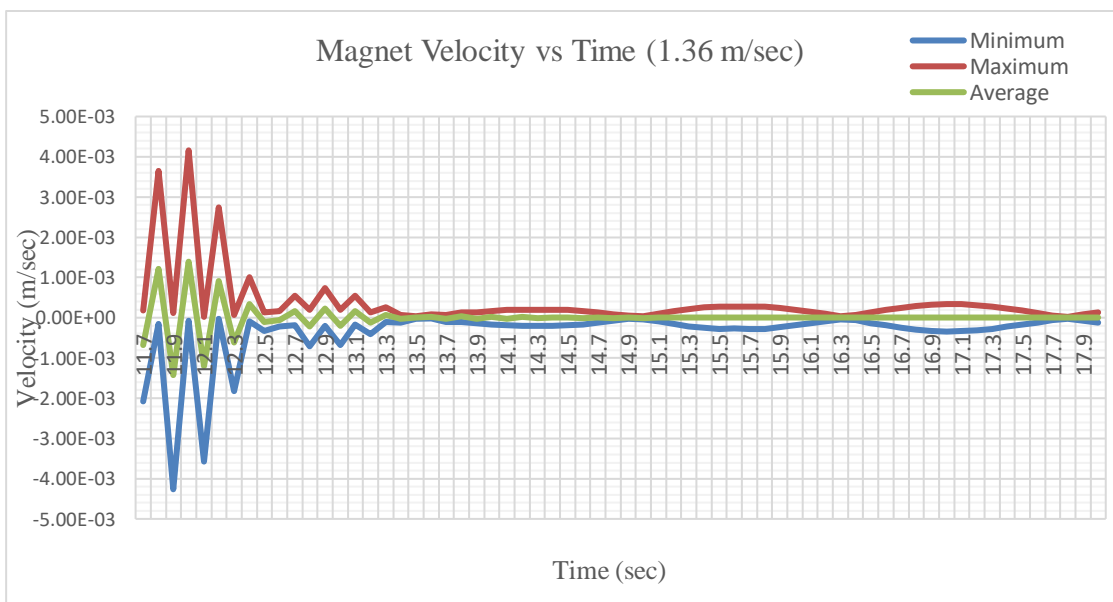


Figure 71. Magnified mean magnet velocity for (V_{water} 1.36 m/sec) between 11.7 sec to 18 sec showing steady cycles.

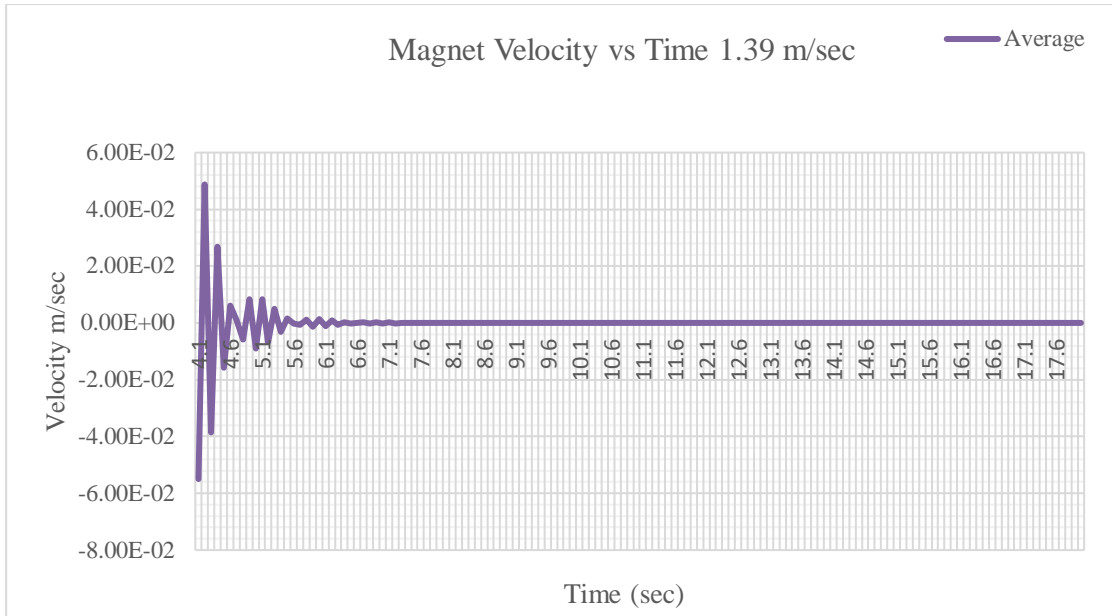


Figure 72. Mean magnet velocity for ($V_{\text{water}} 1.39 \text{ m/sec}$)

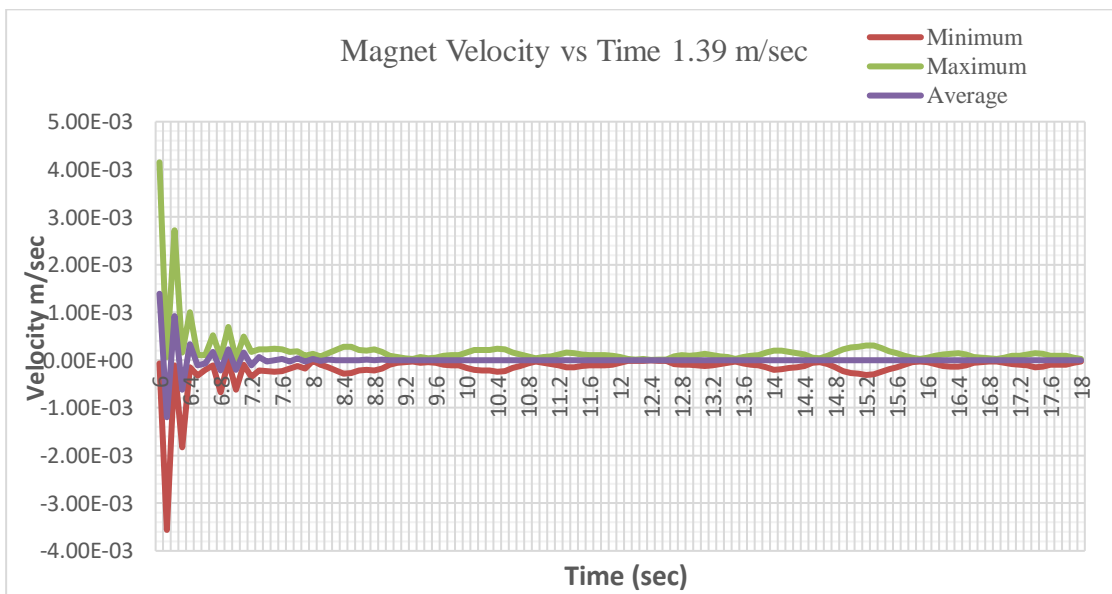


Figure 73. Magnified mean magnet velocity for ($V_{\text{water}} 1.39 \text{ m/sec}$) between 6 sec to 18 sec showing steady cycles.

Based on the magnet velocity and displacement of the magnet, the voltage calculations were done for water velocity 1.36 m/sec and 1.39 m/sec using Faraday's equation (15). It is noticeable that the initial unsteady region from the magnet velocity 1.36 m/sec and 1.39 m/sec were inherited to the electromagnetic voltage as shown in Figure 74 and

Figure 75. In other words, the initial high velocity of the magnet will generate a high voltage due to the water forces impact on the cylinder. As time passes, the water forces transverse and lift will stabilize; thus, the magnet velocity will stabilize, and finally, the electromagnetic voltage will stabilize. To obtain the mean electromagnetic voltage for water speed of 1.36 m/sec, the stabilized time region between 14 to 18 seconds. In like manner, for the water velocity of 1.39 m/sec, the stabilized time region is between 10 to 18 sec.

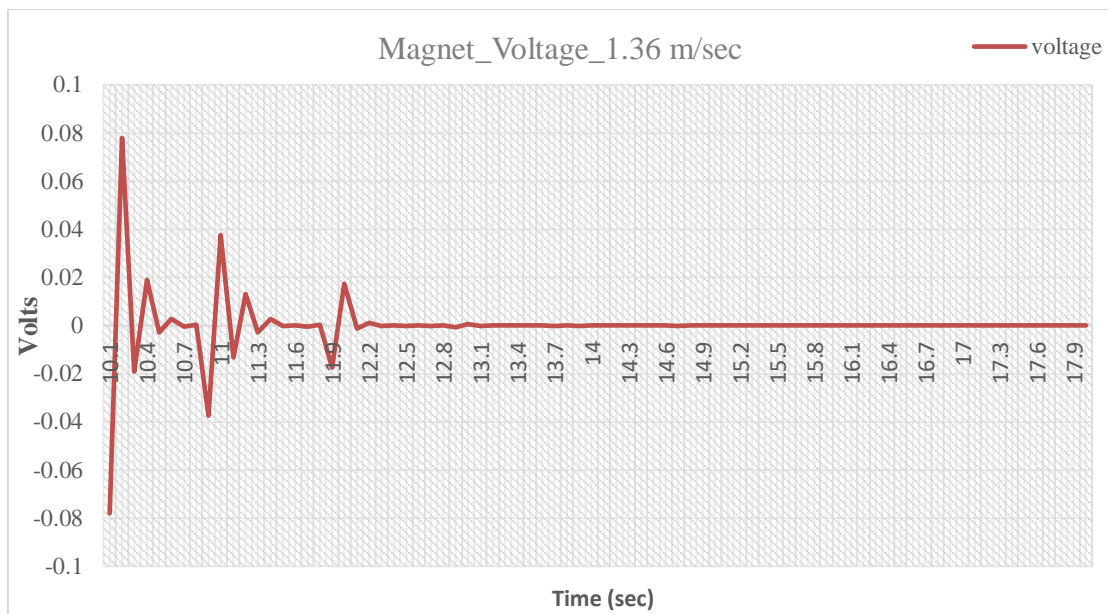


Figure 74. Electromagnetic voltage ($V_{\text{water}} 1.36 \text{ m/sec}$)

Table 34. Summary for electromagnetic voltage for $V_{\text{water}} 1.36 \text{ m/sec}$

Re	$V_{\text{water}}(\text{m/sec})$	$V_{\text{mean}} (\mu\text{V})$	Instantaneous time (sec)
60,000	1.36	49.7	14.0

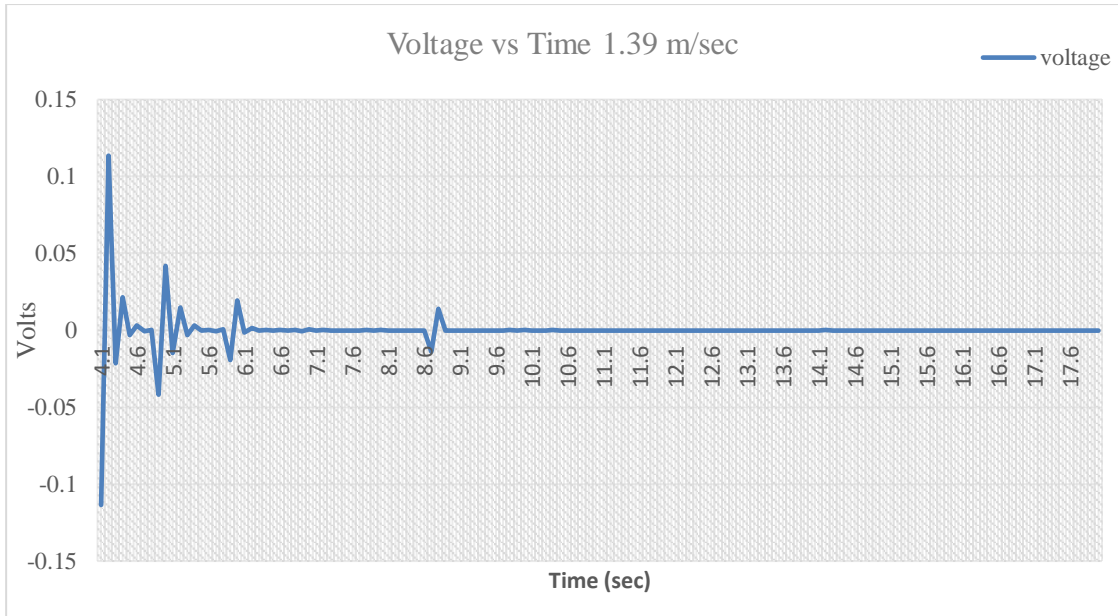


Figure 75. Electromagnetic voltage ($V_{\text{water}} 1.39 \text{ m/sec}$)

Table 35. Summary for Electromagnetic Voltage for $V_{\text{water}} 1.39 \text{ m/sec}$

Re	$V_{\text{water}}(\text{m/sec})$	$V_{\text{mean}} (\mu\text{V})$	Instantaneous time (sec)
62,000	1.39	91.8	14.2

CONCLUSION

To sum up, energy harvesting using smart materials exist from past years to power macroscale technologies such as sensors used in pipeline leak detection. Combining flexible piezoelectric patch (MFC) with electromagnetic induction using one of the world's strongest permanent magnet (Alnico 5) was a great idea to harvest continuous clean energy from water confined in utility pipes. A parametric study was conducted using MATLAB to obtain the piezoelectric voltage using the hydromechanical model proposed by Francesco Cotton demonstrates the actual power and voltage output of the new cylinder dimension. This step was essential to determine the new design capability

and initial results estimation. In 3D simulation section, the piezoelectric voltage in the steady region for the water velocity of 1.36 m/sec was compared to the results hydromechanical model of the same water velocity as shown in Tables 36 and 37. In piezoelectric parametric study, the mean voltage at V_{water} 1.36 is constant versus proportional gain K_p with V_{mean} of 9.1 mV. On the other hand, in 3D simulation, at the same water velocity, the mean voltage (37.6 mV) is instantaneous and gets lower/higher than 9.1 mV by time.

Table 36. Summary of piezoelectric parametric (preliminary study)

V_{water} m/sec	P_{mean} (μW)	V_{mean} (mVolt)
0.34	4.3	-
0.68	13.4	-
1.02	33.6	-
1.36	74.4	9.1

Table 37. Summary of piezoelectric (3D simulation)

V_{water}	Voltage mean (mVolt)	Instantaneous time (sec)
1.36	37.6	16.7
1.39	41.4	8.3

In the electromagnetic induction section, the magnet velocity was estimated using MATLAB by linking hydromechanical variables such as lift coefficient and water velocity. The magnet mean velocity was the main element to obtain the mean voltage of electromagnetic induction through Ansoft Maxwell. Finally, by using ANSYS 3D transient mechanical, the magnet mean velocity was used to acquire the electromagnetic voltage by an equation for both 1.36 m/sec and 1.39 m/sec, and the results were compared as shown in Tables 38 and 39. At V_{water} 1.36 m/sec, the voltage is 65.89 μV using Ansoft Maxwell, having a constant mean velocity of the magnet as this is one of

the major limitations of the software. Unlike in 3D simulation, the researcher could obtain the variable magnet velocity at each fraction of a second and the exact magnet displacement. Moreover, the mean voltage of 49.7 μV is instantaneous and gets higher/lower than 65.89 μV over steady region time.

Table 38. Summary of electromagnetic voltage and power (preliminary study)

V_{water}	Voltage mean (μV)	Power mean (Watt)
0.34	64.31	5.21e^{-7}
0.68	64.65	5.25e^{-7}
1.02	65.73	5.39e^{-7}
1.36	65.89	5.43e^{-7}

Table 39. Summary of electromagnetic voltage (3D simulation)

V_{water}	Voltage mean (μV)	Instantaneous time (sec)
1.36	49.7 μV	14.0
1.39	91.8 μV	14.2

In the future, a further parametric study can be achieved by more advanced piezoelectric smart material or by changing the fluid characteristics such as fluid velocity or using another engineered fluid. Likewise, electromagnetic induction can be further optimized by using a Neodymium-Iron-Boron permanent magnet that has stronger flux or by reducing the magnet spring stiffness.

REFERENCES

- [1] 2021, "uPVC ducting", Hepworth [Online]. Available: <https://hepworth.ae/product/upvc-ducting/>. [Accessed: 10- Feb- 2021].
- [2] Carlton, J., 2019, Marine propellers and propulsion (Fourth Edition).
- [3] 2021, "Dynamic Viscosity of Water", Vaxasoftware.com [Online]. Available: http://www.vaxasoftware.com/doc_eduen/qui/viscoh2o.pdf. [Accessed: 12- Feb- 2021].
- [4] Alcatel Lucent SAS, 2021, "Energy harvester apparatus having improved efficiency."
- [5] Aramendia, I., Fernandez-Gamiz, U., Zulueta Guerrero, E., Lopez-Guede, J., and Sancho, J., 2018, "Power Control Optimization of an Underwater Piezoelectric Energy Harvester", *Applied Sciences*, 8(3), p. 389.
- [6] Designing with Plastic. (2000) (p. 12). USA.
- [7] Maddah, H., 2016, "Polypropylene as a Promising Plastic: A Review", *American Journal of Polymer Science*.
- [8] Mishra, S., Unnikrishnan, L., Nayak, S., and Mohanty, S., 2018, "Advances in Piezoelectric Polymer Composites for Energy Harvesting Applications: A Systematic Review", *Macromolecular Materials and Engineering*, 304(1), p. 1800463.
- [9] Sanchita Abrol , Deepak Chhabra, S., 2018, "Experimental Investigations of Piezoelectric Energy Harvesting with Turbulent Flow", *International Journal of Mechanical and Production Engineering Research and Development*, 8(1), pp. 703-710.
- [10] 2021, "MFC P1 Type", Smart-material.com [Online]. Available: <https://www.smart-material.com/MFC-product-P1.html>. [Accessed: 13- Feb- 2021].
- [11] Davidovits, P., 2013, *Physics in biology and medicine*, Academic Press, London.

- [12] 2021, "GDPR", Byjus.com [Online]. Available: <https://byjus.com/physics/radius-of-gyration/>. [Accessed: 14- Feb- 2021].
- [13] Menter, F., 1994, "Two-equation eddy-viscosity turbulence models for engineering applications", *AIAA Journal*, 32(8), pp. 1598-1605.
- [14] Rahman, M., Karim, M., and Alim, M., 1970, "Numerical investigation of unsteady flow past a circular cylinder using 2-D finite volume method", *Journal of Naval Architecture and Marine Engineering*, 4(1), pp. 27-42.
- [15] Stringer, R., Zang, J., and Hillis, A., 2014, "Unsteady RANS computations of flow around a circular cylinder for a wide range of Reynolds numbers", *Ocean Engineering*, 87, pp. 1-9.
- [16] 2021, "Table of Resistivity", Hyperphysics.phy-astr.gsu.edu [Online]. Available: <http://hyperphysics.phy-astr.gsu.edu/hbase/Tables/rstiv.html>. [Accessed: 23- Feb- 2021].
- [17] Cohen, Brett I. The World's Strongest Permanent Magnet (Neodymium-Iron-Boron): A Chemical Perspective. *Alternate Perceptions (AP) Magazine* (issue 260); November 2019.
- [18] 2021, "Alnico Magnet Datasheet", eclipsemagnetics.com [Online]. Available: https://www.eclipsemagnetics.com/site/assets/files/2418/alnico_magnets_datasheet.pdf. [Accessed: 23- Feb- 2021].
- [19] 2021, "Polypropylene (cop.) | Designerdata", Designerdata.nl [Online]. Available: [https://designerdata.nl/materials/plastics/thermo-plastics/polypropylene-\(cop.\)](https://designerdata.nl/materials/plastics/thermo-plastics/polypropylene-(cop.)). [Accessed: 01- Mar- 2021].

- [20] 2021, "Polyvinylidene fluoride | Designerdata", Designerdata.nl [Online]. Available: <https://designerdata.nl/materials/plastics/thermo-plastics/polyvinylidene-fluoride>. [Accessed: 01- Mar- 2021].
- [21] Costanzo, L., and Vitelli, M., 2020, "Tuning Techniques for Piezoelectric and Electromagnetic Vibration Energy Harvesters", *Energies*, 13(3), p. 527.
- [22] Muthalif, A., and Nordin, N., 2015, "Optimal piezoelectric beam shape for single and broadband vibration energy harvesting: Modeling, simulation and experimental results", *Mechanical Systems and Signal Processing*, 54-55, pp. 417-426.
- [23] Shan, X., Song, R., Liu, B., and Xie, T., 2015, "Novel energy harvesting: A macro fiber composite piezoelectric energy harvester in the water vortex", *Ceramics International*, 41, pp. S763-S767.
- [24] Zhao, J., and Zhang, H., 2017, "A Novel Model of Piezoelectric- Electromagnetic Hybrid Energy Harvester Based on Vortex-induced Vibration", *International Conference on Green Energy and Applications (ICGEA)*, ieeexplore, Beijing.
- [25] Iqbal, M., and Khan, F., 2018, "Hybrid vibration and wind energy harvesting using combined piezoelectric and electromagnetic conversion for bridge health monitoring applications", *Energy Conversion and Management*, 172, pp. 611-618.
- [26] Norberg, C., 2001, "Flow Around A Circular Cylinder: Aspects of Fluctuation Lift", *Journal of Fluids and Structures*, 15(3-4), pp. 459-469.
- [27] 2021, "International - U.S. Energy Information Administration (EIA)", *Eia.gov* [Online]. Available: <https://www.eia.gov/international/analysis/country/JPN>. [Accessed: 17- Apr- 2021].
- [28] Bakhtiar, S., and Khan, F., 2019, "Analytical Modeling and Simulation of an Electromagnetic Energy Harvester for Pulsating Fluid Flow in Pipeline", *The Scientific World Journal*, 2019, pp. 1-9.

APPENDIX “A”: SAMPLE MATLAB CODE FROM LITERATURE

```

Kp=0:0.1:10;
Rhopiezo=5319;
Rhocylinder=920;
Rhowater=997.5;
A=0.01;
k=123;
Ktrans=2;
C=1;
f=0.01;
L1=0.0035;
L=0.08;
Ha=0.05;
a=0.01;
alpha=100;
Jwt=4.2*10^(-7);
Vwater=0.36;
CLmax=1.111;
D=0.01;
Kspring=7.2671*10^(-9);
w0=5930;
a1=0.25*Rhowater*D*Vwater^2*Ha*(2*L-Ha)
a2=(Jwt+L1*Rhopiezo*A*a^2)
a3=(f+alpha^2*a^2./(Kp*Ktrans));
a4=Kspring+(k*a^2/Ktrans)

Pmean=((alpha*a/Ktrans)^2*(1./(2.*Kp))).*(a1*w0*Clmax./sqrt((a4-
a2*w0^2)^2+(a3*w0).^2)).^2;
plot(Kp,Pmean,'r');
grid on
grid minor
xlabel('Kp')
ylabel('Power[W]')
title('Re=3000 Kspring=7.2671x10\it^{-9}')
legend('Power')

```

APPENDIX “B”: PIEZOELECTRIC MATLAB CODES OF PRELIMINARY STUDY

$V_{\text{water}} = 0.34 \text{ m/sec}$

```

Kp=0:0.1:10;
Rhopiezo=1780;
Rhocylinder=920;
Rhowater=997;
A=0.01;
k=123;
Ktrans=2;
C=1.4;
f=0.01;
L1=0.0035;
L=0.020;
Ha=0.08;
a=0.01;
alpha=100;
Jwt=4.021*10^(-5);
Vwater=0.34;
CLmax=0.85;
D=0.04;
Kspring=7.2671*10^(-9);
w0=5930;
a1=0.25*Rhowater*D*Vwater^2*Ha*(2*L-Ha)
a2=(Jwt+L1*Rhopiezo*A*a^2)
a3=(f+alpha^2*a^2./(Kp*Ktrans));
a4=Kspring+(k*a^2/Ktrans)

Pmean=((alpha*a/Ktrans)^2*(1./(2.*Kp))).*(a1*w0*CLmax./sqrt((a4-
a2*w0^2)^2+(a3*w0).^2)).^2;
plot(Kp,Pmean,'r');
grid on
grid minor
xlabel('Kp')
ylabel('Power[W]')
title('Re=15,000 Kspring=7.2671x10\it^{-9}')
legend('Power')
format long
Pmax = max(Pmean)
syms Kp
fun = @(Kp)(-((alpha*a/Ktrans)^2*(1./(2.*Kp))).*(a1*w0*CLmax./sqrt((a4-
a2*w0^2)^2+(f+alpha^2*a^2./(Kp*Ktrans))*w0).^2)).^2)
Kpoptimal = fminbnd(fun,0,10)

```

$V_{\text{water}} = 0.68 \text{ m/sec}$

```
Kp=0:0.1:10;
Rhopiezo=1780;
Rhocylinder=920;
Rhowater=997;
A=0.01;
k=123;
Ktrans=2;
C=1.4;
f=0.01;
L1=0.0035;
L=0.020;
Ha=0.08;
a=0.01;
alpha=100;
Jwt=4.021*10^(-5);
Vwater=0.68;
CLmax=0.375;
D=0.04;
Kspring=3.4594*10^(-8);
w0=5920;
a1=0.25*Rhowater*D*Vwater^2*Ha*(2*L-Ha)
a2=(Jwt+L1*Rhopiezo*A*a^2)
a3=(f+alpha^2*a^2./(Kp*Ktrans));
a4=Kspring+(k*a^2/Ktrans)

Pmean=((alpha*a/Ktrans)^2*(1./(2.*Kp))).*(a1*w0*CLmax./sqrt((a4-
a2*w0^2)^2+(a3*w0).^2)).^2;

plot(Kp,Pmean,'r');
grid on
grid minor
xlabel('Kp')
ylabel('Power[W]')
title('Re=30,000 Kspring=3.4594x10\it^{-8}')
legend('Power')
format long
pmax = max(Pmean)
syms Kp
fun = @(Kp)(-((alpha*a/Ktrans)^2*(1./(2.*Kp))).*(a1*w0*CLmax./sqrt((a4-
a2*w0^2)^2+((f+alpha^2*a^2./(Kp*Ktrans))*w0).^2)).^2)
Kpoptimal = fminbnd(fun,0,10)
```

V_{water} = 1.02 m/sec

```
Kp=0:0.1:10;
Rhopiezo=1780;
Rhocylinder=920;
Rhowater=997;
A=0.01;
k=123;
Ktrans=2;
C=1.4;
f=0.01;
L1=0.0035;
L=0.020;
Ha=0.08;
a=0.01;
alpha=100;
Jwt=4.021*10^(-5);
Vwater=1.02;
CLmax=0.2625;
D=0.04;
Kspring=6.5404*10^(-8);
w0=5867;
a1=0.25*Rhowater*D*Vwater^2*Ha*(2*L-Ha)
a2=(Jwt+L1*Rhopiezo*A*a^2)
a3=(f+alpha^2*a^2./(Kp*Ktrans));
a4=Kspring+(k*a^2/Ktrans)

Pmean=((alpha*a/Ktrans)^2*(1./(2.*Kp))).*(a1*w0*CLmax./sqrt((a4-
a2*w0^2)^2+(a3*w0).^2)).^2;

plot(Kp,Pmean,'r');
grid on
grid minor
xlabel('Kp')
ylabel('Power[W]')
title('Re=45,000 Kspring=6.5404x10\it^{-8}')
legend('Power')
format long
Pmax = max(Pmean)
syms Kp
fun = @(Kp)(-((alpha*a/Ktrans)^2*(1./(2.*Kp))).*(a1*w0*CLmax./sqrt((a4-
a2*w0^2)^2+((f+alpha^2*a^2./(Kp*Ktrans))*w0).^2)).^2)
Kpoptimal = fminbnd(fun,0,10)
```

$V_{\text{water}} = 1.36 \text{ m/sec}$

```
Kp=0:0.1:10;
Rhopiezo=1780;
Rhocylinder=920;
Rhowater=997;
A=0.01;
k=123;
Ktrans=2;
C=1.4;
f=0.01;
L1=0.0035;
L=0.020;
Ha=0.08;
a=0.01;
alpha=100;
Jwt=4.021*10^(-5);
Vwater=1.36;
CLmax=0.22;
D=0.04;
Kspring=1.1627*10^(-7);
w0=5876;
a1=0.25*Rhowater*D*Vwater^2*Ha*(2*L-Ha)
a2=(Jwt+L1*Rhopiezo*A*a^2)
a3=(f+alpha^2*a^2./(Kp*Ktrans));
a4=Kspring+(k*a^2/Ktrans)
format long
Pmean=((alpha*a/Ktrans)^2*(1./(2.*Kp))).*(a1*w0*CLmax./sqrt((a4-
a2*w0^2)^2+(a3*w0).^2)).^2;
%subplot(2,1,2)
figure
hold on
plot(Kp,Pmean,'r');
grid on
grid minor
xlabel('Kp')
ylabel('Power[W]')
title('Re=60,000 Kspring=1.1627x10\it^{-7}')
legend('Power')
format long
Pmax = max(Pmean)
syms Kp
fun = @(Kp)(-((alpha*a/Ktrans)^2*(1./(2.*Kp))).*(a1*w0*CLmax./sqrt((a4-
a2*w0^2)^2+(f+alpha^2*a^2./(Kp*Ktrans))*w0).^2)).^2)
Koptimal = fminbnd(fun,0,10)
hold off
```

Voltage $V_{\text{water}}=1.36$ m/sec

```
Kp=0:0.1:20;
Rhopiezo=1780;
Rhocylinder=920;
Rhowater=997;
A=0.01;
k=123;
Ktrans=2;
C=1.4;
f=0.01;
L1=0.0035;
L=0.020;
Ha=0.08;
a=0.01;
alpha=100;
Jwt=4.021*10^(-5);
Vwater=1.36;
CLmax=0.22;
D=0.04;
Kspring=1.1627*10^(-7);
w0=5876;
a1=0.25*Rhowater*D*Vwater^2*Ha*(2*L-Ha)
a2=(Jwt+L1*Rhopiezo*A*a^2)
a3=(f+alpha^2*a^2./(Kp*Ktrans));
a4=Kspring+(k*a^2/Ktrans)
format long
V1=sqrt(((alpha*a/Ktrans)^2*(1./(2.*(Kp.^2))))).*(a1*w0*CLmax./sqrt((a4-
a2*w0^2)^2+(a3*w0).^2)).^2);
figure
hold on
plot(Kp,V1,'r');
grid on
grid minor
xlabel('Kp')
ylabel('Voltage[V]')
title('Re=60,000 Kspring=1.1627x10\it^{-7}')
legend('voltage')
format long
Vmax = max(V1)
syms Kp
fun = @(Kp)-
sqrt(((alpha*a/Ktrans)^2*(1./(2.*(Kp.^2))))).*(a1*w0*CLmax./sqrt((a4-
a2*w0^2)^2+((f+alpha^2*a^2./(Kp*Ktrans))*w0).^2)).^2)
Koptimal = fminbnd(fun,0,10)
hold off
```

APPENDIX “C”: ELECTROMAGNETIC INDUCTION GOVERNING EQUATION

- *Engineering Dynamic*

$a_r = (\ddot{r} - r\dot{\theta}^2)_{er} + (r\ddot{\theta} + 2\dot{r}\dot{\theta})_{e\theta}$, the second term $e\theta$ is cancelled as magnet moving in radial motion only

$$r = l + x$$

$$\frac{dr}{dt} = \frac{d(l+x)}{dt}$$

$$\frac{dr}{dt} = \frac{dl}{dt} + \frac{dx}{dt}, \text{ (} dl/dt \text{ is cancelled as } l \text{ represent piezo beam which is constant)}$$

$$\frac{dr}{dt} = \frac{dx}{dt}$$

Therefore,

$$\dot{r} = \dot{x}$$

$$\ddot{r} = \ddot{x}$$

Also

$$\dot{\theta} = w(t)$$

$$\dot{\theta} = w^2(t)$$

Where,

$$w(t) = \frac{a_1 w_0 C L_{\max}}{\sqrt{(a_4 - a_2 w_0^2)^2 + (a_3 w_0)^2}} \sin(w_0 t)$$

- *Newton First Law*

$$\sum \vec{F} = ma$$

$$mg \cos \theta - kx = m(\ddot{r} - r\dot{\theta}^2)_{er}$$

Re-arranging and multiplying by -ve

$$m\ddot{x} + x(k + m\dot{\theta}^2) = mg \cos \theta + ml\dot{\theta}^2$$

Let $mg \cos \theta + ml\dot{\theta}^2 = 0$ (General Solution for 2nd order differential equation)

Using discriminant $r = \frac{-b \pm \sqrt{b^2 - 4c}}{2a}$

$$\therefore x(t) = C_1 e^t \cos \sqrt{-2(k + \dot{\theta}^2)}_t + C_2 e^t \sin \sqrt{-2(k + \dot{\theta}^2)}_t \dots \dots \dots \text{Solution 1}$$

(Particular solution)

$$x(t) = at^2 + bt + c \text{ (the general form)}$$

$$x(t)' = 2at + b \text{ (first derivative)}$$

$$x(t)'' = 2a$$

Therefore, and solving

$$m\ddot{x} + x(k + m\dot{\theta}^2) = mg \cos \theta + ml\dot{\theta}^2$$

$$2am + (k + m\dot{\theta}^2)(at^2 + bt + c) = mg \cos \theta + ml\dot{\theta}^2$$

When $a=0, b=0$, solving for c is

$$\therefore C = \frac{mg \cos \theta + ml\dot{\theta}^2}{k + m\dot{\theta}^2} \dots \dots \dots \text{solution 2}$$

Final solution is general + particular solution

$$x(t) = x_g + x_p$$

$$x(t) = C_1 e^t \cos \sqrt{-2(k + \dot{\theta}^2)}_t + C_2 e^t \sin \sqrt{-2(k + \dot{\theta}^2)}_t + \frac{mg \cos \theta + ml\dot{\theta}^2}{k + m\dot{\theta}^2}$$

Deriving $x(t)$

$$x(t)' = \left[C_1 e^t \cos \sqrt{-2(k + \dot{\theta}^2)}_t + C_1 e^t 0.5 \cos(-2kt - 2t\dot{\theta}^2)^{-0.5} - \sin(-2kt - 2t\dot{\theta}^2)^{0.5} * (-2k - 2\dot{\theta}^2 + 2t2\dot{\theta}\ddot{\theta}^2) \right] + \dots$$

$$\left[C_2 e^t \sin \sqrt{-2(k + \dot{\theta}^2)}_t + C_2 e^t * 0.5 \sin(-2kt - 2t\dot{\theta}^2)^{-0.5} * \cos(-2kt - 2t\dot{\theta}^2)^{0.5} * (-2k - 2\dot{\theta}^2 + 2t2\dot{\theta}\ddot{\theta}^2) \right] + \dots$$

$$\left[\frac{(g\dot{\theta} - \sin \theta + 2l\dot{\theta}\ddot{\theta})(k + m\dot{\theta}^2) - (2m\dot{\theta}\ddot{\theta})(mg \cos \theta + ml\dot{\theta}^2)}{(k + m\dot{\theta}^2)^2} \right]$$

APPENDIX “D”: MATLAB CODES FOR ELECTROMAGNETIC INDUCTION

V_{water} **0.34 m/sec**

```

Kp = 1.814;
Rhopiezo=1780;
Rhocylinder=920;
Rhowater=997; % at 25 oC
Apizo=0.01;%section of piezoelectric
kstiff=123;
Ktrans=2;
f=0.01;
L1=0.0035;
L=0.020;
Ha=0.08;
aforce=0.01;%force application distance
alpha=100;
Jwt=4.021*10^(-5);
Vwater=0.34
l=0.07;
CLmax=0.85
D=0.04; %cylinder diameter
Kspring=7.2671^(-9);
w0=5876; %angular pulsation
a1 = 0.25*Rhowater*D*Vwater^2*Ha*(2*L-Ha);
a2 = (Jwt+L1*Rhopiezo*Apizo*aforce^2);
a3 = (f+alpha^2*aforce^2./(Kp*Ktrans));
a4 = Kspring+(kstiff*aforce^2/Ktrans);

format long
m = 0.178 %magnet mass is 178 grams
g = 9.81;
B = 0.5; %Alnico Magnet see reference
Acoil = pi*(0.02)^2; % pi r^2 (r=2 cm)
kmagspr=35.3; %spring constant
Nmax=33;% number of turn
Lwire=2*pi*0.02*Nmax; % L=4.14 Meter
dwire = 0.0015 %cross section area of wire for diameter= 1.5mm
rhocopper = 1.68*10^(-8); %resistivity of copper ohm*meter
syms x(t) t
w = a1*w0*CLmax/sqrt((a4-a2*w0^2)^2+(a3*w0)^2)
%theta = int(w,t)
E = m*diff(x,t,2)+(kmagspr+m*w^2)*x == m*g+m*l*w^2 %The expression of
(E) the differantial equation
Dx = diff(x,t);
x0 = x(0) == 0; %the initial condition (distance)
Dx = Dx(0) == 0; % The initial condition(speed of magnitude)
x(t) = dsolve(E, x0, Dx) %resolve the differential equation
v(t) = diff(x,t) % The expression of v=dx/dt
v1= matlabFunction(v)

```

```

v2 = matlabFunction(-v)
Tmax = fminbnd (v1,0,0.5)
Vmax = v2(Tmax)
Vmag = ((-B*Acoil*v)/(dwire)) % voltage
subplot(2,1,1)
fplot(v) %plot v
axis ([0 5 -2 2])
xlabel('time(sec)')
ylabel('Velocity Magnitude(m/sec) ')
grid on
grid minor

```

V_{water} = 0.68 m/sec

```

Kp = 1.8175;
Rhopiezo=1780;
Rhocylinder=920;
Rhowater=997; % at 25 oC
Apizo=0.01;%section of piezoelectric
kstiff=123;
Ktrans=2;
f=0.01;
L1=0.0035;
L=0.020;
Ha=0.08;
aforce=0.01;%force application distance
alpha=100;
Jwt=4.021*10^(-5);
Vwater=0.68;
l=0.07;
CLmax=0.375;
D=0.04; %cylinder diameter
Kspring=3.459^(-8);
w0=5876; %angular pulsation
a1 = 0.25*Rhowater*D*Vwater^2*Ha*(2*L-Ha);
a2 = (Jwt+L1*Rhopiezo*Apizo*aforce^2);
a3 = (f+alpha^2*aforce^2./(Kp*Ktrans));
a4 = Kspring+(kstiff*aforce^2/Ktrans);

format long
m = 0.178 %magnet mass is 178 grams
g = 9.81;
B = 0.5; %Alnico Magnet see reference
Acoil = pi*(0.02)^2; % pi r^2 (r=2 cm)
kmagspr=35.3; %spring constant
Nmax=33;% number of turn
Lwire=2*pi*0.02*Nmax; % L=4.14 Meter

```

```

dwire = 0.0015 %cross section area of wire for diameter= 1.5mm
rhocopper = 1.68*10^(-8); %resistivity of copper ohm*meter
syms x(t) t
w = a1*w0*CLmax/sqrt((a4-a2*w0^2)^2+(a3*w0)^2)
%theta = int(w,t)
E = m*diff(x,t,2)+(kmagspr+m*w^2)*x == m*g+m*1*w^2 %The expression of
(E) the differantial equation
Dx = diff(x,t);
x0 = x(0) == 0; %the initial condition (distance)
Dx = Dx(0) == 0; % The initial condition(speed of magnitude)
x(t) = dsolve(E, x0, Dx) %resolve the differential equation
v(t) = diff(x,t) % The expression of v=dx/dt
v1= matlabFunction(v)
v2 = matlabFunction(-v)
Tmax = fminbnd (v1,0,0.5)
Vmax = v2(Tmax)
Vmag = ((-B*Acoil*v)/(dwire)) %voltage
subplot(2,1,1)
fplot(v) %plot v
axis ([0 5 -2 2])
xlabel('time(sec)')
ylabel('Velocity Magnitude(m/sec) ')
grid on
grid minor

```

V_{water} = 1.02 m/sec

```

Kp = 1.833;
Rhopiezo=1780;
Rhocylinder=920;
Rhowater=997; % at 25 oC
Apiezo=0.01;%section of piezoelectric
kstiff=123;
Ktrans=2;
f=0.01;
L1=0.0035;
L=0.020;
Ha=0.08;
aforce=0.01;%force application distance
alpha=100;
Jwt=4.021*10^(-5);
Vwater=1.02;
l=0.07;
CLmax=0.2625;
D=0.04; %cylinder diameter
Kspring=6.5404^(-8);
w0=5876; %angular pulsation
a1 = 0.25*Rhowater*D*Vwater^2*Ha*(2*L-Ha);

```

```

a2 = (Jwt+L1*Rhopiezo*Apizo*aforce^2);
a3 = (f+alpha^2*aforce^2./(Kp*Ktrans));
a4 = Kspring+(kstiff*aforce^2/Ktrans);

format long
m = 0.178 %magnet mass is 178 grams
g = 9.81;
B = 0.5; %Alnico Magnet see reference
Acoil = pi*(0.02)^2; % pi r^2 (r=2 cm)
kmagspr=35.3; %spring constant
Nmax=33;% number of turn
Lwire=2*pi*0.02*Nmax; % L=4.14 Meter
dwire = 0.0015 %cross section area of wire for diameter= 1.5mm
rhocopper = 1.68*10^(-8); %resistivity of copper ohm*meter
syms x(t) t
w = a1*w0*CLmax/sqrt((a4-a2*w0^2)^2+(a3*w0)^2)
%theta = int(w,t)
E = m*diff(x,t,2)+(kmagspr+m*w^2)*x == m*g+m*l*w^2 %The expression of
(E) the differential equation
Dx = diff(x,t);
x0 = x(0) == 0; %the initial condition (distance)
Dx = Dx(0) == 0; % The initial condition(speed of magnitude)
x(t) = dsolve(E, x0, Dx) %resolve the differential equation
v(t) = diff(x,t) % The expression of v=dx/dt
v1= matlabFunction(v)
v2 = matlabFunction(-v)
Tmax = fminbnd (v1,0,0.5)
Vmax = v2(Tmax)
Vmag = ((-B*Acoil*v)/(dwire)) %voltage
subplot(2,1,1)
fplot(v) %plot v
axis ([0 5 -2 2])
xlabel('time(sec)')
ylabel('Velocity Magnitude(m/sec) ')
grid on
grid minor

```

V_{water} = 1.36 m/sec

```

Kp = 1.8311;
Rhopiezo=1780;
Rhocylinder=920;
Rhowater=997; % at 25 oC
Apizo=0.01;%section of piezoelectric
kstiff=123;
Ktrans=2;
f=0.01;

```

```

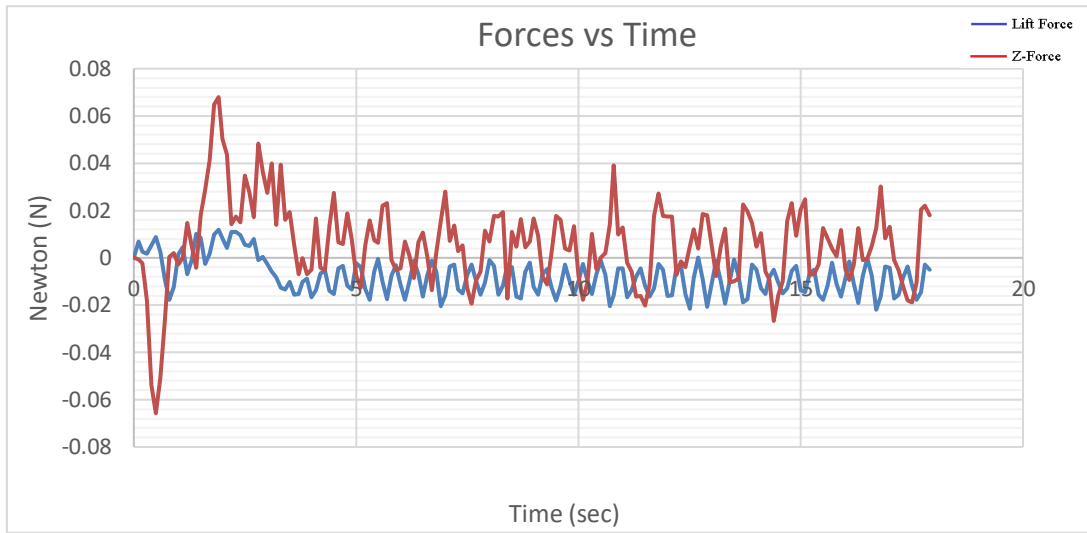
L1=0.0035;
L=0.020;
Ha=0.08;
aforce=0.01;%force application distance
alpha=100;
Jwt=4.021*10^(-5);
Vwater=1.36;
l=0.07;
CLmax=0.22;
D=0.04; %cylinder diameter
Kspring=1.1627^(-7);
w0=5876; %angular pulsation
a1 = 0.25*Rhowater*D*Vwater^2*Ha*(2*L-Ha);
a2 = (Jwt+L1*Rhopiezo*Apizo*aforce^2);
a3 = (f+alpha^2*aforce^2./(Kp*Ktrans));
a4 = Kspring+(kstiff*aforce^2/Ktrans);

format long
m = 0.178 %magnet mass is 178 grams
g = 9.81;
B = 0.5; %Alnico Magnet see reference
Acoil = pi*(0.02)^2; % pi r^2 (r=2 cm)
kmagspr=35.3; %spring constant
Nmax=33;% number of turn
Lwire=2*pi*0.02*Nmax; % L=4.14 Meter
dwire = 0.0015 %cross section area of wire for diameter= 1.5mm
rhocopper = 1.68*10^(-8); %resistivity of copper ohm*meter
syms x(t) t
w = a1*w0*CLmax/sqrt((a4-a2*w0^2)^2+(a3*w0)^2)
%theta = int(w,t)
E = m*diff(x,t,2)+(kmagspr+m*w^2)*x == m*g+m*l*w^2 %The expression of
(E) the differantial equation
Dx = diff(x,t);
x0 = x(0) == 0; %the initial condition (distance)
Dx = Dx(0) == 0; % The initial condition(speed of magnitude)
x(t) = dsolve(E, x0, Dx) %resolve the differential equation
v(t) = diff(x,t) % The expression of v=dx/dt
v1= matlabFunction(v)
v2 = matlabFunction(-v)
Tmax = fminbnd (v1,0,0.5)
Vmax = v2(Tmax)
Vmag = ((-B*Acoil*v)/(dwire)) % voltage
subplot(2,1,1)
fplot(v) %plot v
axis ([0 5 -2 2])
xlabel('time(sec)')
ylabel('Velocity Magnitude(m/sec) ')
grid on
grid minor

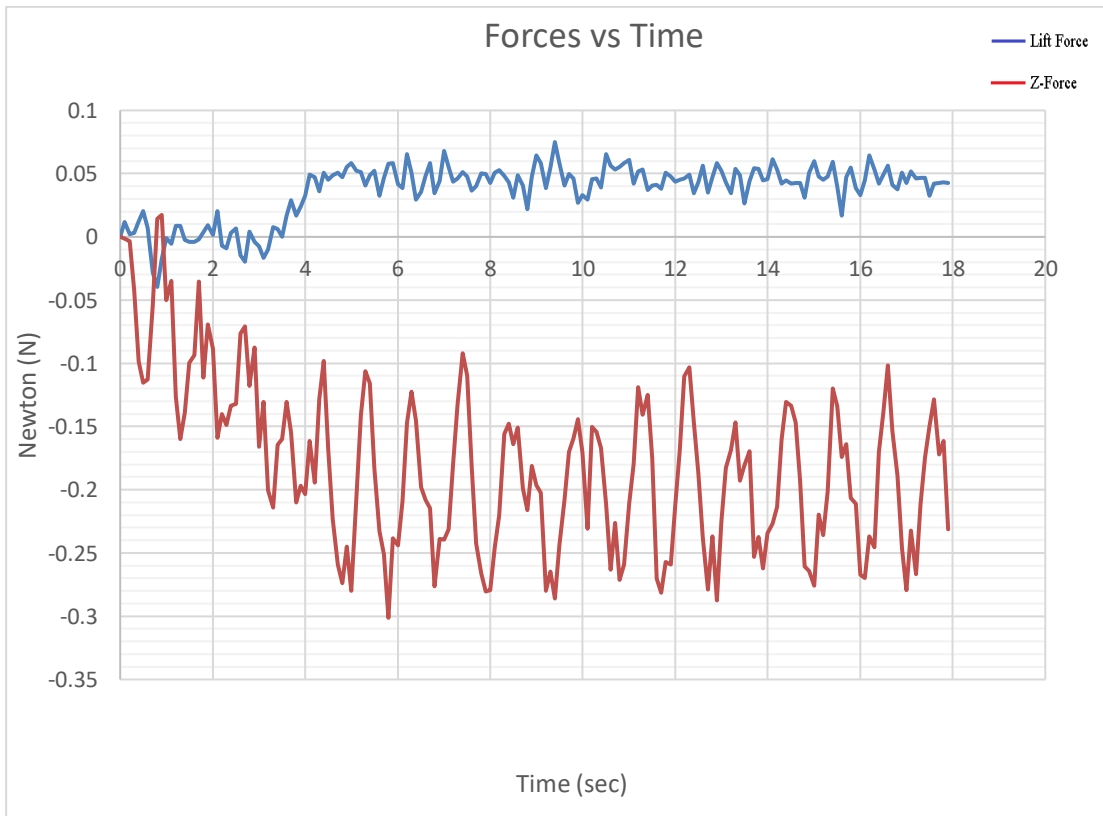
```

APPENDIX "E": NON-SELECTED WATER VELOCITIES

$V_{\text{water}} = 1.29 \text{ m/sec}$



$V_{\text{water}} = 1.80 \text{ m/sec}$



$V_{\text{water}} = 2.72 \text{ m/sec}$

